The Development of a "Genetic Eyewitness" Profiling System For Low Template Forensic Specimens: Identification of Novel Protein, RNA, and DNA Biomarkers

2008

Erin Hanson
University of Central Florida

THE DEVELOPMENT OF A "GENETIC EYEWITNESS" PROFILING SYSTEM FOR LOW TEMPLATE FORENSIC SPECIMENS: IDENTIFICATION OF NOVEL PROTEIN, RNA, AND DNA BIOMARKERS

by

ERIN K. HANSON
B.S. University of Central Florida, 2001
M.S. University of Central Florida, 2003

A dissertation submitted in partial fulfillment of the requirements
for the degree of Doctor of Philosophy in Biomolecular Science
in the Department of Chemistry
in the Burnett School of Biomedical Sciences
in the College of Medicine
University of Central Florida
Orlando, Florida

Fall Term
2008

Major Professor: Jack Ballantyne

ABSTRACT

In many criminal investigations, valuable information regarding the physical appearance of suspected perpetrators or the time and order of events that transpired are provided by eyewitness accounts. However, the information obtained from eyewitnesses is often constrained by human recollection or subjective accounts and provides a biased description of the perpetrator's appearance or an inaccurate time line of events. Additionally, in numerous situations eyewitness accounts may not be available. An increasing reliance therefore is placed on the biological evidence recovered during criminal investigations to act as a silent witness, providing unbiased and scientific information that may aid in the resolution of criminal investigations. While the current capabilities of operational forensic crime laboratories include analytical methods to allow for a determination of the origin of a biological stain and for the recovery of a genetic profile of the donor, the sensitivity of such methods is not always sufficient to accommodate the limited amounts of biological material often recovered in forensic casework, Therefore, it is critical that continual advancements in the analysis of low template samples be made. In this report, we have sought to identify novel protein, RNA and DNA biomarkers that, in combination with enhanced profiling strategies, would allow for a determination of the time since deposition, the body fluid of origin and the genetic profile of the donor ("genetic eyewitness") of forensic low template specimens.

First, we have developed a novel strategy for the determination of the time since deposition of dried bloodstains using spectrophotometric analysis of hemoglobin. An examination of the Soret band (λmax = 414nm) in aged bloodstains has revealed a

previously unidentified hypsochromic shift as the age of the stain increases. The extent of this shift permits a distinction to be made between stains that differ in age by only minutes, hours, days and months thus providing the highest resolution of any previously developed method. We also demonstrate that it may be possible to utilize a decline in enzyme activity to determine the age of a forensic biological stain. Second, we demonstrate that the differential expression of a panel of nine miRNAs allows for the identification of the body fluid origin of forensic biological stains using as little as 50pg of total RNA. This is the highest reported sensitivity of any RNA-based approach and this assay has demonstrated a high degree of specificity for each body fluid tested. The final task of this work was to identify novel DNA biomarkers and to develop enhanced profiling strategies to allow for greater sensitivity and reliability in the genetic profiling of low template samples. We demonstrate that the use of laser capture micro-dissection and enhanced amplification strategies resulted in the ability to obtain genetic profiles from as few as 2-5 epithelial cells and 5-10 sperm cells with greater reproducibility than previously reported studies. The use of a novel whole genome amplification method provided the ability to not only increase the quantity of genetic material obtained from micro-dissected cells but also the ability to recover additional genetic information from individual samples using novel DNA biomarkers.

The novel biomarkers and profiling strategies described in this report provide the basis for the establishment of a molecular "genetic eyewitness" from low template forensic samples and demonstrate the future potential for routine and reliable analysis of trace amounts of genetic material recovered from low template biological evidence.

To Barbara, Michael, Janelle, Damon, Claire, Ed and Em

ACKNOWLEDGMENTS

To Jack Ballantyne, my advisor and mentor, thank you for your wisdom, guidance and good humor. Simple words could not begin to express my appreciation and gratitude for everything you have taught me and every opportunity you have given me. You approached every day with a genuine sense of dedication and enthusiasm that inspired the same in me, allowing me to grow from a graduate student to a scientist. There is no thank you that would be truly sufficient for such a gift. Just know that it is out of honor and respect for you that I will continue to face every opportunity and every challenge with the same intensity and integrity as you have taught me to have.

I would like to thank the members of my committee, Dr. Cristina Calestani, Dr. James Hickman, and Dr. Saleh Naser for their support and encouragement throughout this project. I would also like to acknowledge Dr. Helge Lubenow and Subu Yerramilli of Qiagen for their support and technical assistance, Barbara Koons of the Federal Bureau of Investigation Laboratory for her support, and Jeanette Vance for her time and her phlebotomy skills. I would also like to express my appreciation to everyone who has donated samples throughout this project. This research would not have been possible without your contributions.

Finally, I would like to thank my family and friends for their love and support through this long process. To my family, Barbara, Michael, Janelle, Damon and little Claire, I know it felt like this day would never get here, but I couldn't have made it without your support, understanding and encouragement. I love you all more than you know and I hope I have made you proud. To Paulina Berdos, thank you for friendship and

for never letting me give up. To Jamie Del Papa, thank you for your friendship and for reminding me that it's ok to take a break!

Portions of this project were funded by the State of Florida, the National Institute of Justice (Grant # 2005-MU-BX-K071) and the Federal Bureau of Investigation (Contract # J-FBI-05-177)

TABLE OF CONTENTS

LIST OF FIGURES

LIST OF TABLES

LIST OF ACRONYMS/ABBREVIATIONS

Abs	absorbance
ADI	allele drop in
ADO	allele drop out
bp	base pairs
Ct	cycle threshold
CT	Christmas tree stain
ΔCt	delta Ct; delta cycle threshold
Δλ	change in wavelength
DEPC	diethylpyrocarbonate
DNA	deoxyribonucleic acid
DNase	deoxyribonuclease
dNTPs	deoxynucleotide triphosphates
DTT	dithiolthreitol
EDTA	ethylenediaminetetraacetic acid
Hb	hemoglobin
H&E	hematoxylin & eosin stain
ICN	increased cycle number
LCM	laser capture micro-dissection
LCN	low copy number
MaxV	maximum velocity

mIPEP	modified improved primer extension pre-amplification
miRNA	micro ribonucleic acid
MP	multiplex
mRNA	messenger ribonucleic acid
OSC	outside, covered
OSUC	outside, uncovered
PCR	polymerase chain reaction
proK	proteinase K
qPCR	real-time PCR/quantitative PCR
RFU	relative fluorescence unit
RNA	ribonucleic acid
RNase	ribonuclease
RT	reverse transcriptase/transcription
RT-PCT	reverse transcription-PCR
snoRNA	small nucleolar RNA
snRNA	small non-coding RNA
STR	short tandem repeat
TSD	time since deposition
UHD	ultra high discrimination
UV	ultra violet
UV-VIS	ultraviolet - visible spectrum

WGA	whole genome amplification
Y-STR	Y chromosome short tandem repeat

CHAPTER ONE: INTRODUCTION

In many criminal investigations, valuable information regarding the physical appearance of suspected perpetrators or the time and order of events that transpired are provided by eyewitness accounts. However, the information obtained from eyewitnesses is often constrained by human recollection or subjective accounts and provides a biased description of the perpetrator's appearance or an inaccurate time line of events. Additionally, in numerous situations eyewitness accounts may not be available. An increasing reliance therefore is placed on the biological evidence recovered during criminal investigations to act as a silent witness, providing unbiased and scientific information that may aid in the resolution of criminal investigations. While the current capabilities of operational forensic crime laboratories include analytical methods to allow for a determination of the origin of a biological stain and for the recovery of a genetic profile of the donor, the sensitivity of such methods is not always sufficient to accommodate the limited amounts of biological material, or low template samples, often recovered in forensic casework.

Low template samples are those containing less than 100pg of template DNA, which is equivalent to approximately 15 diploid or 30 haploid cells. Low template sample analysis (typically referring only to the recovery of DNA profiles) is often not possible due to the sensitivity limits of the analytical techniques currently used by operational crime laboratories. The frequency of occurrence of low template samples in forensic casework therefore necessitates continual advancements in the strategies used to analyze

such samples. However, these advancements should not only be limited to the recovery of genetic profiles, but should include improved methodologies to recover other probative information from these samples as well. The aim of this work was to identify novel macromolecular biomarkers and to develop enhanced profiling strategies to establish a molecular "genetic eyewitness" from low template forensic samples. This "genetic eyewitness" ideally would be able to provide a determination of the time since deposition of biological stains, an identification of the body fluid of origin of biological stains, and an identification of the donor's genetic profile with greater reliability and discrimination.

The determination of the time since deposition of biological stains remains an unsolved problem in forensic casework. Currently, no reliable and accurate methods to determine the age of a stain have been developed for standard samples and certainly not for low template samples. Early TSD methods for bloodstains focused on the molecular changes to hemoglobin that occur over time such as oxidation and degradation of the protein chains [1-5]. One example of such a method reported the use of HPLC chromatography to measure the of α-chain:heme ratio in ageing stains [2]. With this method, a linear decrease in the α-chain area/heme area was observed, on a logarithmic scale, as stain age increased. In a subsequent study, a peak designated as "X" was detected only in aged stains, and the area of this peak increased as the age of the stain increased [3]. Various other studies have utilized HPLC analysis of hemoglobin to determine the age of bloodstains [1,5]. While these studies demonstrated a crude linear relationship between the age of a stain and the degradation of hemoglobin, the reported methods possess limited resolution for TSD estimates. Several previous methods have

been proposed that utilize changes in the characteristic α and β bands (~540 and 576nm respectively) of the visible spectral profile of hemoglobin or involve an assessment of potential mRNA degradation products in aged bloodstains. However, these methodologies have failed to gain widespread acceptance due to poor analytical sensitivity (large sample consumption) and inadequate resolution between different stain ages (often requiring years difference in age). Two recent studies involving attempts to determine approximate age of biological stains have examined RNA degradation, using both mRNA and rRNA [6,7]. The first utilized semi-quantitative duplex and competitive RT-PCR methods to estimate the approximate age of bloodstains based on the assumption that degradation to mRNA occurs from the 5'end and that the degradation of two housekeeping genes is different over time [7]. However, the authors did not adduce any evidence that mRNA in biological stains degrades in this manner and, in any case, the resolution afforded by these methods was too low (5 years) to be of forensic use [7]. The other RNA study examined ratios of β-actin mRNA and 18S rRNA as a function of time using real-time PCR and demonstrated a linear relationship over time [6]. However, this study produced low-resolution time estimates (approximately 30 days) and did not take into account differing environmental conditions [6]. Based on the results of these studies, it is evident that novel strategies are needed in order to obtain higher-resolution and accurate time-since-deposition determinations. Therefore, the first aim of this work was to determine if novel protein biomarkers could be identified to allow for a determination of the time since deposition of low template forensic biological evidence.

Another aspect of the analysis of forensic biological evidence that needs improvement in order to be able to accommodate low template samples is body fluid identification. In the past, standard practice in forensic casework analysis typically included a preliminary screening of evidentiary items recovered during the investigation of criminal offenses in order to identify the presence, and possible tissue origin, of biological material. The presence of biological material such as blood, semen and saliva stains can indicate the location of potential sources of DNA that, once recovered, could be used to identify the donor of the biological material. Typically, conventional methods for body fluid stain analysis are carried out in a serial manner, with a portion of the stain being tested for only one body fluid at a time. Frequently multiple tests are required to first presumptively identify the presence of biological fluids followed by additional testing in order to confirm the presence of the fluid or identify the species of origin. Therefore these methods are costly not only in the time and labor required for their completion, but also in terms of the amount of sample consumed during the performance of each assay. While these conventional methods can confirm the presence of human blood and semen, none of the routinely used serological and immunological tests can definitely identify the presence of human saliva or vaginal secretions. With the large volume of cases that operational crime laboratories are faced with processing every year, a significant amount of the total time spent on an individual case can be devoted solely to the screening of evidentiary items for the presence of biological materials. The inability to positively confirm the presence of certain biological fluids, the consumption of valuable samples and the time and labor required has resulted in a trend to bypass

conventional body fluid identification methods and proceed straight to the analysis of DNA present in forensic samples. After all, it is argued, the recovery of human DNA from evidentiary items would directly indicate the presence of human biological material and thereby eliminate the need for conventional body fluid testing.

There are several disadvantages to bypassing the body fluid identification step during bio-molecular forensic analysis. First, the analytical methods used to analyze DNA are considerably more expensive that basic serological testing. Therefore the use of DNA analysis as a means to identify the presence of human biological material may not be justifiable from a budgetary standpoint. Additionally, a smaller number of samplings from an individual piece of evidence may be collected in an attempt to reduce the associated cost of analysis. Critical evidence may be missed using this type of approach that might have been identified using a larger preliminary screen with basic serological methods. A second disadvantage of the disuse of body fluid identification methods is that often the identification of the biological material present is crucial to the investigation and prosecution of the case. For example, consider a sexual assault of a child with a step father suspect where the step-father's DNA profile was recovered from samples taken from the child's underwear and bedding. The step-father could argue that the source of the DNA was from his skin cells deposited from casual and frequent contact with the child's clothing and bedding. However, the finding that his DNA originated from a semen stain and not skin cells would be more problematic for him to explain away and would more strongly support the allegation of a sexual assault. Another example of a case demonstrating the importance of identifying the body fluid could be that DNA from

a sexual assault victim is found in a suspect's vehicle and the suspect claims it was present due to casual contact since the victim had ridden in his car numerous times. However, the significance of this evidence would increase if the source of the DNA could be shown instead to originate from the victim's vaginal secretions, a circumstance which would be more difficult to attribute to casual contact as opposed to a sexual assault. A final example of the importance of determining the body fluid of origin involves the presence of blood in a sexual assault case. If blood is present in the vaginal canal, it needs to be proven that the blood is venous blood resulting from trauma rather than menstrual blood originating from a victim's regular menstrual cycle. In this instance, it is necessary to make a distinction between menstrual blood and venous blood which cannot be accomplished using conventional methods.

The routine use of body fluid identification methods prior to DNA analysis awaits the development of suitable molecular genetics based methods that are fully compatible with the current DNA analysis pipeline. In order for any new body fluid assay to be suitable for forensic casework it must demonstrate a high degree of specificity for each body fluid, permit parallel analysis of the different biological fluids, be completed in a timely and labor efficient manner and must be sufficiently sensitive. Messenger RNA (mRNA) profiling of tissue specific gene transcripts with forensic samples for the identification of body fluids has recently been reported and appears to satisfy most of these criteria [8-10].

The mRNA in aged and compromised dried appears to be sufficiently stable for forensic analysis [11]. However, as with DNA, heat and humidity is detrimental to RNA

stability and results in a time dependent fragmentation of the polynucleotide chain [11]. Typically forensic assays employ some biomarkers whose amplicon sizes are > 250 bases which results in amplification failure when highly degraded samples are encountered [12]. Thus reduced size amplicons for STR and mitochondrial DNA profiling methods are being increasingly used for the analysis of degraded samples [13-22]. Similarly smaller amplicons could be designed for use in mRNA based forensic assays although they may present additional technical assay design challenges because of the need to ensure that contaminating genomic DNA does not confound the analyses. In theory, another way to reduce the amplicon size would be to employ short RNA biomarkers in stead of mRNA. Recently, there has been an explosion on interest in a class of small non-coding RNAs, microRNAs, whose regulatory functions in various developmental and biological processes have been identified [23-40]. The role of miRNAs in various cancers and diseases are also being evaluated [41-52]. Several studies have examined the relative abundance of miRNAs in human tissue with numerous miRNAs reported to be tissue-specific [53-63]. However, as yet no studies have described miRNA expression in forensically-relevant, dried biological fluids (blood, semen, saliva, vaginal secretions and menstrual blood). In theory, it should be possible to identify miRNAs that, due to their differential tissue expression, could be used to identify the body fluid origin of forensic biological stains with a high degree of sensitivity and specificity and thus ideally suited for low template samples. Therefore, the second aim was to determine if miRNA expression assays could be used to determine the body fluid source of forensic low template samples.

The determination of the genetic profile of the donor of low template or low copy number (LCN) samples is a current challenge facing operational crime laboratories. Currently, no methods that allow for sufficient reproducibility and ease of interpretation are available for use in forensic casework. Since only a small number of cells are present in LCN samples, recovery of genetic profiles is difficult using standard STR methods and often results in total failure or recovery of a partial profile. Hence LCN methods have been developed (based upon increasing the PCR cycle number (ICN) to increase allelic signal intensity) to permit profile recovery from limited quantity samples. Interpretation of the data obtained from these LCN analyzed samples requires novel considerations [64-66]. The occurrence of allelic drop-out or drop-in is significantly higher in LCN samples due to stochastic effects, and can result in false homozygous classifications and in false heterozygous classifications, respectively. Additionally, LCN samples exhibit significant peak height imbalance and are more susceptible to interference from contamination. The frequency of LCN samples in forensic casework warrants development of additional methodologies to ICN that allow for more successful recovery of genetic information.

While it has been demonstrated that single cells can be isolated from certain tissue samples with micro-dissection techniques, the ability to consistently recover a DNA profile from single cells has not been demonstrated [67-74]. Most work done with single cells has involved the use of tumor cells, and the analysis of these cells is limited has normally been limited to one genetic marker. The success of recovery of genetic profiles from these single cells is often not consistent. No studies have demonstrated the ability to

consistently recover full autosomal STR profiles from single cell samples, which is the routine method of DNA analysis in forensic casework [68].

In an attempt to increase the recovery of DNA profiles from LCN samples, the use of increased cycle number has been suggested, with the assumption that sufficient amounts of the amplified product would be produced to allow for detection and analysis [6]. However, this method may not always be efficient, with additional cycles at high temperatures leading to a decrease in inefficiency of Taq DNA polymerase [75]. This results in less amplified product being produced, unless the process is halted for fresh enzyme to be added before the additional cycles. However, no studies have demonstrated successful analysis of single cells using only increased cycle number. Another approach to the analysis of LCN samples utilizes whole genome amplification (WGA) strategies, including primer extension pre-amplification (PEP), degenerate oligonucleotide-primed PCR (DOP) and multiple displacement amplification (MDA) [69,76-88]. These WGA methods employ various random-sequence primers with typically low stringency annealing conditions to amplify large tracts of the genome in an attempt to increase the effective number of starting templates prior to any downstream analysis. By pre-amplifying the limited amount of genetic material in the sample, sufficient quantities of template theoretically can be produced to overcome stochastic effects resulting from low copy number templates. However, few studies have demonstrated the suitability of these WGA methods for use with forensic casework samples [89-92]. The application of these WGA methods to cells isolated using laser capture micro-dissection techniques has also not been widely examined [93]. Therefore, it is evident that it may be possible to improve

low template sample analysis with additional research efforts. As a result, the final task of this work was to identify novel DNA biomarkers and to develop enhanced profiling strategies to allow for greater sensitivity and reliability in the genetic profiling of low template samples.

In summary, the overall aim of this work was to identify novel protein, RNA and DNA biomarkers that, in combination with enhanced profiling strategies, would allow for the development of a "genetic eyewitness" profiling system to provide investigators with the *who*, *what* and *when* of forensic low template samples. The "*when*" or time since deposition was accomplished through spectrophotometric analysis of hemoglobin. Additionally, we demonstrate that it may be possible to utilize a decline in enzyme activity to determine the age of a forensic biological stain. The "*what*" or identification of the body fluid of origin was accomplished by the development of the miRNA profiling assays using a panel of nine differentially expressed miRNAs. The *"who"* or determination of the genetic profile of the donor of low template samples was achieved using laser capture micro-dissection and enhanced amplification strategies. Collectively, our findings constitute the basis for the establishment of a molecular "genetic eyewitness" from low template forensic samples.

CHAPTER TWO: RESEARCH DESIGN AND METHODOLOGY

Preparation of Body Fluid Stains

General

Body fluids were collected from volunteers using procedures approved by the University of Central Florida's Institutional Review Board. Informed written consent was obtained from each donor. Blood samples were collected by venipuncture into additive-free vacutainers and 50 µl aliquots were placed onto cotton cloth and dried at room temperature. Blood samples from 12 non-primate animal species (dog, cat, horse, crane, cow, sheep, coyote, tortoise, lamb, Patagonian cavy, ferret, deer) and 10 primate species (spider monkey, rhesus macaque, pig-tailed macaque, brown lemur, chimpanzee, baboon, howler monkey, cynomolgous monkey, African green monkey, and spot-nosed guenon) were obtained from various sources: Tuscawilla Oaks Animal Hospital, Oviedo, FL (dog, cat); HemoStat Laboratories, Dixen, CA (sheep, cow, horse); Central Florida Zoo, Sanford, FL (brown lemur, howler monkey, spot-nosed guenon); Brevard Zoo, Melbourne, FL (crane, coyote, tortoise, lamb, Patagonian cavy, spider monkey, rhesus macaque, pig-tailed macaque); donation from laboratory members (coyote, deer); West End Animal Hospital, Gainesville, FL (ferret). Liquid blood samples from African green monkey, cynomolgus monkey, baboon and chimpanzee were obtained from

Bioreclamation, Inc. (Westbury, NY). For all blood samples, fifty microliter aliquots were placed on cotton cloth and dried overnight at room temperature.

Freshly ejaculated semen was provided in sealed plastic tubes and stored frozen until they were dried onto sterile cotton swabs. Saliva samples were provided in sealed plastic tubes and stored frozen until they were dried onto sterile cotton swabs. Buccal samples were collected from donors using sterile swabs by swabbing the inside of the donor's mouth. Saliva samples from two cats and two dogs were collected by swabbing the inside of the animal's mouth using sterile cotton swabs. A primate saliva sample (spot-nosed guenon) was obtained by donation from the Central Florida Zoo (Sanford, FL). Semen-free vaginal secretions and menstrual blood were collected using sterile cotton swabs.

Preparation of Bloodstains (Time Since Deposition)

Blood samples were collected by venipuncture into additive-free vacutainers and 50 µl aliquots were placed onto non-sterile cotton cloth The bloodstains were stored at various temperatures (22^{o}C, 30^{o}C, 37^{o}C) and humidity levels (50%, 75%, 80%, 85%, 90%) for varying lengths of time (15 minutes, 30 minutes, 1 hour, 3 hours, 6 hours, 12-18 hours, 24 hours, 48 hours, 1 week, 1 month, 3 months, 6 months, 1 year, and 2 years). All bloodstains were collected at the desired time intervals, placed in a sealed plastic bag and stored at -47^{o}C until needed. Experiments were conducted either in the laboratory (22^{o}C, 50% humidity) protected from light, in incubators (specified temperatures, 50%

humidity), or in a MicroClimate® Humidity Chamber MCH-3 (Cincinnati Sub-Zero, Cincinnati, OH).

Environmental Samples (Time Since Deposition)

50 µl aliquots of human blood were dried onto non-sterile cotton cloth. The samples were placed inside a glass tank to protect them from rain with a vented bottom to allow for free air-flow into the tank. The samples were placed on a roof top to allow for direct exposure to sunlight for various lengths of time including 15 minutes, 30 minutes, 1 hour, 3 hours, 6 hours, 18 hours, 24 hours, 48 hours, and 1 week. Upon collection, all samples were placed into sealed plastic bags and stored at -47^{o}C until needed.

Environmental Samples (miRNA)

50 µl aliquots of human blood, semen and saliva were dried onto cotton cloth. Vaginal secretion samples were collected using sterile cotton swabs. These samples were exposed to different environmental conditions including various temperatures and environmental influences including humidity and rain. The environmental conditions were as follows: (i) room temperature storage (22^{o}C), (ii) 37^{o}C storage, (iii) outside covered (OC) – exposed to heat, light and humidity, and (iv) outside uncovered (OUC) – exposed to heat, light, humidity and rain. Samples from all sets of conditions were collected at varying lengths of time and the following samples were used in the present

study: room temperature (1 year, 18 months-2 years), 37°C (3 months, 6 months), OC (3 days, 7 days, 1 month), and OUC (1 day, 3 days, and 7 days). Temperature ranges, humidity levels, and amount of rain were recorded for the samples placed in outside conditions.

Menstrual Cycle Samples (miRNA)

Two female individuals donated vaginal swabs over the course of a 28-day period. Females at two different life stages participated in the study, one experiencing menstruation at regular intervals and one in perimenopause. Participants were asked to collect a single semen-free vaginal swab during each day of the study, with the first day of collection starting on the first day of menstruation if applicable.

Multiple Source Samples (miRNA)

Five-donor pooled samples were used for the initial miRNA screening in forensically relevant fluids. Total RNA from each individual sample was extracted and quantitated as described above. Equal quantities of total RNA from each donor were combined in order to produce a 1ng/μl pooled sample for blood, saliva, vaginal secretions and menstrual blood, and a 5ng/ μl pooled sample for semen. A 1μl aliquot of each pooled sample was used in the reverse transcription assay.

Admixed body fluid samples (blood-semen, blood-saliva, blood-vaginal secretions, semen-saliva, semen-vaginal secretions and saliva-vaginal secretions) were created by combining two different body fluid stains or swabs (50 µl stain for blood, semen and saliva, or a single vaginal secretion swab) in the same tube. Total RNA was extracted as described above.

Tissue Samples (miRNA)

Total RNA from 20 human tissues (adipose, bladder, brain, cervix, colon, esophagus, heart, kidney, liver, lung, ovary, placenta, prostate, skeletal muscle, small intestine, spleen, testes, thymus, thyroid, and trachea) included in the FirstChoice® Human Total RNA Survey Panel was obtained from Applied Biosystems/Ambion (Austin, TX). All tissues included in the panel were 3-donor pooled samples and were certified to contain small RNAs including miRNAs and snRNAs. Total RNA from human skin was obtained from Biochain Institute, Inc (Hayward, CA).

Mock Casework Samples (miRNA)

Swabs of a beverage container lid (plastic coffee cup lid, water bottle) using a sterile cotton swab were collected after being deposited by volunteers. Saliva from a male donor was deposited onto the skin of a female donor. After the saliva was allowed to dry, the skin was swabbed using a sterile cotton swab. Portions of the outer wrapping of used

cigarette butts (collected from a male and female donor) were removed for extraction. Total RNA was extracted as described above.

An adhesive bandage that was used to cover a small cut on a donor's finger was obtained. The cotton pad in the center of the bandage had a reddish-brown appearance. The entire cotton pad was removed from the bandage for extraction. Total RNA was extracted as described above.

A post-coital sample was obtained from a female volunteer who recovered the sample 18 hours post-coitus. A swabbing of both the vaginal canal and the cervicovaginal region was collected. The volunteer was instructed to take the cervicovaginal swab by brushing the cervix multiple times for at least thirty seconds. To insure that residual semen from prior encounters were not present, a pre-coital cervicovaginal swab was also obtained before coitus commenced but after an abstinence period of seven days.

Laser Capture Micro-dissection Slide Preparation

Body fluid swabs were removed from storage at -47^{o}C and allowed to sit at room temperature for at least 15 minutes prior to preparation of the cell suspension. A 1.5mL microcentrifuge tube was filled with 1X PBS and a Spin-Ease extract basket was added. The body fluid swab was placed in the liquid within the basket and agitated in order to collect the cells. The tubes were centrifuged for 5 min at 13,000rpm in order to pellet the cells. The PBS was then removed using a plastic transfer pipet and approximately 500µl of fresh PBS was added. The cell pellet was agitated until the pellet was disrupted until

an even cell distribution was achieved. The cell suspension was then heat fixed onto a clean glass slide (for use with the Arcturus PixCell II system) or onto a proprietary membrane slide (for use with the Leica LMD system). The heat fixation involved placement of the slides onto a heat plate (low heat setting) for approximately 3-5 minutes.

Cell staining

Christmas Tree Stain (Nuclear Fast Red/Picroindigocarmine)

The nuclear fast red solution was prepared by dissolving 2.5g of aluminum sulfate in 100mL of warm water. Fifty milligrams of nuclear fast red was then added to the solution. The solution was filtered into amber bottles. The picroindigocarmine solution was prepared by dissolving 1g of indigocarmine in 300mL of picric acid. The solution was dispensed into small amber bottles. For slides prepared using the Christmas Tree stain, the entire sample area was covered with the nuclear fast red solution for 15 minutes. Excess stain was removed by gentle flooding with deionized water. The sample area was then covered with the picroindigocarmine solution for 10 seconds. Excess stain was removed by gentle flooding with room temperature absolute ethanol.

Hematoxylin and Eosin (H&E)

The components for the Harris Hematoxylin/Eosin stain were obtained from a commercial source (Sigma-Aldrich). For slides prepared using the H&E stain, the entire sample area was covered with the Harris hematoxylin solution for 1.5 minutes. Excess stain was removed by gentle flooding with deionized water. The sample area was then covered with Eosin for 30 sec. Excess stain was removed by gentle flooding with deionized water.

Leica LMD Slides

Upon completion of the staining procedures described above, slides prepared for use with the Leica LMD system were then dried at room temperature and then placed in slide storage boxes for storage at 4^{o}C.

Arcturus PixCell II Slides

The presence of moisture on slides to be used with the Arcturus PixCell II system would result in failure of the instrument to remove cells from the glass slide. Therefore additional processing of these slides was required during the staining procedures describe above in order to remove any moisture. After slide preparation but prior to staining, the specimen slide was placed in a glass jar containing approximately 25mL of 75% ethanol for 30 seconds. It was then transferred to a glass jar containing 25mL of deionized water

for 30 seconds. The procedure for staining with the Christmas Tree stain or the H&E stain was then performed as described above. The slide was then transferred to a glass jar containing 25mL of deionized water. The slide was then transferred to glass jars containing 25mL of ethanol (75%, 95%, and 100%) for 30 seconds each. The slide was then transferred to a glass jar containing 25mL of xylene for 5 minutes (performed in a fume hood). The slide was allowed to air dry at room temperature and was stored in a dessicator at room temperature. Prior to use, if the slide had acquired any moisture the dehydration steps were repeated.

Laser Capture Micro-dissection

Leica LMD System

0.2ml flat-capped PCR tubes were inserted into the four tube holder positions. Ten microliters of lysis buffer were added to the cap of each tube. The tube holder was placed in position underneath the stage. The specimen slide was placed face down in the slide holder and placed on the instrument. The specimen was brought into focus and the laser power and speed and specimen balance were adjusted. Epithelial cells were collected using a 40x objective (400x magnification) using the following laser settings: power – 33, speed – 8, specimen balance – 28. Sperm cells were collected using a 63x objective (630x magnification) using the following laser settings: power – 30, speed – 8, specimen balance – 25.

Arcturus PixCell II System

The specimen slide was placed on the microscope stage and help in position by the use of the small vacuum on the stage. The area of interest was brought into view using a joystick. The laser power and pulse duration were adjusted to ensure optimal laser settings. A CapSure® HS LCM cap (Molecular Devices, Sunnyvale, CA) was placed onto of the specimen slide. The appropriate number of cells was collected onto the cap. Once all cells were collected, the cap was lifted and placed onto a clean slide to ensure that the cells had been lifted from the specimen slide. The cap was then inverted and placed into a sample tray. An ExtracSure™ device (Molecular Devices) was placed over the cap and lysis buffer was added. A 0.5mL thin walled reaction tube was placed over the ExtracSure™ device. The entire sample tray was covered with a pre-heated heat block and the sample tray then placed in an incubator for lysis.

Extraction

DNA – Organic Extraction

DNA was extracted using a standard phenol: chloroform method [94]. Stains or swabs were cut into small pieces and placed into a Spin-Ease tube (Gibco-BRL, Grand Island NY). The tubes were incubated overnight in a 56^{o}C water bath using 400 µl DNA Extraction Buffer (100mM NaCl, 10mM Tris-HCl, pH 8.0, 25mM EDTA, 0.5% SDS),

0.1mg/mL Proteinase K, and 10% 0.39 M DTT (added to semen containing samples). After the overnight incubation, swab or stain fabric was placed into a Spin-Ease basket, the basket inserted back into the original tube, and the samples centrifuged at 14,000 rpm for 5 minutes to remove the absorbed fluid from the swab material. A volume of phenol/chloroform/isoamyl alcohol equal to the volume of the crude extract was added and vigorously intermixed by shaking. The aqueous layer, containing the DNA, was removed. Precipitation of the DNA was accomplished by the addition of cold absolute ethanol (two and a half times the volume of the aqueous layer extract) and allowed to progress overnight at –20°C. The DNA was pelleted by centrifugation, washed once using 70% ethanol and re-solubilized with 100 µl of TE^{-4} (10 mM Tris-HCl, 0.1 mM EDTA, pH 7.5) overnight at 56°C.

DNA - Direct Lysis

Direct lysis of micro-dissected cells was performed using a modified commercially available lysis buffer (Quick Extract, Epicenter). The Quick Extract lysis solution was prepared by adding 9µl of Quick Extract buffer and 1µl of 0.39M DTT (final concentration 0.039M) per sample. The DTT was made fresh daily. 10µl of lysis solution per sample was used for both the Leica and Arcturus systems. For Leica samples, the 0.2ml PCR tubes were briefly centrifuged and the lysis performed in a thermocycler. For Arcturus samples, the lysis was performed in an incubator. The Quick Extract lysis protocol is as follows: 65°C for 6 minutes, 98°C for 2 minutes.

RNA

Total RNA was extracted from blood, semen, saliva, vaginal secretions and menstrual blood with guanidine isothiocyanate-phenol:chloroform and precipitated with isopropanol [95]. Briefly, 500 µl of pre-heated (56°C for 10 minutes) denaturing solution (4M guanidine isothiocyanate, 0.02M sodium citrate, 0.5% sarkosyl, 0.1M β-mercaptoethanol) was added to a 1.5mL Safe Lock tube extraction tube (Eppendorf, Westbury, NY) containing the stain or swab. The samples were incubated at 56°C for 30 minutes. The swab or stain pieces were then placed into a DNA IQ™ spin basket (Promega, Madison, WI), re-inserted back into the original extraction tube, and centrifuged at 14,000 rpm (16,000 x g) for 5 minutes. After centrifugation, the basket with swab/stain pieces was discarded. To each extract the following was added: 50 µl 2 M sodium acetate and 600 µl acid phenol:chloroform (5:1), pH 4.5 (Applied Biosystems/Ambion). The samples were placed at 4°C for 30 minutes to separate the layers and then centrifuged for 20 minutes at 14,000 rpm (16,000 x g). The RNA-containing top aqueous layer was transferred to a new 1.5ml microcentrifuge tube, to which 2 µl of GlycoBlue™ glycogen carrier (Applied Biosystems/Ambion) and 500 µl of isopropanol were added. RNA was precipitated for 1 hour at -20°C. The extracts were then centrifuged at 14,000 rpm (16,000 x g). The supernatant was removed and the pellet was washed with 900 µl of 75% ethanol/25% DEPC-treated water. Following a centrifugation for 10 minutes at 14,000 rpm (16,000 x g), the supernatant was removed and the pellet dried using vacuum centrifugation (56°C) for 3 minutes. Twenty

microliters of pre-heated (60°C for 5 minutes) RNA*secure*™ solution (Applied Biosystems/Ambion) was added to each sample followed by an incubation at 60°C for 10 minutes. Samples were used immediately or stored at -20°C until needed.

DNase I digestion

Six units of TURBO™ DNase I (2U/µl) (Applied Biosystems/Ambion, Inc.) and 2.2 µl of Turbo DNase I Buffer (10X) were added to each RNA extract and incubated at 37°C for 1 hour. The DNase was inactivated at 75°C for 10 minutes. The samples were used immediately or stored at -20°C until needed. Alternatively, DNase digestion was performed using the Turbo DNA-*free*™ kit (Applied Biosystems/Ambion) according to the manufacturer's protocol.

Protein

Approximately half of a 60 µl bloodstain was placed in a 1.5mL microcentrifuge tube with 750 µl of 0.2M Tris-HCl, pH 8.0. The samples were allowed to extract overnight at room temperature (protected from light). After the overnight incubation, the stain pieces were placed in a spin basket and the samples were centrifuged at 14,000 rpm (16,000 x g) for 3 minutes. The stain pieces and basket were then discarded. All extracts were stored at -20°C until needed.

Quantitation

DNA

DNA extracts and whole genome amplification products were quantitated with the Quantifiler® Human or Quantifiler® Y Human Male Real-Time PCR Quantitation Kits (Applied Biosystems, Foster City, CA) according to manufacturer's recommended conditions.

RNA

RNA extracts were quantitated with Quant-iT™ RiboGreen® RNA Kit (Invitrogen, Carlsbad, CA) as previously described [8]. Fluorescence was determined using a Synergy™ 2 Multi-Mode microplate reader (BioTek Instruments, Inc., Winooski, VT).

Protein

All bloodstain extracts were quantitated using the Quant-It™ Protein Assay Kit according to manufacturer's recommended conditions. The quantitation was performed using a Synergy 2 Microplate Reader (BioTek, Winooski, VT). All samples were run in duplicate and an average of the two measurements obtained.

cDNA Synthesis

For the reverse transcriptase (RT) reaction, the miScript Reverse Transcription Kit (Qiagen, Valencia, CA) was used according to manufacturer's protocols. One nanogram of total RNA from blood, semen, vaginal secretions and menstrual blood extracts and 5 ng of total RNA from semen extracts were used in the RT reactions. A reverse transcription negative reaction (containing total RNA and reaction buffer but no reverse transcriptase enzyme mix) was performed for each sample.

Polymerase chain reaction

Autosomal STR Amplification

DNA extracts were amplified with commercially available STR amplification kits including AmpFlSTR® Profiler Plus®, COFiler®, Minifiler™ and Identifiler® (Applied Biosystems). Amplifications were either performed using standard conditions according to manufacturer's instructions (with the exception of Profiler Plus® and COFiler® where a decreased reaction volume to 25 μl and 2X Taq Gold polymerase was used) or using increased cycle number (from 28 cycles to 32 or 36) and an alternative polymerase (Expand High Fidelity Polymerase, Roche Applied Science, Indianapolis, IN).

Y Chromosome STR Amplification

DNA Extracts were amplified with a commercially available Y-STR amplification kit (Yfiler® PCR Amplification kit, Applied Biosystems) or using multiplex systems developed in our laboratory as previously described [96-100].

Whole Genome Amplification

The modified improved primer extension pre-amplification method was used to pre-amplify DNA extracts and cell lysates as previously described [90].

Post-PCR Purification

Purification using the Qiagen MinElute columns was performed according to manufacturer's instructions. Ten microliters of product was eluted from the columns and the entire 10 µl was used for capillary electrophoresis.

Capillary Electrophoresis

PCR products were detected using the ABI Prism 310 capillary electrophoresis system. A 1.75 µl aliquot of each amplified sample was added to 24 µl Hi-Di™ formamide (Applied Biosystems) and 1 µl of GeneScan™ 500 ROX™ or 500 GeneScan™ 500 LIZ™ internal lane standard (Applied Biosystems). Tubes were heated

at 95°C for 3 min and snap cooled on ice for 2 min. Samples were injected through the capillary using the module GS STR POP4 (1ml)F (5s injection, 15 kV, 60°C, run time 28 min, filter set F) or module GS STR POP4 (1ml)G5 (5s injection, 15 kV, 60°C, run time 28 min, filter set G5). An allelic ladder for each amplification kit was run with the samples to allow for genotyping. Samples were subject to laser induced fluorescence, and analyzed with GeneScan 3.1.2 Software.

Alternatively, PCR products were detected using the ABI Prism 3130 capillary electrophoresis system. A 0.75 µl aliquot of each amplified sample was added to 9.7 µl Hi-Di™ formamide (Applied Biosystems) and 0.3 µl of GeneScan™ 500 ROX™ or GeneScan™ 500 LIZ™ internal lane standard (Applied Biosystems). The 96-well plates were heated at 95°C for 3 min and snap cooled on ice for 2 min. Samples were injected through the capillary using the FragmentAnalysis36_POP7_1 module (16s injection, 15 kV, 60°C, run time 20 min, filter set G5 or F). An allelic ladder for each amplification kit was run with the samples to allow for genotyping. Samples were subject to laser induced fluorescence, and analyzed with GeneMapper 3.2 Software.

Real-Time (Quantitative) Polymerase Chain Reaction

Real-time PCR was performed using the Relative Quantitation protocol on an ABI Prism 7000 Sequence Detection System (Applied Biosystems). One microliter of the 1 ng RT-reaction (blood, saliva, vaginal secretions, menstrual blood) and two microliters of the 5 ng RT-reaction (semen) were amplified using the miScript SYBR® Green PCR

kit and a 10x miScript primer assay (Human miScript Primer Assay Set v1.0, Qiagen) according to manufacturer's protocols, with minor modifications. A reduced reaction volume of 25 µl was used as well as an increased number of amplification cycles (from 35-40 to 50 cycles). Additional snRNA (U6b) and snoRNA (U26, U27, U28, U29, U30, U31, U38B, U43, U44, U48 and U90) primer assays for normalization studies were obtained from Qiagen.

UV-Visible Spectroscopy

Microplate Reader

UV-Visible spectral profiles were obtained using a Synergy 2 Microplate Reader. Spectral data was collected from 200-700nm in 1nm increments. Samples were run in a clear, flat-bottomed 96-well reaction plate using 7.5 µg of total protein and brought to a final reaction volume of 75 µl per well using 0.2M Tris-HCl, pH 8.0. All spectral data was blank corrected using 75 µl of 0.2M Tris-HCl. All data was run in triplicate and an average of the data was used in subsequent analysis.

Standard Bench-Top Spectrophotometer

UV-Visible spectral profiles were also obtained using a U-0080D Photodiode Array Spectrophotometer (Hitachi, Pleasanton, CA). Spectral data was collected from

200-700nm in 1 nm increments using a 5 μl cell (7.5 μg total protein used for analysis). All spectral data was blank corrected using 5 μl of 0.2M Tris-HCl. All data was run in triplicate and an average of the data was used in subsequent analysis.

Portable "Point-of-Use" Spectrophotometer

UV-Visible spectral profiles were also obtained using the portable NanoPhotomer™ (Implen, Inc., c/o LABREPCO, Horsman, PA). Spectral data was collected from 350-600nm in 1 nm increments. A 1μl aliquot of the bloodstain extracts was added directly to the spectrophotometer for analysis. All data was run in triplicate and an average of the data was used in subsequent analysis.

Enzyme Activity Assays (MTT-PMS colorimetric assays)

All assays were run on the Synergy 2 Microplate Reader using a kinetic absorbance program: 3 minutes hold, absorbance read: 565mm for 30 minutes in 1 minute intervals. Each reaction was run in duplicate and the average maximum velocity of each reaction was obtained. Two negative controls, including a no-substrate control and a no-NAD/NADP control, were run with each assay in order to ensure that the measured activity was resulting from the enzyme itself and not other non-specific interaction between reaction components. All enzyme assays were performed in 200 μl reactions using 3 μg of total protein, 7 mM MTT and 26 mM PMS. The reaction mixtures

for each enzyme assay were prepared as follows: *Lactate dehydrogenase* – 16 mM calcium lactate, 15 mM NAD in 0.05M Tris-HCl; *Malate dehydrogenase* – 100 mM L-malic acid, 15 mM NAD in 0.1M Tris-HCl; *Alcohol dehydrogenase* – 60% Absolute ethanol, 15 mM NAD in 0.05M Tris-HCl; *Glycerate dehydrogenase* – 160 mM DL-Glyceric acid hemicalcium salt hydrate, 15 mM NAD in 0.1M Tris-HCl; *3-hydroxybutyrate dehydrogenase* – 150 mM (±) Sodium 3-hydroxybutyrate, 50 mM $MgCl_2$, 300 mM NaCl in 0.1M Tris-HCl; *Glucose-6-phosphate dehydrogenase* – 16 mM D-Glucose 6-phosphate disodium salt hydrate , 25 mM $MgCl_2$, 4 mM NADP in 0.2M Tris-HCl; *Phosphogluconate dehydrogenase* – 24 mM 6-Phosphogluconic acid trisodium salt, 30 mM $MgCl_2$, 4 mM NADP in 0.5M Tris-HCl; *Isocitrate dehydrogenase* – 38 mM DL-Isocitric acid trisodium salt, 30 mM $MgCl_2$, 4 mM NADP in 0.5M Tris-HCl; *Phosphoglucomutase* – 30 mM glucose-1-phosphate dipotassium salt hydrate, 2U glucose-6-phosphate dehydrogenase, 30 mM $MgCl_2$, 4 mM NADP in 0.05M Tris-HCl; *Gluconate dehydrogenase* – 15 mM 6-phosphogluconic acid, 30 mM $MgCl_2$, 4 mM NADP in 0.2M Tris-HCl; *L-xyulose reductase* – 33 mM xylitol, 4 mM NADP in 0.5M Tris-HCl. All reagents used in the enzyme assays were obtained from Sigma-Aldrich (St. Louis, MO), except for NADP which was obtained from USB Corporation (Cleveland, OH).

CHAPTER THREE: RESULTS – TIME SINCE DEPOSITION

Spectral Analysis of Hemoglobin

Initial work to determine the time since deposition of forensic biological stains involved an examination of dried bloodstains. The ultra-violet-visible (UV-VIS) spectrum of hemoglobin was examined for any possible changes that could serve as "molecular estimators" of the time since deposition. A characteristic spectral profile for hemoglobin can be seen in Figure 1. A strong absorption peak, known as the Soret band, can be observed at approximately 414 nm. Additionally, smaller absorption peaks occurring at approximately 576 and 541 nm, known as the α and β peaks respectively, can also be observed. It is the presence of these peaks that provide an indication of the presence of blood. These peaks, as well as those found in the UV region of the hemoglobin spectrum were examined for possible changes as the age of the bloodstain increased.

Initial studies performed to examine changes in the spectral profiles of hemoglobin involved a small number of room temperature bloodstains of different ages (15 minutes, 6 hours, 24 hours, 1 month, 3 months, 6 months and 1 year). These samples were selected since there was a significant difference in their age and would hopefully provide an indication of whether visible differences between bloodstains could be observed. Spectral profiles from 200-450nm and 500-600nm were obtained because they contained the characteristic hemoglobin absorption peaks and it was thought these areas might be of

interest. An examination of the UV region (200-400 nm) of the hemoglobin spectral profile did not result in the identification of any significant peaks of interest (Figure 2A). However, several observations were made regarding the Soret band at ~414 nm (Figure 2A). A decrease in the Soret band absorption maximum was observed as the age of the stain increases, as well as a possible shift in the wavelength where this band occurs (Figure 2A). An examination of the remaining portion of the visible hemoglobin spectrum, from 500-600nm including the characteristic β_{541nm} and α_{576nm} absorption peaks, was also observed in these samples (Figure 2B). As can be seen from these spectral profiles, deterioration of the α_{576nm} and β_{541nm} peaks can be observed in stains as early as 1 month of age, with a progressive decline of these peaks as the age of the stain increases. The peaks are completely unidentifiable in stains one year in age (Figure 2B). Additionally, it was thought that the rate of decline of the α_{576nm} and β_{541nm} peaks may not occur at the same rate. The absorbance values for the α_{576nm} and β_{541nm} peaks appear to be similar for the 15 minutes and 6 hour samples. However, a slight difference in the absorbance maxima can be seen starting with the 24 hour sample. It was therefore thought that a ratio of the α_{576nm} and β_{541nm} peak absorbance values may also demonstrate a correlation with the time since deposition.

As a result of these initial findings, a set of spectral shift parameters were developed in order to further examine possible correlations with the time since deposition (Figure 3). Five spectral parameters were identified and included: 1) change in the maximum absorbance of the Soret band (ΔAbs_{Soret}); 2) change in the wavelength of the λmax for the Soret band ($\Delta\lambda_{Soret}$); 3) change in the absorbance of the β_{541nm} band relative to the

minimum at 560nm ($\Delta Abs_{\beta(541-560)}$); 4) change in the absorbance of the α_{576nm} band relative to the minimum at 560nm ($\Delta Abs_{\alpha(576-560)}$); 5) the ratio of absorbance change of the α_{576nm} and β_{541nm} bands ($\Delta Abs_{\beta(541-560)}/ \Delta Abs_{\alpha(576-560)}$).

Initially, an examination of the parameters involving changes in absorbance values for the Soret band and the α_{576nm} and β_{541nm} bands was performed. Previous attempts in classic literature to determine the time since deposition using spectroscopic methods typically involved changes to the α_{576nm} and β_{542nm} bands. However, in our experiments parameters 1, 3, 4 and 5 (ΔAbs_{Soret}, $\Delta Abs_{\beta(541-560)}$, $\Delta Abs_{\alpha(576-560)}$, $\Delta Abs_{\beta(541-560)}/ \Delta Abs_{\alpha(576-560)}$) did not provide a reliable correlation with the age of the stain. Figure 4 depicts the relationship obtained between the age of the stain and the change in absorbance of the $\beta_{(541-560nm)}$ band. As can be seen from this data, month differences in stain age were required before a possible correlation could be developed. The resulting r^2 values were also $\leq$ 0.78 with a large standard error for several samples. There was also a large separation between the two individuals within each storage condition. Similar results were also obtained with the $\alpha_{(576-560nm)}$ peak was examined (Figure 5). The r^2 values were higher (> 0.80) than those obtained for the $\beta_{(541-560nm)}$ band. However, month differences in stain age were still required. This resolution would not be sufficient for use in forensic casework.

Previous studies had demonstrated a difference in the morphology of the α_{576nm} and β_{541nm} bands as the age of the stain increased. Therefore, the final parameter utilizing a change in absorbance that was examined was an evaluation of the ratio of the ΔAbs of the α_{576nm} and β_{541nm} bands (Figure 6). When a ratio of the two ΔAbs values was used, a

stronger correlation with the age of the stain was observed ($r^2 > 0.94$, except for one data set whose $r^2 = 0.87$). However, month differences in stain age were still required and there was still a significant variation between the two sample sets stored at 37°C (Figure 6).

As a result of the poor resolution of the spectral parameters involving absorbance changes in the three characteristic hemoglobin bands (Soret, α_{576nm}, β_{541nm}), attempts were made to further examine the possible λSoret shift that was observed during initial testing. This parameter was of particular interest since, to the best of our knowledge, it had not been reported in any previously published studies. The λSoret was graphed as a function of stain age for bloodstains that had been stored at room temperature (22°C) and 37°C samples for 15 minutes to 1 year (Figure 7A). From this data, a strong correlation between the age of the stain and the ΔλSoret was observed ($r^2 = 0.96$ and 0.84 for the 22°C and 37°C samples, respectively). A larger and more pronounced decrease in the λSoret was observed for the samples stored at 37°C indicating a possible effect of temperature on the shift. With the range of samples examined, it was difficult to see the relationship in the early time points. In order to further examine the early time points, only the 15 minutes to 2 days samples were plotted (Figure 7B). When this smaller set of samples was examined, a strong correlation between the wavelength shift and the age of the stain was demonstrated (r^2 values of 0.95 and 0.98 for 22°C and 37°C samples, respectively). As a result of the significant correlation observed in the minutes to year and minutes to day intervals, additional time intervals were examined to determine if this method could be utilized to distinguish samples minutes, hours, days, weeks and months

different in age. The r^2 values for each of the time intervals (15 min - 2 days, 15 min - 1 week, 15 min – 1 month, and 15 min – 1 year) for both bloodstains stored at both 22°C and 37°C are provided in Table 1. The r^2 value for each time interval for both temperatures (except for the 15 min – 1 year interval for the 37°C samples) was $\geq$ 0.95. The slightly lower r^2 value for the 15 min – 1 year 37°C sample set could be a result of exposure to such a high temperature (~98°F) for a long period of time. It is unlikely, except for in extreme cases, that bloodstains would be exposed to this level of constant temperature. However, it does indicate that TSD estimates may be more accurate for younger stains at extreme temperatures. Overall, this data demonstrated the potential to distinguish bloodstains differing in age by minutes, hours, days, weeks and months.

Instrumentation

All previous data had been obtained using the BioTek Synergy 2 microplate reader. Before any further work was conducted, an evaluation of the same sets of bloodstains was performed using the bench-top Hitachi U-0080D Spectrophotometer. This was performed in order to ensure that the Soret band shift would still be observed on a different instrument and that it was not the result of the microplate reader itself. Table 2 provides a comparison of the λSoret obtained for bloodstains stored at 22°C for 15 minutes – 1 year using both the microplate reader and the bench-top spectrophotometer (Hitachi U-0080D). As can be seen from this data, the same hypsochromic shift in the λSoret was observed using both instruments. There were differences in the obtained

wavelength values between the two spectrophotometers, with the values for the bench-top spectrophotometer typically 0.7-1.7 nm higher (average = 1.1nm) than what was observed for the microplate reader (Table 2). The total wavelength shift between the 15 minute and 1 year samples was generally the same between the two instruments for both data sets (Table 2). The 22^{o}C data set when run on the bench-top spectrophotometer had a slightly larger overall shift, 7.7nm, compared to the 5nm overall shift that was observed when the same samples were run on the microplate reader (Table 2). However, the 1 year data point on the spectrophotometer had a larger standard error and therefore likely caused the larger shift that what was observed on the microplate reader.

When the $\Delta\lambda$Soret was plotted against the age of the stain, the r^2 for the 22^{o}C data sets (15 minutes to 2 days) on both instruments was greater than 0.91 (Figure 8). The same trend was observed in the data from both instruments, with the wavelengths from the spectrophotometer slightly higher than the microplate reader which was indicated in Table 2. From this data it was evident that the observed shift is a genuine occurrence in aged stains and can be observed on different types of spectrophotometers. The data also indicated a need to calibrate any spectrophotometer that would be used for TSD measurements using this method. A series of standards would need to be run prior to any unknown samples. Table 3 provides a summary of the r^2 values obtained on both instruments for the 22^{o}C and 37^{o}C using both a 15 minute – 2 day and a 15 minute – 1 year data set. For all data sets, the r^2 values from the microplate reader were slightly higher than those obtained from the spectrophotometer, although all r^2 values were

acceptable. As observed with previous data, the r^2 value for the extended range (15 minutes – 1 year) 37°C sample set was < 0.9 using both instruments.

The results of these experiments demonstrate the reproducibility of the ΔλSoret measurements was using different spectrophotometers. The microplate reader does offer the advantage of being able to run replicates of the same sample at the same time, as well as the ability to run more samples at one time (96-well plate vs. a single cuvette with the spectrophotometer). It also allows for the use of a disposable 96-well plate whereas a standard bench-top spectrophotometer would require the re-use of a cuvette which would need to be cleaned in between samples.

Environmental Influences

Humidity

Initial experiments demonstrated that temperature may have an effect on the rate of or extent of the Soret band shift. Therefore the affects of temperature and humidity on the ΔλSoret were further examined. All sample sets used previously had been stored at room temperature (22°C) or in a 37°C incubator. The average humidity and temperature for the laboratory (measurements taken in the mornings) were approximately 22°C and 50% humidity. However, small changes throughout the day may have occurred. In order to more accurately control the temperature and humidity to which the samples were exposed, a Cincinnati Sub-Zero MicroClimate® Humidity Chamber MCH-3 was used

(Figure 9). This chamber allowed for a range of temperatures from -65^{o}C to 190^{o}C and a range of humidity from 10% to 95% to be used. The chamber is digitally controlled and monitored. Samples were placed inside the chamber and were thus exposed to constant temperatures and humidity levels.

Prior to performing the experiments, national temperature and humidity level averages were examined in order to determine if ranges could be selected that would be appropriate for most regions of the country (Figure 10). Most of the country experiences humidity levels between 56% and 85% for most of the year with western states experiencing lower humidity levels (35-50%) for most of the year (Figure 10A). Therefore some states, such as Arizona or New Mexico, humidity levels above 60% might not be that relevant. Additionally, humidity levels below 65% might not be that relevant for states such as Florida which maintains humidity levels of 65% or higher through the year. There appeared to be distinctive regions of average daily temperatures throughout the country as well, with large variation within specific months through the year (Figure 10B). This data indicated that different regions of the country will be affected by differing humidity and temperatures and might therefore need to conduct simple experiments using temperatures and humidity levels relevant to their particular region and relevant to different times of the year in order to establish reference data for their geographical region. As a result of this data, a range of humidity levels from 50-90% (50, 75, 80, 85 and 90%) were selected for use with two different temperatures, 22^{o}C and 30^{o}C.

The affects of humidity on the ΔλSoret measurements for bloodstains stored at 22°C can be seen in Figure 11A. As the humidity level increases, the hypsochromic shift is reduced (lower r^2 value) and is essentially not observed with 90% humidity (Figure 11A). As a result of the differences observed between different humidity levels, in order to determine the age of an unknown stain the storage conditions to which the sample was exposed would need to be known (or estimated.) The affects of 50, 75, 80 and 85% humidity on samples stored at 30°C can be seen in Figure 11B. Again, as the humidity level increases, the hypsochromic shift is reduced (lower r^2 value).

It is evident from the graphs provided in Figure 11 that the affects of humidity are different depending on what temperature the sample is exposed to. For example, for bloodstains stored at 22°C, there is a progressive reduction in the hypsochromic shift as the humidity level increases (Figure 11). It was expected that the same trend would be observed for the bloodstains stored at 37°C. However, it can be seen that the extent of the hypsochromic shift with 50% and 75% humidity is quite similar (Figure 11). Therefore it is possible that at higher temperatures the affect of humidity is lessened and a higher humidity level is needed to cause a reduction in the hypsochromic shift.

Temperature

The previous experiments had examined the affects of different humidity levels at a constant temperature. An indication of the additional affect of temperature was also obtained. Therefore to further examine the affects of temperature, samples were placed at

a constant humidity (50%) at various temperatures, including -20°C, 4°C, 22°C (one set at room temperature lab storage and one set stored in the humidity chamber), 30°C and 37°C. The λSoret was plotted for each temperature as a function of stain age (Figure 12). The hypsochromic shift was more significant and occurred at a faster rate with increased temperature (Figure 12). This data again indicated the need to have some knowledge or reasonable estimate of the environmental conditions that any unknown bloodstain sample was subjected to prior to collection and analysis.

Of additional interest was the -20°C sample set. As can be seen from Figure 12, almost no change in the λSoret was observed. This data suggested that bloodstains removed from a crime scene and brought back to the laboratory for future analysis could be stored at -20°C without any further change to the λSoret. In order to further demonstrate the ability to store bloodstains at -20oC without affecting ΔλSoret measurements, three data sets were prepared: 1) samples extracted immediately upon collection, 2) samples collected and stored at -20°C for two to three weeks, and 3) "original" storage consisting of a mixture of samples stored at -47°C (15 minutes through 24 hours) prior to analysis and samples tested immediately (2 days, 1 week). The results of the various storage conditions can be seen in Figure 13. Similar ΔλSoret plots were obtained for bloodstains stored at each of the conditions described above. Therefore, it would be possible for bloodstains to be collected at a crime scene and stored frozen (-20°C) until ready for analysis without any significant alteration of the ΔλSoret values. This would be of vital importance to crime laboratories where evidence is often not examined immediately upon arrival at the laboratory.

Outside Storage

The previous experiments examined the affects of storage at constant temperatures and humidity levels. However, many criminal offenses will not occur indoors in a controlled environment with relatively stable temperatures and humidity levels. Often crime scenes are located outside with samples exposed to fluctuating temperatures and humidity levels, sunlight, moisture, bacterial growth, and possible smog or other air pollutants. Therefore, it was necessary to examine bloodstains that were stored outside. Bloodstains were placed outside and covered (OSC), exposed to direct sunlight but protected from rain and collected at various times through a one week period (15 minutes, 30 minutes, 1 hour, 3 hours, 6 hours, 18 hours, 24 hours, 48 hours and 1 week). During this week period the samples were exposed to a reported average temperature of 27.1^{o}C (low – 22.7^{o}C, high – 35.7^{o}C) and an average humidity of 81.1% (low - 46%, high – 97.9%). Previous experiments had involved samples stored at 22^{o}C, 30^{o}C and 37^{o}C. It was therefore assumed that the graph of the $\Delta\lambda$Soret for the OSC samples would be observed in between the graphs for the 22^{o}C and 37^{o}C samples.

The $\Delta\lambda$Soret of the OSC samples was graphed along with the 22^{o}C data sets (50%, 75%, 80%, 85%, 90% humidity). As anticipated, the hypsochromic shift for the OSC sample set was greater and occurred at a faster rate compared to all of the 22^{o}C data sets (Figure 14A). Even though the average temperature that the OSC samples were exposed to was 27.1^{o}C, it was thought that the $\Delta\lambda$Soret could still be slightly greater than that of the 30^{o}C sample set as a result of the exposure of the OSC samples to an average

high of 35.7°C. As can be seen in Figure 14B, the ΔλSoret for the OSC samples was greater than the 30°C sample sets (50%, 75%, 80% and 85% humidity). Additionally, the ΔλSoret for the OSC samples was also greater than that of the 37°C data set (Figure 15). While the average high temperature for the OSC data set was 35.7°C, there were three days where the recorded high temperature was greater than 37°C (38.1°C – 39.4°C) which could have accelerated the ΔλSoret in the OSC samples. Additionally, since the bloodstains were exposed to direct sunlight at various times during the day, it is possible that they experienced temperature much higher than the reported temperatures which are often recorded in shaded areas. Without a direct and continuous measurement of the actual temperature, the reported average temperature and humidity levels can only be used as a crude approximation of the actual temperatures. It is also possible that sunlight or smog and other air pollutants could also contribute to an increase in the ΔλSoret of samples exposed to outside environmental conditions. Additional work will need to be conducted to further examine the environmental influences affecting the ΔλSoret for samples stored outside as it appears that environmental conditions could significantly confound TSD determinations.

Non-Probative Samples – Car Trunk

In an attempt to further examine the affects of heat and humidity using samples more akin to casework samples, bloodstains were stored inside the trunk of a car for various lengths of time ranging from 25 minutes to 1 week, including 25 minutes, 1 hour,

3 hours, 18 hours, 24 hours, 48 hours, 5 days (112 hours), and 1 week (Figure 16A). A small digital thermometer with humidity gauge was placed inside the car trunk to allow for continuous monitoring of temperature and humidity. During the week period, the bloodstains were exposed to an average temperature of 44.2^{o}C (high – 44.6^{o}C, low – 43.4^{o}C) and an average humidity of 49% (high – 60%, low – 40%). Due to the extreme temperature, a more significant hypsochromic shift compared to previous data sets was expected. The $\Delta\lambda$Soret was determined in comparison to the OSC samples and the 37^{o}C samples since the highest temperatures were observed with these sample sets (Figure 16B). As can be seen from Figure 16B, the car trunk data was located in between the OSC and 37^{o}C sample exhibiting a greater than 7 nm hypsochromic shift. It is also evident from this data that the OSC samples, as previously discussed, likely experienced temperatures much higher than the reported daily temperatures. From the data shown in Figure 16B, it is predicted that the OSC bloodstains would have experienced temperatures greater than 44^{o}C (112^{o}F) as evidenced by the greater hypsochromic shift.

Molecular Basis for the Hypsochromic shift

Before further experiments were conducted, a molecular basis for the hypsochromic shift needed to be developed that could explain the observed affects of humidity and temperature. The precise mechanism for the observed shift is unknown but a possible mechanism can be posited. As the age of the stain increases, protein conformational changes (loss of secondary structure, disruption of hydrogen bonding,

etc) may occur. The previously protected heme cavity may become more exposed as a result of these structural changes. Water, if allowed entry into the cavity, will successfully compete with the His residue (from Hb) coordinated to Fe(II) in the 6^{th} hexa-coordinate position. The presence of the more electronegative oxygen will then cause the Fe(II) electrons to change from a low spin (paired) state to a high spin (unpaired) state. This causes Fe(II) to be more susceptible to oxidation. Over time, Fe(II) would then be oxidized to Fe(III). As a result of this oxidation, the electron configuration for the Fe molecule will therefore be altered and can interact with the π bonds of the porphyrin ring structure of hemoglobin. This interaction may cause an increase in energy of π to π^* transitions thereby resulting in absorbance at a shorter wavelength or a hypsochromic shift.

It is more difficult to explain the effects of temperature and humidity on the extent of the hypsochromic shift. With regard to temperature it's well characterized effect on chemical reaction rates (such as the oxidation of Fe(II) $\rightarrow$ Fe (III)) may explain a greater shift with increasing temperature. With humidity, one might have expected that the higher humidity would result in more retained water and the bigger the hypsochromic shift. However the converse is found in that higher humidity results in less of a hypsochromic shift. Perhaps the more water retained with higher humidity leads to the dehydrated protein regaining more of its native structure with a concomitant reduction in the hypsochromic shift.

Validation

Sensitivity

All previous data that had been collected involved the use of 7.5 μg of total protein into a 75 μl reaction in an individual well in a 96-well plate. A range of input volumes was tested in order to determine if the Soret band shift could still be observed with smaller amount of input total protein. Hemoglobin spectral profiles from 1.1 – 8.8 μg of total protein are shown in Figure 17. It can be seen from these profiles that 2.2 μg of total protein is needed to obtain the characteristic α_{576nm} and β_{541nm} bands needed for the identification of the stain as blood. As little as 1.1 μg (0.5 μl) is needed to analyze the hypsochromic shift to determine the age of the stain (Figure 18). However, the sensitivity of this assay was determined to be 2.2 μg of total protein since that amount was needed for a complete hemoglobin spectral profile to be obtained. While this is not an optimal input level, it is still sufficient to allow for a determination of the time since deposition.

The samples used in the previous experiment were simply smaller aliquots of a standard bloodstain extract. In order to further test the sensitivity of the developed method, bloodstains were prepared using a smaller initial volume of blood. Bloodstains ranging in size from 10 μl down to as small as 0.2 μl were prepared (Figure 19). For the sensitivity testing, the 0.2 – 1 μl bloodstains were extracted in only 25 μl of 0.2M Tris-HCl buffer (as compared to the standard 75 μl). Initially a range of input volumes, from 10 to 120 nanoliters (0.25 – 3 μl of the 25 μl extract), from a 1 μl bloodstain extract were

tested. The spectral profiles obtained using these input volumes are shown in Figure 20, with the Soret band shown in greater detail in Figure 20B. While the Soret band is visible using as little as 20 nanoliters, in order to obtain a spectral profile including the α_{576nm} and β_{541nm} bands, 40 nanoliters (1 μl of the 25 μl extract) was required (Figure 20).

Since as little as 40 nanoliters was required to obtain spectral profiles of sufficient quality for analysis, attempts were made to obtain similar spectral profiles using bloodstains smaller than 1 μl. It was expected that the smaller bloodstains would result in a lower hemoglobin concentration in the resulting extract and therefore increased nanoliter volumes were tested. As can be seen from Figure 21, analysis of up to 300 nanoliters of blood from a 0.5 μl stain did not result in suitable spectral profiles including unclear α_{576nm} and β_{541nm} bands (Figure 21A) and a broad Soret band (Figure 21B). Similar results were observed with 0.75 μl even with increased nanoliter input (up to 450 nanoliters) (Figure 21C and 21D). The inaccuracy of the ΔλSoret measurements using the 0.5 and 0.75 μl bloodstains is demonstrated in Figure 22. The broadness of the Soret band resulting from the low hemoglobin concentration of the extracts, the λSoret measurements are significantly different from that obtained using the standard stain size (~60 μl). Therefore the sensitivity of the ΔλSoret assay was demonstrated, allowing for the analysis of bloodstains as small as 1 μl in size using as little as 40 nanoliters of extract.

Bloodstain Size

While it was necessary to demonstrate the ability to obtain accurate and reliable ΔλSoret measurements from small bloodstains needed, it was equally as important to demonstrate that ΔλSoret measurements would not be affected by significant larger bloodstains. Large bloodstains or pools of blood can frequently be encountered at crime scenes. The outer regions of the bloodstain may dry quicker than the center of the bloodstain which contains a greater amount of blood. Therefore it is possible that different oxidation rates could be occurring within the same larger bloodstain. Therefore, the ΔλSoret was determined for the 60 μl bloodstains and compared to that of 600 μl bloodstains. As can be seen from Figure 23, the large 600 μl bloodstain had a lighter colored outer portion with a denser center portion. Samplings from the outer and central portions of the 600 μl bloodstain were collected and the ΔλSoret determined for each. As can be seen from Figure 24, the size of the bloodstain or the location of the sampling did not affect the ΔλSoret allowing crime scene analysts to collect samplings from various regions of suspected bloodstains.

Portable "Point-Of-Use" Spectrophotometer

The ability to obtain ΔλSoret measurements and characteristic blood spectral peaks from bloodstains as small as 1 μl was previously demonstrated. However, for the ΔλSoret assay to be of greater use in forensic casework, the ability to perform such measurements

directly at crime scenes could be useful. This would allow investigators to identify if a stain was blood and possibly how old the stain was prior to packaging samples to submit to the crime laboratory for further analysis. In order to do this, a portable spectrophotometer would have to be available at the crime scene. Recently, a portable spectrophotometer has become commercially available from Implen called the NanoPhotometer^{TM}. The instrument has no moving parts making it more durable during transport to a crime scene and weighs less than 10 lbs. Concentration measurements (protein, DNA, RNA), full wavelength scans (190-1100nm), standard curves, ratio calculations and kinetic measurements can be performed on the instrument with as little as 0.7 μl of sample. The cuvette is inserted into the holder and the sample is then placed on the top of the cuvette. The mirrored lid is then placed on top of the cuvette and the measurement can be taken. Once a measurement is made, the sample can be collected from the top of the cuvette and the area cleaned between measurements. The wavelength data obtained from the instrument is provided in 1 nm intervals, which is the same resolution that is provided by the microplate reader used in all previous studies. When a sample measurement is taken, the data can be printed directly from a built in printer or can be connected to a computer through a USB or Bluetooth wireless connection. If the data is printed from the built-in printer, a small receipt-like print out is obtained. The print out contains the date and time the measurement was made, the serial number of the instrument is was collected on, and provides a full spectral profile including the wavelength and absorbance of recorded peak maxima. If the data is sent to a computer, the same data is provided in a report generated in the software that accompanies the

instrument. Additionally, the data can be sent directly into an Excel file which creates its own graph of the data which can then be modified.

Initial work was performed with the NanoPhotometer^{TM} to determine if it would be possible to obtain reliable ΔλSoret measurements. Bloodstains stored at 22^{o}C and 50% humidity from 15 minutes to 1 week were analyzed using the NanoPhotometer and then compared to the original data obtained using the microplate reader. The results of this comparison can be seen in Figure 25. The r^2 value for the data set on both instruments was above 0.9, however was slightly lower for the NanoPhotometer (0.9089) compared to the microplate reader (0.9861). As was seen with the standard bench-top spectrophotometer, the wavelength for the whole data set using the NanoPhotometer was slightly higher then what was observed with the microplate reader. Again, this simply indicated the need to calibrate any instrument before measurements with unknown samples could be made.

Despite the slight differences observed in the r^2 values obtained from data collected using the NanoPhotometer^{TM}, the initial data indicated the potential utility of this instrument (or one like it) for use at crime scenes. Further validation of this instrument may also help improve the results. An optimization of the sample volume and concentration would need to be performed in order to determine the proper amount of sample to use for analysis.

Enzyme Activity Assays

As an alternative approach to the determination of the time since deposition of dried bloodstains, the stability of enzyme activity in aged bloodstains was examined. It was expected that a decline of enzyme activity as the age of a stain increases would be observed and could possibly be used to estimate the age of the stain. The microplate reader used in the ΔλSoret assay was used to perform enzyme kinetic assays with a determination of the maximum velocity of each reaction.

Numerous candidate enzymes were selected for initial screening (Table 5). These candidates were selected from the classical serological and human biochemical genetics literature where they were typically analyzed by gel electrophoresis. There are several detection methods available for use with these candidates. Initially, both fluorescence and colorimetric detection methods were evaluated. Many of the candidates utilized a NAD or NADP fluorescence detection scheme, which could also be coupled to a MTT colorimetric detection scheme. Several 4-methlyumbellifry-labeled assays were also evaluated which result in the production of a fluorescent product without the use of NAD or NADP. Additionally, there were also numerous enzyme candidates that use a direct MTT, NBT, or other colorimetric detection scheme.

To initially evaluate the reaction to determine if the reaction was working, 100µl of this extract was tested with the reaction mixture. A 'no sample' blank was also run to ensure that any reaction obtained was due to the enzyme itself and not enzyme-independent substrate conversion. If enzyme activity was detected, the sample input was

varied from 5-100µl (5, 10, 20, 40, 60, 80, and 100µl). The linearity of sample input versus MaxV (as determined by the instrument software) for fluorescence-based assays and colorimetric-based assays was evaluated. Adjustments to sample and reagent concentrations were made to develop an optimized reaction.

Numerous candidate enzymes were rejected for a variety of reasons (inefficiency of assay to detect enzymes, lack of solubility/compatibility of reagents with recommended buffers). It was determined that the colorimetric assays (detection at 565nm, for MTT-formazan reactions) provided the most reliable results and were therefore used to examine potential activity differences between bloodstains of different ages. Two sets of room temperature bloodstains, ranging in age from 1 month to 1 year (1 month, 3 months, 6 months and 1 year) were tested using each assay. For each assay, two different samples for every time point were tested, and each sample was run in triplicate. The triplicate data for each sample was averaged, and then the average for the two samples was averaged as well to given an overall MaxV for each time point. The average MaxV was then plotted against the age of the stain in order to determine if any trends could be identified (Figure 26). A decrease in enzyme activity as the age of the stain increases was observed for size enzymes, including lactate dehydrogenase, malate dehydrogenase, phosphogluconate dehydrogenase, isocitrate dehydrogenase, glycerate dehydrogenase, and alcohol dehydrogenase (Figure 26). The individual enzymes also exhibited varying rates of enzyme activity loss. This initial data indicated that it might be possible to use the amount of residual enzyme activity detected in a dried bloodstain in order to determine the time of deposition of that stain.

The data was also examined in order to determine the amount of time required for a complete loss of activity to be observed for each enzyme. If the enzymes lost activity at various times, it could be possible to determine an approximate age of an unknown stain based on which enzymes were still active and which enzymes were lost assuming that the protein input was normalized. The amount of time required for each enzyme to totally lose its activity (by direct observation or by extrapolation from the activity-time graph) is listed in Table 6. Glycerate dehydrogenase, lactate dehydrogenase, and isocitrate dehydrogenase lost activity in slightly less than one year (10.1, 11.4 and 11.8 months respectively). Alcohol dehydrogenase, phosphogluconate dehydrogenase, and malate dehydrogenase lose activity between one and two years (14.4, 16.0, and 20.7 months respectively). L-xyulose reductase and 3-hydroxybutyrate dehydrogenase lose activity after two years or more (28.7 and 144.7 months respectively). Interestingly, phosphoglucomutase (PGM), glucose-6-phosphate, and gluconate dehydrogenase can be considered relatively stable enzymes which may be useful in future experiments for use as potential normalizers or positive controls.

While this initial data requires month differences in age in order for TSD estimates to possible be made, it did provide an indication that enzyme activity measurements may be useful in estimating the age of the dried bloodstain. Only a small number of enzymes were evaluated and therefore additional enzymes may require smaller time differences for relationships to be seen and therefore provide better resolution. This method could also be applied to other biological fluids in addition to blood whereas the previous Soret band hypsochromic shift method is limited to bloodstains.

CHAPTER FOUR: RESULTS – miRNA PROFILING FOR BODY FLUID IDENTIFICATION

Presence of miRNAs in Forensically Relevant Dried Body Fluid Stains

In order to determine whether miRNAs were present in the total RNA isolated from the stains, a reverse transcriptase-polymerase chain reaction (RT-PCR) detection strategy was employed. Complementary DNA (cDNA) was synthesized from total RNA using the miScript Reverse Transcription kit (Qiagen). The miRNAs were simultaneously polyadenylated and reverse transcribed using both random and oligo-dT primers. The oligo-dT primers contain a 5' end universal tag which is utilized as a primer binding site for subsequent real time PCR detection. Individual miRNAs were subsequently detected using the miScript SYBR® Green PCR kit. Each single-plex reaction utilizes a universal primer (complementary to the 5' universal tag on oligo-dT primer used in the reverse transcription reaction) and a miRNA-specific primer (Human miScript Primer Assay Set V1.0, Qiagen). Figure 27 depicts the absolute Ct values for twenty-five miRNAs in blood, semen, saliva, vaginal secretions and menstrual blood. The detection of numerous miRNAs, with expression values well below the recommended 40 cycle limit, indicated that miRNAs are present in total RNA extracts from dried biological stains.

Identification of Differentially Expressed miRNA in Biological Fluids

Numerous studies have been published describing miRNA expression in both normal and cancerous human tissue samples. A small number of miRNAs have been identified as "tissue-specific," demonstrating a high abundance in an individual tissue with low or no abundance in others. While a majority of these studies evaluated a wide range of human tissues they did not include, with the notable exception of blood, most of the physiological fluids of relevance to forensic analysis such as semen, saliva, vaginal secretions, and menstrual blood. Such body fluids typically comprise secretions from multiple tissues and hence the resulting miRNA*ome* would be expected to comprise miRNAs from the contributing tissues. Moreover it is possible that a miRNA designated as "tissue-specific" in previous studies may be found in high abundance in these previously untested forensically relevant fluids. Therefore, we made no prior assumptions regarding the tissue specificity of particular miRNAs. In order to identify highly abundant or possible fluid-specific miRNAs in forensic biological stains, an extensive survey of the expression of 452 miRNAs was conducted.

For the initial screening experiments, five-donor pooled body fluid samples were used in order to take into account any possible inter-individual sample variation. All samples were run in duplicate and the average Ct value was used for comparison. Negative controls for each of the pooled body fluid samples, to which no reverse transcriptase was added (RT-), were also run in duplicate to ensure that the miRNAs were the source of amplification products being detected. Initially, only 50 pg of cDNA was

used for real-time PCR based detection in order to facilitate the identification of highly abundant miRNAs.

Graphs of absolute Ct values obtained for each body fluid were created which allowed for an evaluation of the relative expression levels for individual miRNAs (Figure 27). No truly fluid-specific miRNAs, with high to moderate abundance of the miRNA in a single body fluid (and no expression in the other body fluids), were identified. However, it was evident that a significant number of the 452 miRNAs evaluated were differentially expressed in the various body fluids. Figure 27 depicts the expression of 25 miRNAs in blood, semen, saliva, vaginal secretions and menstrual blood. Numerous miRNAs demonstrated similar expression levels in all of the body fluids (data not shown). However, other miRNAs demonstrated a significant difference in expression between the body fluids. For example, miR16 (Figure 27), was found in much higher abundance in blood and menstrual blood compared to semen, saliva, and vaginal secretions ($\Delta Ct \sim 8$). Overall, a significant number of miRNAs (~20%) were found in higher abundance in blood than any of the other body fluids. Numerous potential menstrual blood (n = 38), saliva (n = 32), semen (n = 17) and vaginal secretions (n = 7) candidates were also identified (data not shown).

During the course of the initial screening, numerous miRNAs were identified that were not readily detected in all or most of the body fluids using only 50 pg of input cDNA. In order to not overlook potentially useful miRNA candidates present in lower abundance, additional screening of previously undetected or poorly detected miRNAs ($Ct \geq 38$) was conducted using 500 pg (10-fold increase) of cDNA for detection (data not

shown). The use of additional cDNA input resulted in the identification of additional potential menstrual blood (n = 7), semen (n = 30) and saliva (n = 10) candidates, but failed to identify any additional vaginal secretion candidates.

Further screening of 179 of the most abundant miRNA candidates was accomplished by constructing an expression 'heat map' in order facilitate identification of those candidates that exhibited significant differential expression between the various body fluids (Figure 28). Examples of potential body fluid candidate miRNAs are indicated in color (red – blood, yellow – semen, blue – saliva, green – vaginal secretions, pink – menstrual blood). It was expected that a large number of the heat-map selected candidate miRNAs would not ultimately be ideal for inclusion in body fluid identification assays. For example, the expression data up to this point had not been subjected to any rigorous normalization strategies (apart from input quantity of the total RNA isolate) and was obtained from pooled samples rather than separate individuals. It was thus important to evaluate other normalization strategies and the variation of expression levels between different individuals instead of from pooled samples.

Normalization

The success and accuracy of any biological assay involving the use of quantitative expression analysis depends on proper normalization of data. The purpose of normalization is to minimize potential variation that can mask or exaggerate biologically meaningful changes. Quantitative assessments of total RNA in a sample can be affected

by various factors including extraction efficiencies of RNA from different body fluids and substrates upon which they were deposited as well as potential RNA degradation. The currently available RNA quantitation methods are not human-specific and therefore RNA quantity estimations can also be affected by the presence of contaminating non-human species. Potential normalization strategies for use in miRNA expression analysis include the use of housekeeping genes (mRNA), small RNAs such as 5S rRNA or U6b (a small nucleolar RNA), and universally expressed miRNAs. Ideally a normalizer should be present in relatively high and consistent abundance in all tissues or cell types, should be of similar size and found in similar cellular environments as the target molecule, and be compatible with the analysis methods utilized for the target molecule. Messenger RNAs from housekeeping genes may not be the most suitable targets for normalization of miRNA expression data due to abundance, degradation rates and amplimer size differences. Presumably universally (and approximately) equally expressed 'housekeeping' miRNAs could be used as normalizers but appropriate candidates still need to be identified by additional studies. Accordingly we used a normalization method that involved standardization of total RNA input and measurement of the relative expression of the miRNA in comparison to the small nuclear RNA, U6b. Total RNA extracts were first quantitated using a RiboGreen fluorescence assay and equal amounts of total RNA were used in subsequent reverse transcription assays. However, this normalization strategy was not sufficiently precise enough on its own due the potential presence of differing levels of non–human sources of RNA in some forensic samples (e.g. bacteria in saliva and vaginal secretions). Therefore, we chose to also employ a

delta Ct (ΔCt) metric which measured the relative abundance of a particular miRNA in relation to the small nucleolar RNA, U6b. U6b was chosen based on its high abundance and apparent stability in different body fluid stains of forensic interest (data not shown). For high abundance miRNA candidates whose expression was greater than U6b, the ΔCt metric was obtained by subtracting the Ct value of miRNA from the Ct value of the U6b, whereas for miRNAs present in lower abundance than U6b, the ΔCt was obtained by subtracting the Ct value of U6b from the Ct value of the miRNA.

Candidate Selection

U6b-normalized expression of the miRNA candidates with individual samples rather than the previously-used pooled samples resulted in the rejection of several candidates due to either too much variation between individuals or insufficient variation between different body fluids (data not shown). This additional screening process resulted in the identification of differentially expressed miRNAs that were good candidates for blood, semen, saliva, vaginal secretions, and menstrual blood.

Strong candidates were those miRNAs found in higher abundance than U6b in an individual body fluid but present at lower levels than U6b in other body fluids. Two strong candidates for blood, miR451 and miR16, were identified. As can be seen from the relative expression plot in Figure 29A, expression of these miRNAs in blood (higher abundance than U6b) was significantly higher compared to all other body fluids (lower abundance than U6b). While no miRNAs were found in semen in higher abundance than

U6b, two good candidates, miR135b and miR10b, were identified that demonstrated a higher abundance in semen relative to the other body fluids (Figure 29B). Two strong candidates were identified for saliva (miR205 and miR658) (Figure 29C). Only one strong candidate, miR124a, was identified for vaginal secretions (Figure 29D). Two other potential vaginal secretion candidates were identified, miR372 and miR195. Expression of miR372 was relatively similar in all body fluids, but was found in slightly higher abundance in vaginal secretions (Figure 29E). The other potential candidate, miR195, was least abundant in vaginal secretions (Figure 29F). Despite its low abundance, it was considered as a possible candidate because the near absence of this miRNA in combination with the presence of miR124a or miR372 may be indicative of vaginal secretions. Potential menstrual blood markers included miR451 (Figure 29G) and miR412 (Figure 29H) chosen on the basis of differential expression compared to other body fluids rather than being the most abundant miRNA species in menstrual blood.

Development of miRNA Body Fluid Identification Assays (miRNA BodyFlu*ID*)

While none of the miRNA candidates were found to be truly body fluid-specific in the sense that they were expressed in one tissue and not in any other, it was hypothesized that a panel of differentially expressed miRNAs could be used to develop a unique expression profile that would be characteristic of an individual body fluid. For initial assay development, normalized expression data for each of the previously identified miRNA candidates (miR16, miR451-blood; miR135b, miR10b-semen;

miR205, miR658-saliva; miR124a, miR372, miR195-vaginal secretions, miR451, miR412-menstrual blood) was obtained for blood, semen, saliva and vaginal secretion samples from different individuals (n=5). The ΔCt values were used to create two-dimensional scatter plots in order to determine if differentiation of each body fluid would be possible. Significantly, distinct clustering of each body fluid was observed for each miRNA pair, with the body fluid of interest in each assay clearly separated from the other body fluid expression data (Figure 30A-F). It became apparent that such differential clustering could form the basis of a body fluid identification assay. Therefore, the nine candidates were selected for inclusion in a miRNA panel for body fluid identification (Table 7).

The degree of separation between the body fluid of interest and the other fluids differed between miRNA pairs. For example the blood identification assay, using the two strong blood miRNA candidates (miR16 and miR451), provided an approximate 7-8 ΔCt difference in both dimensions from the next closest body fluid (Figure 30A). However, with the vaginal secretion assays using the stronger vaginal secretions candidate, miR124a, only a 2-3 ΔCt difference was observed between vaginal secretions and the next closest body fluid (Figure 30D and 30E). In an attempt to improve the resolution between body fluids for the vaginal secretion assay, a three-dimensional scatter plot was created using miR124a, miR372 and miR195 (Figure 31). While distinct body fluid clusters were visible using the 3D scatter plot, combination of all three miRNA candidates did not significantly improve the distance between the various body fluid clusters. As a result, the 2D scatter plot was determined to be sufficient for the vaginal

secretion assay. It was decided that the miR124a-miR372 assay would be used for further validation due the fact that miR372, while a weak candidate, still provided a positive result. MiR195 was least expressed in vaginal secretions and considered a negative result. The potential for false positive results can be increased with a "negative" marker if degradation is present. For example, miR195 would be detected in a pristine blood sample in relatively high abundance and would be clustered away from the vaginal secretions data using this assay. However, if a degraded blood sample was analyzed and miR195 was not detected, this would produce a "negative" result which could be interpreted as a false positive for vaginal secretions. It is not known if the strength of the other vaginal secretion candidate, miR124a, would be sufficient to prevent such false positive results. Therefore, the inclusion of miR372 in the vaginal secretion assay was deemed more appropriate.

In order to ensure that the miRNAs were the true source of the obtained expression data, reverse transcription negative (RT-) samples, to which no reverse transcriptase had been added, were evaluated with the miRNA panel. The average Ct value for 10 RT- samples for each body fluid was determined (Table 8). For several of the miRNAs including miR451, miR16, miR135b, miR10b, and miR372, no signal was detected in any of the RT- samples. However, for the remaining miRNAs (miR658, miR205, miR124a, miR195 and miR412), Ct values were obtained for the RT- samples (Table 8). The average Ct value for the RT- samples for miR658, miR205, miR195 and miR412 were slightly above 40, which is the manufacturer's recommended maximum number of amplification cycles, and would therefore be undetected if a 40-cycle limit was

utilized. However, lower Ct values were observed for miR124a (avg. = 37.3) and U6b (avg. = 35.7). While the presence of a signal in the RT- samples could be a concern, none of the RT- signals were close to the Ct values obtained for the body fluid samples of interest (Table 8). For example, the average Ct for miR124a for the RT+ vaginal secretion samples (n=10) was 25.1 whereas the RT- value was 37.1, an approximately 4096 fold difference in expression. For the assays with no signal detection in the RT- samples (miR451, miR16, miR135b, miR10b, miR372), a Ct value of <50 was accepted as a valid result. However, different detection thresholds needed to be established for the assays where a signal was detected in the RT- sample (miR658, miR205, miR124a, miR195, miR412 and U6b). For these assays, only Ct values below the RT- average could be considered valid. To determine an acceptable value range for these assays, the average Ct value minus three standard deviations (rounded to the nearest 0.5 number) was calculated and the obtained value was used as the maximum acceptable Ct value (Table 8). Any unknown sample whose Ct value for these assays was above the determined threshold value was considered invalid and could not be used for further analysis.

All valid Ct values were used to obtain ΔCt's for each of the miRNAs included in the body fluid identification panel. Previous ΔCt calculations were performed in such a manner as to result in the body fluid of interest being plotted in the positive/positive quadrant of the two dimensional scatter plot if possible. However, in an attempt to simply analysis and to provide a more accurate representation of the expression of each miRNA in relation to U6b, all normalization in subsequent studies was performed by subtracting

the miRNA Ct value from the U6b Ct value. For strong candidates, whose expression was higher than that of U6b, this would result in a positive value. For weaker candidates, whose expression was lower than that of U6b, this would result in a negative value. As a result, a visual examination of the constructed 2D scatter plots also provides additional information regarding the relative abundance of each miRNA in each biological fluid.

The initial assay design demonstrated that the panel of selected miRNAs (blood – miR451, miR16; semen – miR135b, miR10b; saliva – miR205, miR658; vaginal secretions – miR124a, miR372; menstrual blood – miR451, miR412) seemed suitable for the differentiation of forensically relevant biological fluids (Table 7). The miRNA based body fluid identification assays (named 'miRNA BodyFlu*ID'*) were thus subjected to more extensive validation studies.

miRNA BodyFlu*ID* Specificity

Body Fluid/Tissue Specificity

The initial studies were performed using only five samples per body fluid. In order to ensure the specificity of each assay, additional body fluid samples were tested (n=10-20 for the body fluid of interest, n=8-10 for the other body fluids not being assayed for).

Blood

Nineteen human blood samples (including the five previously tested samples) were analyzed using the blood miRNA assay (miR16/ΔCt miR451). The blood sample donors, both male and female, ranged in age from 15 months to 84 years old. As before, all of the human blood samples were found in a distinct cluster in the upper right quadrant separated from all other body fluids (Figure 32A). All vaginal secretion samples were found in the lower left quadrant and there was considerable overlap of the semen and saliva samples, which were spread out over the two lower quadrants and the upper right quadrant. The buccal samples were located closer to the blood samples than any of the other fluids but were still well separated from each other.

Saliva

Eighteen human saliva samples (including the five previously tested samples) were tested using the saliva miRNA assay (miR205/miR658). Samples were obtained from both male and female donors ranging in age from 26 – 58 years old, and included both liquid whole saliva samples (n=9) and buccal swabs (n=9). As can be seen from Figure 32B, all of the liquid saliva and buccal scrapings samples were located together in a distinct cluster separate from the other body fluids tested. They were clustered in the upper right quadrant with the exception of one buccal sample which, although part of the cluster, was slightly outside the quadrant. The vaginal secretions, blood and semen samples were mainly located in the lower left quadrant with a few samples just inside the

lower right quadrant (Figure 32B). The ability to identify both liquid saliva and buccal samples is an important finding since both whole saliva and buccal cells are encountered in forensic specimens.

Semen

Eleven human semen samples (five previously tested samples included) were tested using the semen miRNA assay (ΔCt miR135b and ΔCt miR10b). Samples were obtained from adult males ranging in age from 26 – 52 years old. As can be seen from Figure 32C, all of the semen samples are found in a distinct cluster separated from all other body fluids. However, the separation between body fluids using this assay is not as significant as was observed with the blood assay. As previously discussed, neither of the miRNAs used in the semen assay were identified as strong candidates (i.e. found in higher abundance than U6b) and all data points are found in the lower left quadrant (Figure 32C). Therefore while the semen samples are found in a distinct cluster, the identification of stronger semen miRNAs will be necessary in order to improve the separation between body fluids.

Samples from two vasectomized males were included in the study in order to determine if the semen assay was specific to sperm cells. Both of the samples from the vasectomized males (orange squares) were detected amongst the semen samples from non-vasectomized males, thereby demonstrating the ability of the assay to accommodate non-sperm containing semen samples (Figure 32C). The detection of semen from both

vasectomized and non-vasectomized males could indicate that the two semen miRNA candidates are present in seminal fluid or in epithelial cells from the male reproductive tract. Overall, fewer miRNAs were detected in semen compared to the other biological fluids and those that were present were often found in much lower abundance. The low abundance of these miRNAs may be explained if detection is obtained from the low level of non-sperm cells present in semen. The cellular and non-cellular components of semen could be separated and examined for the presence of both of the semen miRNA candidates to determine if the miRNAs used in the semen assay are cellular based. If the miRNAs were present in the cellular component, then sperm cells would need to be specifically isolated from other non-sperm cells that may be present which could be accomplished using laser capture micro-dissection. Regardless of the origin of the miRNAs used in the current semen assay, further work will be needed to identify stronger semen candidates and to identify possible sperm-specific miRNAs.

Vaginal Secretions

Eleven vaginal secretion samples (including the five previously analyzed samples) were collected from adult females ranging in age from 28 – 65 years old and tested using the vaginal secretions miRNA assay (miR124a/ΔCt miR372). As can be seen from Figure 32D, all vaginal secretion samples, except for one 'false negative', were located together in a distinct cluster in the lower right quadrant separate from the other body fluids. Since the whole saliva sample set was the closest to the vaginal cluster,

additional saliva samples comprising five buccal epithelial samples were tested using the vaginal secretions assay in order to determine whether the vaginal epithelial and oral epithelial cells were distinguishable. While the buccal epithelial cells clustered closer to the vaginal secretion data points than the whole saliva samples, there was still a clear separation between the two body fluids (Figure 32D). Since only one strong miRNA candidate (i.e. more abundant than U6b) was identified for vaginal secretions, it is possible that the separation between buccal and vaginal secretion samples could be improved if a second strong candidate was subsequently identified.

Other Human Tissues

Despite reports in the current literature of the identification of tissue-specific miRNAs, it has been suggested that a majority of miRNAs will be expressed in the majority of tissues [101]. While all of the miRNAs included in the body fluid identification panel described above were detected in each body fluid, their differential expression enabled each of the four body fluids to be distinguished. A more detailed study to evaluate tissue specificity of the miRNA BodyFlu*ID* assays was carried out using a wide variety of human tissues.

Total RNA from twenty-one human tissues including adipose, brain, cervix, heart, liver, lung, placenta, prostate, skeletal muscle, testes, thyroid, trachea, bladder, spleen, thymus, ovary, kidney, colon, esophagus, small intestine (FirstChoice® Human Total RNA Survey Panel, Applied Biosystems/Ambion) and skin (Biochain Institute, Inc.), was

analyzed using the miRNA panel. Each total RNA sample included in the FirstChoice® panel comprised RNA from at least three different donors and was certified to contain small RNAs (miRNA, siRNA and snRNA). As expected, the miRNAs included in the panel were detected in each of the tissue samples but again in varying abundance. The high degree of specificity of each of the miRNA body fluid identification assays was confirmed since all of the tissue samples exhibited expression profiles that differed from that of the appropriate body fluid in each of the four assays (Figure 33).

For the blood assay, both miR16 and miR451 were detected in all twenty-one tissues with the exception of the small intestine where miR451 was not detected (data not shown). MiR451 was found in the highest abundance in lung and placenta whereas miR16 was found in the highest abundance in lung and prostate. However, despite their higher abundance in these tissues compared to the rest of the samples, their abundance was still lower than that in human blood samples. When the tissue samples were evaluated using blood assay and the data analyzed using the 2D scatter plot, all of the tissue samples were present in the lower left quadrant of the scatter plot whereas the blood samples were tightly clustered in the upper right quadrant (Figure 33A).

One of the saliva miRNA candidates, miR658, was present in low abundance in all of the tissue samples (data not shown). MiR205 was present in moderate abundance in the cervix, placenta and prostate tissue but in low abundance in all other tissues. The 2D plot showed the tissue samples located in the lower left quadrant with a significant separation from the saliva samples, which were located in the upper right quadrant (Figure 33B).

Both the semen candidates, miR135b and miR10b, were also detected in all of the twenty-one tissues with many present in moderate to high abundance. MiR135b was detected in highest abundance in testes and thyroid, whereas miR10b was detected in high abundance in numerous tissues including testes, adipose, cervix, ovary, kidney and colon. As a result of the high abundance of these miRNAs in numerous tissues, the separation between the human semen sample cluster and the tissue samples was not as great in the 2D scatter plot as that observed for the blood assay (Figure 33A and 33C). As can be seen from Figure 33C, the tissues are all present in close proximity to the human semen samples although still distinct there from. This data indicates the need to monitor the continually-expanding miRNA*ome* for more specific semen candidates.

For the vaginal secretions assay all tissue samples were located in the lower left quadrant separated from the vaginal secretions samples that were located in the lower right quadrant (Figure 33D). Several published studies have identified miR124a as a brain-specific miRNA [56,58,59]. While miR124a was found in highest abundance in brain compared to the other tissues examined, the expression level observed in brain was still lower than that we observed for vaginal secretions. Due to these differences in expression, the brain sample was located closer to the vaginal secretions samples on the two-dimensional plot but was still present in the lower left quadrant (Figure 33D). The Ct values for miR372 ranged from 32 to >40 for all tissue samples, with the lowest Ct value obtained from placenta. So despite the presence of only one strong candidate, the specificity of this assay for vaginal secretions is supported by the tissue data.

Species Specificity

Optimal forensic analysis not only requires an assay to possess tissue specificity but it also should exhibit restricted species specificity. To check this, a number of non-human blood samples were analyzed including twelve animal species (dog, cat, horse, crane, cow, coyote, sheep, tortoise, lamb, Patagonian cavy, ferret, deer) and ten non-human primate species (spider monkey, rhesus macaque, pig-tailed macaque, brown lemur, chimpanzee, baboon, howler monkey, cynomolgus monkey, African green monkey, spot-nosed guenon). A smaller number of non-human saliva samples were available tested and included cat, dog and one primate (spot-nosed guenon). Semen and vaginal secretion samples from non-human species were not available for testing, but such body fluids from non-human species are rarely encountered in casework.

For all of the non-human species blood samples, miR451, miR16, and U6b were detected in significant abundance. As can be seen from Figure 34A, all of the non-human samples were found in close proximity to the human blood data points. Two animals (ferret and coyote) and four primates (chimpanzee, baboon, African green monkey, and cynomolgus monkey) were located directly within the human blood cluster (Figure 34A). While only a small number of the species tested were clustered within the human blood samples, the small distance between the human data points and the remaining animal species would make it difficult to differentiate human and non-human blood samples with any degree of confidence using this assay.

Saliva samples from two dogs and two cats were used to examine the species specificity of the saliva miRNA assay. As can be seen from Figure 34B, negative results

(i.e. not found in the human saliva data cluster) were obtained for the both of the cat and dog samples. While an extensive number of animal saliva samples were not available for testing, cat and dog represent animals that could be frequently encountered at crime scenes in forensic casework. One primate saliva sample from a spot-nosed guenon was also tested using the saliva miRNA assay. However, the U6b value for this sample was invalid (Ct > 34.5, Table 8) and therefore could not be used in further analysis.

As a result of the poor species specificity of the original blood assay, it was evident that modifications would need to be made in order to provide a more forensically relevant assay. Attempts were made to identify an alternative small RNA to be used for normalization of the miRNA expression data that would also allow for a differentiation of human and non-human blood stains. The expression of 11 small nucleolar RNAs (snoRNAs), including U26, U27, U28, U29, U30, U31, U38B, U43, U44, U48 and U90, was examined in both human and non-human blood samples in order to determine if a human specific normalizer could be identified (Table 9). Several of the snoRNAs, including U26, U28, U30, U44, and U90, were found in very low abundance or were not detected in the non-human samples. However, the abundance of these snoRNAs in the some of the human body fluids was also quite low (Table 9). For example, the Ct value for U44, U26, U28, and U90 in semen was over 40 whereas the Ct for U30 was acceptable for semen but was close to 40 for blood and saliva (Table 9). Therefore, none of the snoRNAs tested were determined to be suitable for use a universal normalizer for all body fluids.

While an alternative universal normalizer was not identified, several of the snoRNAs, including U26, U28 and U44, were present in low abundance in non-human blood samples and in higher abundance in human blood samples. Therefore, it was possible that one of these snoRNAs could be used to normalize only the blood assay and provide the desired species specificity. U44 was selected as the top snoRNA candidate due to its high abundance in blood, its low abundance in the animal blood samples, but also because of its low abundance or absence in most of the primate samples. When the 2D scatter plot was constructed using the U44-normalized data, the clustering that was achieved with the U6b-normalized assay was not achieved and overlap of the semen, saliva and blood data was observed (data not shown). However, it was evident from the 2D scatter plot that there was a clear separation between the human blood data points and the non-human blood samples (Figure 35). As can be seen from the U44-normalized scatter plot, only chimpanzee was found clustered with the human blood data points (Figure 35). Based on these results, it was determined that the U44-normalized assay could be used to identify the presence of human or higher primate blood if a positive result for an unknown sample was obtained using the U6b-normalized blood assay.

miRNA BodyFlu*ID* Stability

Environmentally Compromised Samples

Forensic biological evidence is often exposed to various damaging environmental influences including heat, light, humidity and rain. In order for an assay to be useful in forensic casework, the ability of the assay to accommodate environmentally impacted samples must be demonstrated. Until recently, the analysis of biological samples in forensic casework has largely been limited to DNA-based methods. Therefore, numerous studies have been published that demonstrate the ability to recover genetic profiles from degraded or compromised samples. The use of RNA in forensic assays, however, has only recently been proposed and therefore few studies have examined the stability of RNA in forensic biological samples. Recently, we have reported the results of an extensive evaluation of the persistence and stability of mRNA in forensic samples in which it was demonstrated that mRNA profiling can be performed successfully on environmentally impacted biological stains [11]. While mRNA stability was demonstrated in samples stored at room temperature, heat and humidity appeared to be detrimental to RNA stability [11]. However, since mRNAs are significantly larger in size compared to miRNAs, it was therefore hypothesized that miRNAs could be less susceptible to degradative processes due to their significantly smaller size and thus potentially be better suited for the analysis of environmentally impacted forensic samples. A recent study has reported more robust isolation and analysis of miRNAs compared to mRNAs in FFPE tissue samples [102].

In order to assess the stability of miRNAs and to determine if the miRNA assays could accommodate environmentally impacted samples, body fluid stains were exposed to varying storage conditions such as storage at room temperature (22^{o}C), storage at 37^{o}C, exposure to heat, light, humidity, and rain (outside uncovered, OUC), and exposure to heat, light and humidity (outside covered, OC). The samples were collected at various time intervals and the following samples from each condition were examined in this study: room temperature – 1 year, 18 months or 2 years (2 year sample examined for blood only); 37^{o}C – 3 months, 6 months; outside uncovered (i.e. directly exposed to any precipitation) – 1 day, 3 days, 1 week; outside covered (i.e. protected from direct exposure to precipitation) – 3 days, 1 week, 1 month. Table 10 provides a summary of the range of temperatures and humidity levels that the samples were exposed to, in addition to the amount of precipitation (rainfall) that was observed during collection of the outside uncovered samples. The samples placed outside were typically exposed to average high temperatures of greater than 90^{o}F and average high humidity levels of greater than 85%. All samples placed outside and uncovered were exposed to various amounts of rain. After one week of storage the blood, semen and saliva samples had received 2.7 inches of rain and vaginal secretions samples had received 7.6 inches of rain. Total RNA was recovered from each of the above mentioned samples in sufficient quantity for analysis and the miRNA panel was used to determine if the presence of the body fluid of origin could be detected. The results of this study are summarized in Table 11 and depicted in Figure 36.

Blood

A positive result for blood was obtained for samples stored at room temperature for 2 years and 37^{o}C for 6 months whereas the outside (both covered and uncovered) gave results at 1 week (Table 11, Figure 36A). All samples generating a positive result were located in upper right quadrant cluster with the known human blood samples (Figure 36A). The sample stored at 37^{o}C for 3 months was also located in the upper right quadrant but was significantly separated from the human blood cluster closer to the location of the saliva samples (Figure 36A). Again, the appearance of the 37^{o}C 3 month sample near the location of the saliva samples does not indicate that this sample would be identified as saliva. It simply indicates a negative result for blood for this sample as blood is the body fluid being tested using this assay. However, to ensure that the 37^{o}C 3 month sample would not be identified as a saliva sample, the location of this sample on the saliva two-dimensional scatter plot was determined after testing with the miRNA saliva assay. A negative result for saliva was obtained (data not shown). Despite the false negative result for blood obtained for the particular 37^{o}C 3 month sample and the OUC 3 day sample, other samples stored at each condition for a longer period of time (37^{o}C 6 months, OUC 7 days) provided a positive result (Table 11, Figure 36A). Such sample variability could be due to differing microbiota colonization of the stains. The identification of blood in the most exposed sample for each condition (room temperature 2 years, 37^{o}C 6 months, OC 1 week, OUC 1 week) demonstrates the excellent stability of the blood miRNA candidates.

Saliva

Saliva was detectable up to a year at room temperature (22^{o}C) (Table 11, Figure 36B). The recovery of miRNAs from the saliva samples stored at the other environmental conditions was significantly reduced compared to the other body fluids. The negative results in four of the samples (two stored at 37^{o}C and the 3 day and 1 week OC) were due to the non-detection of the U6b normalizer and not the absence of detectable miRNA species. The failure to detect U6b was somewhat surprising since U6b was detected in the other body fluids under the same storage conditions. A reduced expression of miR205 was observed for all samples stored outside both covered and uncovered (data not shown).

Semen

A positive result for semen was obtained for samples stored at room temperature for 18 months and 37^{o}C for 6 months whereas the outside samples gave results out to 1 week (covered) and 1 day (uncovered) (Table 11, Figure 36C). All samples for which a positive result were obtained were located in the upper portion of the lower left quadrant clustered with the known human semen samples (Figure 36C). For the three samples with the negative result, U6b and miR10b were detected, however a Ct value of over 40 was obtained for miR135b for the OUC 3 day and 7 day samples and was undetected for the OC 1 month sample. The OUC 3 day sample, located near the vaginal secretion data, was

tested using the vaginal secretions assay to ensure that a false positive result would not be obtained. A negative result for vaginal secretions was obtained (data not shown). The ability to identify semen in samples stored at 37^{o}C for 3-6 months and stored outside for 1 week with exposure to almost 3 inches of rain and high temperatures and humidity demonstrates a high degree of stability of the miRNA biomarkers used in the semen assay. The detection of U6b and miR10b in the samples for which a negative result was obtained indicates that the stability of this assay could be even more improved if a better candidate were to be identified that could replace miR135b.

Vaginal Secretions

A positive result for vaginal secretions was obtained for samples stored at room temperature for 18 months and 37^{o}C for 6 months whereas the outside covered samples gave results out to 3 days (Table 11, Figure 36D). The failure to detect miRNA in the outside uncovered samples could be due to sample wash out by the amount of rain that these samples were exposed to (e.g. the 1 week sample received over 7 inches of rain).

In general, miRNAs appeared to be relatively stable in all body fluid samples stored at room temperature and 37^{o}C for extended intervals. While exposure to environmental elements such as heat, humidity, light and rain appeared to be detrimental for the recovery of miRNAs in saliva and vaginal secretions, blood and semen were not as adversely affected. It is not possible to preclude the possibility that the poor results with saliva and vaginal secretions are due to the overrepresentation within these samples

of co-extracting commensal or exogenous microbiota-derived RNA, the quantity of which is expected to increase with time in environmentally exposed samples. The results of this initial work indicate a high degree of stability for some of the miRNA candidates and indicate their potential suitability for their use with forensic casework samples.

Menstrual Cycle

The final study conducted to evaluate the stability of the miRNA BodyFlu*ID* assays involved an assessment of the identification of vaginal secretions in samples collected daily during a full 28-day cycle. Menstrual cycles are controlled by a complex interaction of numerous hormones that affect gene expression levels and therefore it is possible that the expression of certain miRNAs may also vary. Additionally the onset of menopause in older females results in a significant disruption and eventual complete loss of regular hormone levels. In order to ascertain whether changes in female reproductive hormone levels would affect the identification of vaginal secretions using the miRNA assay, vaginal swabs from a female experiencing regular menstrual cycles and from a female in perimenopause were collected daily for a 28-day period. For the menstruating female, day 1 was indicated by the start of menstruation.

As can be seen from Figure 37, vaginal secretions were identified in all samples from both the menstruating female (Figure 37A) and the female in perimenopause (Figure 37B). All samples were located in the lower right quadrant clustered with the known vaginal secretion samples. The samples with reported menstrual blood also were

positive for the presence of vaginal secretions (Figure 37A). However this is expected since menstrual blood will contain vaginal cells and secretions. Thus no significant changes in the expression of the vaginal secretions miRNA candidates were observed during different female reproductive stages and also during regular menstrual cycles.

Simulated Forensic Casework Samples

The initial studies described above demonstrated the sensitivity (50pg of input cDNA), specificity (no cross-reactivity with human tissues) and stability (detection in environmentally compromised samples) of the developed miRNA assays for body fluid identification. However, forensic evidentiary items may contain only trace amounts of genetic material and may also include the presence of multiple different biological fluids. Thus it is important to test the performance of the miRNA BodyFlu*ID* assays with such samples and we accomplished this by the preparation and analysis of simulated casework samples.

Saliva

Genetic profiles can be routinely recovered from trace amounts of salivary fluids from items such as used cigarette butts and beverage containers. Therefore if the presence of trace amounts of saliva could be detected on these items, it may provide investigators with an indication of which evidentiary items may be useful for the subsequent recovery

of DNA. Furthermore, saliva recovered from the skin of a victim could be useful in the investigation of oral assault cases. In order to determine if the saliva miRNA assay could detect trace amounts of saliva in such samples, total RNA was recovered from swabs of beverage container lids, human skin on which saliva had been deposited, and used cigarette butts. All of the simulated casework samples, except for one of the swabs taken from a beverage container lid, were located clustered with the known human saliva samples in the upper right quadrant (Figure 38A).

Blood

Total RNA was recovered from the cotton pad of an adhesive bandage used to cover a small cut on the finger of a female donor. The cotton pad of the bandage contained blood in the form of a small reddish-brown stain. When the bandage sample was evaluated with the blood assay, the sample data was located in the upper right quadrant on the two-dimensional scatter plot clustered with the known blood samples (Figure 38B). The same sample was subsequently evaluated with the U44-normalized blood miRNA assay in order to determine if the blood present on the bandage was of human origin. The location of the sample on the two-dimensional U44-normalized scatter plot was upper right quadrant clustered with the known human blood samples confirming the presence of human blood present on the bandage (data not shown).

Semen and Vaginal Secretions

A significant number of samples processed in an operational forensic DNA laboratory involve the analysis of evidence recovered from sexual assaults. Often only a small amount of semen from the perpetrator will be present amongst a vast excess of a female victim's biological material. For an assay to be useful in forensic casework, it must be able to detect the small amount of semen that may be present and not be masked by the excess vaginal material present. In order to determine the potential utility of the semen miRNA assay for the analysis of sexual assault evidence, a vaginal and cervicovaginal swab was collected from a female donor 18 hours post-coitus. The vaginal and cervicovaginal swabs were collected in order to determine if semen would be detected in different regions of the vaginal canal. To insure that residual semen from prior sexual relations were not present, a pre-coital cervicovaginal swab was also obtained before coitus commenced but after an abstinence period of seven days. The presence of semen was detected on both the vaginal and cervicovaginal swabs taken 18 hours post-coitus (Figure 38C). The pre-coital swab was negative for the presence of semen (Figure 38C). The presence of vaginal secretions was detected in the vaginal swab, cervicovaginal swab and the pre-swab using the vaginal secretions assay (data not shown).

Body Fluid Mixtures

Body fluid mixtures other than the common semen-vaginal secretions encountered in sexual assault cases may also be present in forensic evidentiary samples. Thus additional body fluid mixtures samples, including two blood-semen (Figure 39) and one semen-saliva (Figure 40) mixtures were also evaluated. The miRNA expression profile for each mixture using all four body fluid assays (blood, semen, saliva, and vaginal secretions) was determined. Blood and semen were correctly identified in both of the blood-semen mixture samples (Figure 39). On the blood assay, the admixed samples were located in the upper right quadrant clustered with the known blood samples (Figure 39A). On the semen assay, the samples were located in the upper portion of the lower right quadrant clustered with the known semen samples (Figure 39C). The absence of saliva and vaginal secretions was also demonstrated with the blood-semen mixture samples located in the lower left quadrants (Figure 39B and 39D). Semen and saliva were also correctly identified in the semen-saliva mixture sample with the sample clustered with the known samples on each plot (Figure 40B and 40C). The absence of blood and vaginal secretions was also demonstrated (Figured 40A and 40D).

Development of a Menstrual Blood miRNA BodyFlu*ID* Assay

The ability to detect the presence of menstrual blood may prove invaluable in certain forensic cases, such as in sexual assault investigations, where the facts of the case

may be in dispute. For example, the presence of a victim's blood on the clothing of a potential rape suspect may be explained as venous blood originating from a nose bleed resulting from a physical, rather than sexual, assault of the victim. However, if the blood was determined to be menstrual blood, it would indicate a more intimate contact between the victim and a potential suspect.

During the female reproductive cycle, if fertilization does not occur hormonal changes catalyze the breakdown of the endometrium lining of the uterus. Menstrual discharge therefore consists of tissue from the degenerating endomentrium as well as blood resulting from associated blood vessel rupture as the endometrium breaks away from the uterus. Menstrual blood is thus a complex mixture consisting of endometrium derived stromal, epithelial, endothelial, vascular smooth muscle, and bone marrow derived cells, as well as capillary blood [103,104]. Menstrual blood will therefore contain products that would also be detectable in venous blood or vaginal secretions. Menstrual blood samples were examined using the miRNA assays for all body fluids in order to determine if the menstrual blood samples would interfere with the identification of the body fluid of interest on each assay (Figure 41). The menstrual blood samples were separately clustered compared to venous blood using the miRNA blood assay (Figure 41A). As can be seen from Figures 41B and 41C, the menstrual blood samples on the semen and saliva assays also did not overlap with the body fluid of interest. However when the menstrual blood samples were evaluated using the vaginal secretions miRNA assay, the presence of vaginal secretions was identified in many of the samples (Figure 41D). While this is not necessarily a false positive result since menstrual blood samples

will contain vaginal secretions and cells, it demonstrates the need for a separate assay to be developed that would allow for menstrual blood and vaginal secretions samples to be distinguished.

During the initial screening of the 452 miRNAs several candidates for the identification of menstrual blood were identified. MiR451, which is used in the blood assay, was also present in high abundance in menstrual blood as well. Most of the miRNAs demonstrating a moderate to high abundance in menstrual blood were also found in significant amounts in blood or vaginal secretions. Therefore, while two specific miRNA candidates for menstrual blood (i.e. higher abundance in menstrual blood than U6b) were not identified, an assay was developed using miR451 and miR412 that nevertheless permitted a distinct clustering of menstrual blood samples separate from all other body fluids (Figure 42A). As can be seen from Figure 42A, both the venous blood and menstrual blood samples are located in the lower right quadrant with a majority of the other body fluid samples located in other quadrants. Two of the menstrual blood samples were not located within the cluster of other known menstrual blood samples (Figure 42A). While one of these samples was present in the lower right quadrant, it was not located within the cluster of menstrual blood samples (Figure 42A). A false negative result was obtained from the other menstrual blood sample that was located in the lower left quadrant (Figure 42A). Despite these two discordant samples, a clear distinction can be made between the venous blood and menstrual blood samples. There is no overlap between the menstrual blood and vaginal secretions samples with the vaginal samples located in the lower left quadrant (Figure 42A). Importantly, therefore, a menstrual blood

sample should provide a positive result for the vaginal secretion and menstrual blood assays whereas a vaginal secretions sample should only provide a positive result on the vaginal section assay. The specificity of the menstrual blood assay was further demonstrated with the location of all twenty-one previously tested tissue samples located in the lower left quadrant clearly separated from the known menstrual blood samples (Figure 42B).

Similar to the vaginal secretions assay, the expression of the menstrual blood miRNA candidates during a 28-day period (Day 1 = first day of menstruation) were evaluated to ascertain whether significant changes in expression would occur. Menstrual blood was reported on days 1 – 4, with a significant reduction in the amount of menstrual blood present on day 4. As can be seen from Figure 43, menstrual blood was detected in the day 1 – 3 samples but was not detected in the day 4 sample. All other samples collected during the 28-day period (days 5 – 28) were also negative for the presence on menstrual blood (Figure 43).

Venous blood and vaginal secretions were located at opposite ends of the two-dimensional scatter plot in the lower right and lower left quadrants respectively (Figure 42-44). Since menstrual blood was located somewhat in between these two body fluid clusters, it needed to be demonstrated that a mixture of venous blood and vaginal secretions would not be located within the cluster of menstrual blood samples. When two different venous blood-vaginal secretion mixtures were evaluated with the menstrual blood assay, both were located in the lower right quadrant clustered with the known

venous blood samples (Figure 44). This further supported the specificity of the developed assay for menstrual blood.

miRNA Profiling Schema for the Analysis of Unknown Biological Samples

A proposed experimental schema for the analysis of biological stains of unknown origin using the miRNA body fluid identification assays is provided in Figure 45. First, total RNA is isolated from an unknown biological stain. The use of a standard guanidine isothiocyanate-phenol:chloroform based extraction method allowed for the recovery of miRNAs in total RNA extracts. Numerous non-organic, silica-based extraction kits are now commercially available for the recovery of miRNAs and, in contradistinction to the phenol-chloroforms methods, are easily transferable to an automated platform. Thus these kits may prove more suitable for use in forensic casework although the quantity and quality of the recovered miRNAs from forensic stains would have to be evaluated in separate studies. An appropriate amount of total RNA (~1-5ng) would be used for reverse transcription (RT) (e.g. the miScript system from Qiagen). Unlike other commercially available miRNA systems that employ miRNA-specific reverse transcription strategies, the miScript system allows cDNA to be produced from all RNA species within the sample, including mRNAs and other small non-coding RNAs. This could be advantageous in forensic casework where multiple individual reverse transcription reactions required to analyze a sufficient amount of miRNAs may not be possible due to a limited amount of genetic material recovered from most evidentiary

items. The ability to simultaneously reverse transcribe other RNA species, such as mRNAs, may also be useful if parallel assays need to be performed for the detection of tissue specific mRNAs or housekeeping genes. An appropriate volume of the RT product to obtain 50pg (for the blood, saliva, vaginal secretions and menstrual blood assays) or 500pg (for the semen assay) cDNA would be used in the miRNA quantitative real time PCR (QT-PCR) assay which, in our case, uses the miScript SYBR Green PCR system and a miRNA specific primer. The detection of each miRNA must be performed in a separate reaction well since all assays utilize SYBR Green for detection and therefore cannot be multiplexed. However, the entire miRNA panel (9 miRNAs and 2 normalizers, U6b and U44) can be analyzed from a single RT product. So while the miRNAs cannot be analyzed in a multiplex format, numerous RT reactions are not required for the examination of multiple miRNAs in the same sample. The Ct values for each miRNA are then evaluated to ensure all obtained values are within acceptable ranges (Table 8). Any data not within the acceptable range is rejected and would need to be repeated. All acceptable expression data would then be normalized using U6b in which the Ct value of the miRNA is subtracted from the Ct value of U6b. The ΔCt values for the two miRNAs for each body fluid would then be used to position the unknown sample on the two-dimensional scatter plot for each body fluid. The identification of the presence of the body fluid would be confirmed if the unknown sample was found within the cluster of known body fluid samples. If a positive result is obtained for blood, ΔCt values using U44 for miR451 and miR16 would then be calculated and used to determine the species

of origin. The presence of human (or higher primate) blood would be indicated by the presence of the unknown sample within the cluster of human blood samples.

CHAPTER FIVE: RESULTS –ENHANCED PROFILING STRATEGIES FOR LOW TEMPLATE SAMPLE ANALYSIS

Low Template Samples

Short tandem repeats (STRs) are regions of repetitive DNA where the repeat unit is 2-6 bases in length. The number of repeat units differs between individuals. For autosomal STR loci, one or two alleles can be present at a single locus, providing a homozygous or heterozygous genotype respectively. For standard samples ($\geq$ 500pg of input template DNA), profile recovery and analysis is relatively straightforward. However, forensic casework evidentiary items often contain less than 100 pg of template DNA, which is equivalent to approximately 15 diploid or 30 haploid cells. The presence of such low template samples could be due to several factors including: damaged or degraded DNA, oligospermic or aspermic perpetrators or from extended interval post coital samples, where sperm have been lost over time due to the effects of drainage or host cell metabolism. Other trace biological evidence will also contain small quantities of cells, including fingerprints, particulate matter, and aerosols [105-107]. Since only a small number of cells are present in LCN (short tandem repeat) methods and often results in total failure or recovery of a partial profile. If partial profiles are recovered, interpretation of the data obtained from these LCN analyzed samples requires novel considerations [64-66]. The occurrence of allelic drop-out or drop-in is significantly higher in LCN samples due to stochastic effects, and can result in false homozygous classifications and in false heterozygous classifications, respectively (Figure 46).

Additionally, LCN samples exhibit significant peak height imbalance and are more susceptible to interference from contamination (Figure 46). The frequency of LCN samples in forensic casework warrants development of additional methodologies to ICN that allow for more successful recovery of genetic information.

Laser Capture Micro-dissection

Laser capture micro-dissection is a technology that allows for the isolation of single cells or groups of cells from various samples. The use of laser capture micro-dissection was employed in this study in order to accurately control the number of cells being analyzed in an individual sample. Several laser capture micro-dissection instruments are currently available that utilize either a direct contact or no-contact micro-dissection approach. Direct contact laser capture micro-dissection instruments involve a laser being positioned and fired directly over the cells of interest. This approach may cause damage to targeted cells, particularly if only a small number of cells are collected. No-contact laser capture micro-dissection instruments use a laser to cut around the cell of interest thereby reducing any potential damage that may be caused to the sample by exposure to direct laser contact. For the current work, a direct contact (Arcturus PixCell II) and a no-contact (Leica LMD) laser capture micro-dissection instrument were available for comparison. Each instrument was evaluated for ease of use, time and labor intensity, amenability to downstream applications and recovery of genetic profiles from micro-dissected cells.

Arcturus PixCell II System

The Arcturus PixCell II system utilizes direct-contact laser capture micro-dissection. A specimen on a standard glass microscope slide is prepared and dehydrated. The slide is positioned on the stage of the instrument and held in place by a small vacuum. The stage is then manipulated by a joystick attached to the stage. The highest provided magnification objective is 40X (400x magnification). Cells of interest are brought into focus and the laser power and pulse duration can be adjusted. For sample collection, a sample cap is used that is coated with a thermoplastic polymer. The sample cap is placed directly onto the specimen slide and the laser is fired over cells of interest (Figure 47A). The laser causes the thermoplastic film to "melt" over the cells of interest. As the film quickly cools, the cell is attached to the film and can be removed from the specimen slide by lifting the cap off the surface (Figure 47B). The cap can be placed onto a clean glass slide in order to ensure that the cells have been removed from the specimen slide and are present on the cap surface (Figure 47C). A plastic ExtracSure™ device containing a hollow center is placed over the cap. Lysis buffer is then added into the ExtracSure™ device covering the sample area with the collected cells of interest. A 0.5mL tube is then placed over the ExtracSure™ device. A pre-heated heat block is then placed over the sample tray and placed into an incubator for lysis.

The direct contact laser-capture micro-dissection approach of the Arcturus PixCell II system provides the ability to isolate cells from standard glass slides. This would allow for the collection of cells from archived casework slides. However, several challenges with sample collection using the Arcturus PixCell II system were encountered.

If any moisture was present in the sample, the thermoplastic film would not adhere to the cells. The dehydration steps of the staining procedure had to be repeated in order for the cells to be collected. Often times the additional dehydration steps did not result in successful removal of cells from the prepared slides. On numerous occasions due to the extremely high humidity occurring during Florida afternoons, the slide would acquire moisture during sample collection and therefore would need to be re-dehydrated before additional cells could be collected. Additionally, the size of the laser pulse could not be made small enough to target the size of a sperm cell. Therefore if a sperm cell was adhering to an epithelial cell (Figure 48A), the size of the laser pulse caused the thermoplastic film to coat the sperm cell and a portion of the epithelial cell (Figure 48B). When the cap is lifted, the epithelial cell was collected with the sperm cell (Figure 48B and 48C). The lysis protocol for the PixCell II samples had to be amendable to being performed in an incubator, with no direct contact between the sample and heat. The sample and lysis buffer were enclosed in the plastic ExtracSure^{TM} device. When the lysis is completed the entire sample device has to be inverted and centrifuged in order to collect the sample into the 0.5mL tube. Using various direct lysis methods, hundreds of cells were needed for a partial profile to be recovered using the Arcturus PixCell II system (data not shown).

It was possible that the small amount of nuclear material obtained from lysis of a small number of cells was adhering to the walls of the ExtracSure^{TM} chamber and therefore was lost during sample manipulation. Collection into a 0.5mL tube also required the cell lysate to be transferred to a 0.2mL PCR tube for amplification increasing

the potential for sample loss. Additional collection strategies were attempted in order to reduce the amount of sample manipulation and potential sample loss. The collection area in the thermoplastic film was cut out from the cap surface and the film with attached cells was placed directly into a 0.2mL or 0.5mL tube containing an appropriate amount of lysis buffer. The tubes could then be placed in a heat block or thermocycler for direct contact with heat during the lysis protocol. Additionally, excess film outside of the collection area on the cap surface was removed and the lysis buffer placed directly on the remaining film area where cells were attached. A 0.5mL tube was placed over the cap without the use of the ExtracSure^{TM} device and the lysis performed in an incubator. These modified approaches provided only a slight improvement in profile recovery (data not shown) and required a significant amount of sample manipulation and the use of a disposable scalpel. These methods would not be amenable to the current requirements and resources of operational casework laboratories and therefore no further work was performed using the Arcturus PixCell II system.

Leica LMD

The Leica LMD system utilizes no-contact laser micro-dissection. A specimen is heated fixed to a slide covered with a proprietary membrane and stained. As a result of the need for samples to be placed on the membrane slides, cells could not be easily collected from archived casework glass slides. The highest provided objective for the Leica LMD system is 63x (630x magnification) allowing for easier viewing of sperm cell

samples. The slide is placed sample side down into the slide holder and inserted onto the microscope stage. Manipulation of the stage, microscope focus, light intensity and magnification power are all controlled by a joystick separate from the microscope itself. Underneath the stage are the sample collection tubes. There are four chambers where a flat-capped 0.2mL PCR tube is placed. A small volume of lysis buffer is placed in the sample cap. The power and speed of the laser, as well as the cap position, are all controlled in the software provided with the instrument. Cells of interest are brought into focus (Figure 49A) and then outlined using pre-made shapes or drawn by hand (Figure 49B). The laser then cuts along the specified paths and cuts out the cells of interest from the surrounding membrane (Figure 49C). The cells will then fall by gravity into the sample collection tube located underneath the stage. Once samples have been collected, the tubes can be closed and briefly centrifuged. The lysis can then be performed in a thermocycler and subsequent amplifications can be performed in the same tube.

The no-contact laser capture micro-dissection approach of the Leica LMD systems eliminates potential damage to cells by direct exposure to the laser. Due to the ability of the laser to cut around a small area, an individual sperm cell head can be outlined and cut by the laser (Figure 49). This allows sperm cells adhering to epithelial cells to be isolated without collecting the nucleus of the epithelial cells as well (Figure 50). This is a significant advantage over the PixCell II system particularly when dealing with sexual assault evidence where sperm may frequently be found adhering to epithelial cells. The ability to collect cells into 0.2mL PCR tube allows for the lysis to be performed

in thermocycler with more precision temperature control and allows for subsequent amplifications to be performed in the same tube.

Direct Lysis Strategies

Experiments were conducted to evaluate various direct lysis buffers in order to determine which buffer was the most efficient for epithelial and sperm cell lysis (data not shown). Various proteinase K and alkaline lysis buffers were tested, as well as several commercially available lysis buffers including the Quick Extract™ lysis buffer (Epicentre), Lyse-N-Go (Pierce), and DNAzol® Direct (Molecular Research Center, Inc). In order to evaluate these lysis buffers, cell suspensions were prepared from semen and buccal epithelial cell swabs. Cell numbers were determined using by cell counting using a hemacytometer. Serial dilutions of each extract were prepared, ranging from 1 to 1000-1500 cells. The cell suspensions were lysed with the appropriate buffer and reactions conditions (obtained from published materials or manufacturer's protocols). The samples were amplified with Profiler Plus® (standard conditions) in order to determine the efficiency of lysis using each buffer. Those buffers that allowed for recovery of partial to full profiles from smaller numbers of cells were further examined. In order to ensure that the lysis buffer was responsible for the lysis of the cells, lysis buffer was added to a small aliquot of a cell suspension. This was placed in a hemacytometer and the cell lysis was observed under the microscope as it occurred. Two of commercially available lysis

buffers, Quick Extract™ and Lyse-N-Go, resulted in the most efficient cell lysis (data not shown).

The two commercially available lysis buffers, Quick Extract™ and Lyse-N-Go were then further evaluated in order to determine which buffer would be most suitable for use with LCM samples. Both buffers required only a small volume to be used (10-15μl) and used a short lysis protocol (8-30 minutes). The use of the Quick Extract™ lysis buffer required the use of an alternative polymerase, the Expand High Fidelity polymerase. The High Fidelity polymerase is a mixture of Taq polymerase and Tgo polymerase. The Tgo polymerase is a "proofreading" enzyme, possessing a 3'-5' exonuclease activity. It is reported that the use of this mixture of polymerases results in a three-fold greater accuracy than Taq alone. The Lyse-N-Go buffer allowed for amplification with Taq Gold. Both buffers allowed for recovery of STR profiles from LCM samples; however fewer cells were required with the Quick Extract™ buffer with the alternative polymerase (data not shown). Additionally, increased amounts of allele drop-in were observed for the Lyse-N-Go buffer (data not shown). Therefore it was determined that the Quick Extract™ lysis buffer would be most suitable for use with LCM samples. Optimization of the Quick Extract™ lysis buffer was performed and included an evaluation of the volume of lysis buffer needed, the length and temperatures of the incubation steps, and the addition of additional reagents such as DTT (data not shown). The most efficient cell lysis (for both sperm and epithelial cells) was obtained when the manufacturer's lysis protocol was utilized except for the addition of 0.39M DTT (data not shown).

Evaluation of the Developed Direct Lysis Strategy

Once the laser capture micro-dissection conditions and the lysis protocol had been optimized, the optimized conditions were evaluated by amplification of a range of sperm cells at various amplification cycles (Table 12). One, five, and ten to one hundred sperm cells (in ten cell increments) were collected using the Leica LMD system and lysed using the optimized Quick Extract™ lysis method. The 10µl lysates were then amplified using the Profiler Plus® amplification kit (25µl reaction, 5U High Fidelity polymerase). Various amplification cycle numbers were tested including 28 (standard), 32, 34 and 36. RFU thresholds of 50, 100, and 150 were used to provide an indication of the signal intensities of the recovered alleles. The number of alleles recovered (out of a possible 20 – 9 STRs and AMEL) were recorded (Table 12). Using 28 amplification cycles, 100 or more sperm cells were needed before a full STR profile could consistently be obtained. Even with this number of cells, the signal intensity of many alleles was quite poor and often below 150 RFUs (Table 12). The use of four additional cycles (32 cycles) above the standard 28 cycles resulted in the need for 80-90 sperm cells for consistent profiles to be recovered (Table 12). The use of six additional cycles (34 cycles) above the standard 28 cycles resulted in the need for only 40-50 sperm cells for consistent profiles (Table 12). When eight additional cycles (36 cycles) were used, as few as five to ten sperm cells were required for minimal quality profiles (Figure 51A, Table 12). A minimal quality profile demonstrates typical low template sample problems including peak imbalance and allele drop-out. Ninety sperm cells were needed for a higher quality profile using 36

amplification cycles (Figure 51B, Table 12). With this number of cells, peak imbalance was improved and fewer allele drop-ins were observed. As can be seen from Table 12 in the early stages of the project a significant amount of allele drop-in was observed. As the project progressed, the number of allele drop-ins was significant reduced. As a result, the use of 5U of High Fidelity polymerase and 36 amplification cycles for use with STR amplifications was determined to be optimal.

Analysis of Single Source Low Template Samples

Single source epithelial (buccal and vaginal) and sperm cells were tested to further evaluate the optimized method involving the use of the Leica LMD system and the Quick Extract™ lysis method. Various numbers of sperm cells had been examined during the test of the optimized conditions and the number of cells needed for minimal and optimal quality profiles determined (Table 12). Therefore, single source epithelial cell samples were analyzed using the optimized amplification conditions (36 cycles, 5U High Fidelity polymerase). One to ten epithelial cells were collected and lysed with the Quick Extract™ lysis solution. Two to five epithelial cells were needed in order to obtain minimal quality profiles (data not shown). Full autosomal STR profiles were recovered from a single buccal (Figure 52A) and a single vaginal (Figure 52B) epithelial cell. However, there was only partial success with profile recovery from single epithelial cells (2/5 or 40%).

The previous experiments had involved the collection of full epithelial cells for analysis. Since a direct lysis strategy was developed, proteins and other cell debris are present in the lysate. Additional purification steps could not be incorporated prior to amplification due to the potential to lose the small amount of genetic material that was present with sample manipulations and purification steps. An advantage of the Leica LMD system was that it provided ability to isolate and collect small regions of interest, allowing for portions of epithelial cells to be collected rather than whole cells. For these studies, recovery of DNA from the micro-dissected cells was of particular interest and therefore only the cell nucleus would be required. It was thought that if only cell nuclei were collected, the amount of unwanted protein and cellular debris could be reduced allowing for a possible improvement in the efficiency of profile recovery from the micro-dissected cells. Nucleus-only portions of epithelial cells were collected to determine if full autosomal STR profiles would be obtained. Full autosomal profiles could be obtained from as few as 10 nuclei (data not shown). However, there was not a significant improvement in allelic signal or the number of cells required for a full profile compared to whole cell collections (data not shown).

Analysis of Non-distinguishable Cell Type Mixtures

An advantage of using laser capture micro-dissection techniques is the ability to isolate individual cells. This could be advantageous if a mixture is present, providing the ability to isolate individual contributors. However, in some samples the presence of a

mixture may not be visibly apparent due to the presence of non-distinguishable cell types. In these instances, cells from multiple donors would be collected. It was therefore necessary to ensure that the Leica-Quick Extract™ method and the optimized amplification conditions could accommodate mixture samples and result in the recovery of two STR profiles.

The first type of non-distinguishable cell type mixture that was examined was sperm-sperm cell mixtures. The sperm-sperm mixture was artificially created by combining two semen samples in a 1:1 ratio. Various numbers of sperm cells were then collected ranging from 5 to 100 cells (Table 13). The samples were amplified with Profiler Plus® (5U of High Fidelity polymerase, 36 amplification). As few as thirty cells were required in order to obtain two full autosomal STR profiles from both male contributors (Table 13). Significant partial profiles were recovered when fewer than thirty cells were collected.

The next type of mixture that was examined was epithelial cell mixtures. Vaginal (female) and buccal (male) epithelial cells were mixed in a 1:1 ratio and various numbers of epithelial cells were collected, ranging from five to thirty cells (Table 14). The samples were amplified with the COFiler® PCR Amplification kit (5U of High Fidelity polymerase, 36 amplification cycles). Partial and full profiles were observed for one contributor when five to ten cells were collected (Table 14). Two full autosomal profiles were consistently observed when twenty epithelial cells were collected (Table 14).

These results indicate that the developed lysis and amplification strategy to would be able to provide an indication of the presence of a mixture and to recover a genetic

profile from multiple donors. It was interesting to note that an expect number of cells were needed to recover full profiles from both donors than would have been expected. For example, it was determined that five to ten sperm cells and two to five epithelial cells from single source slides were needed to obtain acceptable STR profiles. Therefore, it would be expected that full two STR profiles would be recovered from 10-20 sperm cells and 4-10 epithelial cells in a two-donor 1:1 mixture. Thirty sperm cells and 20 epithelial cells were necessary to consistently obtained full profiles from both donors. It is possible however that, even though the mixture was created in a 1:1 ratio, unequal amounts of cells were collected from both donors. This is particular evident in the epithelial cell mixture results (Table 14). Three 10-cell collections were analyzed and differing number of male alleles were recovered. It is therefore possible that fewer and differing numbers of male cells were collected in each sample, thus resulting in the failure to recover complete profiles. For example, in the second 10-cell collection 8/14 male and 14/14 female alleles were recovered. It is possible that as few as 2 male cells could have been collected in comparison to 8 female cells and this accounting for the difference in the number of alleles obtained.

Analysis of Mock Casework Samples

The previous samples examined involved single source samples and artificially created mixture samples. Additional studies were conducted that included mock casework samples. These samples included vaginal post coital swabs (distinguishable cell

type mixtures), a semen stained t-shirt that had been stored at room temperature for 3.5 years, a semen sample from a vasectomized male, a menstrual blood swab and a used beverage container lid. The results of these experiments involving mock casework samples demonstrate the potential future application of the optimized Leica-Quick Extract™ method and optimized amplification strategy (36 cycles, 5U High Fidelity polymerase) to the tools available to operational forensic crime laboratories.

3.5 Year Old Semen-Stained T-Shirt

A small portion of the semen-stained t-shirt that had been stored at room temperature for 3.5 years was collected. When the cell suspension from this sample was examined, a large number of cells still adhering to fibers from the t-shirt were observed (data not shown). Several sperm cells were located detached from fibers and were collected for analysis. A full autosomal STR profile was recovered from 15 sperm cells collected from the 3.5 year old semen stained t-shirt with no loss of the larger alleles as is expected with degraded DNA (data not shown).

Semen Sample from a Vasectomized Male

While it is expected that no sperm would be present in a semen sample from a vasectomized male, it was thought that a small number of epithelial cells from the male reproductive tract may be present. A semen sample from a vasectomized male was

obtained and examined for the presence of epithelial cells. A small number of epithelial cells were observed. A single epithelial cell was collected, lysed using the Quick Extract™ lysis method, and amplified using the COFiler® Amplification kit (5U High Fidelity polymerase, 36 amplification cycles). A picture of the actual cell collected for analysis is provided in Figure 53 (bottom left). A full autosomal profile was recovered from the single epithelial cell (Figure 53). Despite the presence of a full profile, significant peak imbalance could be observed particularly at the TH01, CFS1PO and amelogenin loci.

Beverage Container Lid

A beverage container lid that had been used by a male participant was swabbed and a small number of epithelial cells were recovered, lysed using the Quick Extract™ method and amplified (5U High Fidelity polymerase, 36 amplification cycles). Analysis of two (Figure 54A) and three (Figure 54B) epithelial cells from the beverage container lid resulted in the recovery of an STR profile with only one allele drop-out and a full STR profile, respectively.

Menstrual Blood Swab

Blood samples had previously not been included in any studies conducted as it was difficult to recover in tact cells from a blood cell suspension. A menstrual blood

swab was examined since it was possible that a larger number of epithelial cells might be present. A three cell sample from the menstrual blood swab resulted in almost a complete STR profile, with only one allele drop out at the vWA locus (Figure 55A). A five cell sample from the same menstrual blood swab resulted in the recovery of a full STR profile (Figure 55B). There were several alleles present not originating from the donor in the study. While this sample was not examined for the presence of semen, the possibility that these alleles originated from possible trace amounts of semen cannot be eliminated.

Cervico-Vaginal Post Coital Swabs

The final mock casework samples that were examined with vaginal post coital swabs collected 12 and 36 hours after intercourse. Laser capture micro-dissection has been suggested as a differential extraction tool, separating sperm and non-sperm fractions prior to analysis. However, as described previously, often sperm cells are found adhering to epithelial cells and cannot be separated if they are close or on top of the epithelial cell nucleus. Attempts were made to locate and collect sperm cells not fully adhering to epithelial cells. However, due to the overwhelming amount of vaginal material present on the slide, isolated sperm cells were not frequently observed. A full autosomal STR profile was recovered from twenty-five sperm cells collected from the 12 hour sample, with no alleles recovered from the female donor in the study (data not shown). Since a larger number of sperm cells were present in this sample, sperm cells not adhering to epithelial cells were located and collected. However, fewer sperm cells were present in the 36 hour

sample. A full male and female donor autosomal STR profile was recovered from the analysis of twenty-five sperm cells collected from the 36-hour sample. This data indicates the potential advantage of the use of laser capture micro-dissection in the analysis of low template samples, but not necessarily as a replacement for a differential extraction as has been previously suggested.

Evaluation of Whole Genome Amplification (WGA) Strategies

An evaluation of existing whole genome amplification methods was performed in order to determine if their application to low template samples would result in the ability to recover full STR profiles from a smaller input DNA amounts. This survey of existing whole genome amplification methods resulted in the development of the modified improved primer extension pre-amplification (mIPEP) method [90]. A basic diagram of the primer extension pre-amplification is provided in Figure 56. Random 15-mer primers hybridize through the genome and extension from these primers occurs during a larger number of low-stringency (low annealing temperature) amplification cycles. The developed mIPEP strategy is a modified version of and improved PEP method (IPEP). It differs from the IPEP method in several ways: 1) it utilizes a different mixture of polymerases – *Taq* polymerase ("processive") and *Tgo* polymerase ("proofreading"), contained in the Expand High Fidelity polymerase (Roche Applied Science); 2) it utilizes significantly increased concentrations of the High Fidelity polymerase and primers; 3) removes an additional elongation step during the amplification process; 4) eliminates the

addition of gelatin to the amplification mix. These modifications resulted in the ability of the mIPEP method to successfully recover full STR profiles with as little as 5pg of input DNA, recover profiles from environmentally compromised blood samples, and from single dermal ridge fingerprints [90]. However all of the samples used in the initial development of this method were samples extracted using a standard organic extraction, allowing for removal of cell debris and proteins. The mIPEP method needed to be evaluated with micro-dissected cells in order to determine if additional modifications to the reaction components or amplification conditions would need to be made in order to accommodate micro-dissected cell lysates.

Initially, ten microliter cell-lysates were used directly in a mIPEP amplification using original conditions [90]. In order to evaluate the efficiency of the mIPEP amplification method, the mIPEP products were quantitated using the Quantifiler® Human Real-time PCR quantitation kit. Quantitation of sperm (Figure 57A) and epithelial cells (Figure 57B) indicate that amplification of unstained cells results in the highest fold increase after mIPEP amplification. For sperm cells, smaller numbers of unstained cells resulted in higher fold increases (Figure 57A). For epithelial cells, larger fold increases were observed with larger numbers of cells (Figure 57B). For both epithelial and sperm cells, the use of the Christmas tree stain resulted in little to no fold increase. As a result of this study, unstained and H&E stained cells were used in subsequent testing.

Analysis of Micro-dissected Cells with Prior mIPEP Amplification

Single Source Samples

An advantage of the use of prior whole genome amplification is that sufficient amounts of sample are produced that may permit the use of standard amplification conditions in subsequent STR amplifications. The use of the Quick Extract™ buffer resulted in the inability to use Taq Gold polymerase in STR amplifications. In order to determine if standard conditions could be used after prior mIPEP amplification, aliquots of the mIPEP products were amplified with STR amplification kits using standard amplification cycle numbers and standard amounts of Taq Gold. It was determined that for the Profiler Plus® and COFiler® amplification kits, two times the amount of Taq Gold could be used in order to obtain greater sensitivity (data not shown).

Ten buccal epithelial cells were lysed and amplified with mIPEP. The mIPEP products were quantitated and 155pg of the mIPEP product was used for amplification with both COFiler® (Figure 58A) and Profiler Plus® (Figure 58B). Full STR profiles were recovered using both multiplex systems. There appeared to be an improvement in peak height balance at heterozygous loci using prior mIPEP amplification for most loci, with the exception of the D16 locus in the COFiler® profile (Figure 58). Additional STR multiplex systems, including Identifiler® (15 locus multiplex system), Minifiler™ (reduced sized amplicons), and Yfiler® (Y chromosome STR multiplex), were also evaluated for use with the mIPEP amplification products. Each of these multiplex

systems was previously tested with the non-WGA strategy and each failed to result in the recovery of profiles from either sperm or epithelial cells. Since these multiplex systems are more frequently being used in forensic casework, they were re-evaluated with the mIPEP products in order to determine if profiles could be recovered from micro-dissected cells. A partial profile recovered from 5 epithelial cells using the Identifiler™ amplification kit is shown in Figure 59. A genotype was not recovered at two loci (D13 and FGA) and one allele at the heterozygous D3 locus was also not recovered. However, the partial profile that was recovered was a significant improvement compared to the complete failure to recovery any genetic information from the non-mIPEP amplified micro-dissected cells. With more loci contained in this single multiplex system than Profiler Plus® or COFiler®, the partial profile recovered with the Identifiler™ multiplex may still result in a higher discrimination than a complete profile with either of the smaller multiplexes. A full profile was also obtained from 10 micro-dissected epithelial cells pre-amplified with mIPEP using the Minifiler™ multiplex system (Figure 60). This multiplex contains reduced sized amplicons to be more suitable for use with degraded or low template samples. However, frequently only limited partial profiles were obtained.

In addition to the numerous autosomal STR multiplex systems available, a Y-chromosome STR multiplex (Yfiler®) that specifically targets male DNA, is also available. Figure 61 shows a Y-STR profile recovered from 10 mIPEP-amplified micro-dissected epithelial cells, with only one locus not recovered (DYS392). This multiplex system could be advantageous for use with low template samples since Y-STR loci are

hemizygous in nature and would therefore eliminate potential interpretation difficulties due to peak imbalances.

In additional to epithelial cells, micro-dissected sperm cells were also evaluated using mIPEP pre-amplification. Figure 62 shows two autosomal STR profiles recovered from 10 mIPEP-amplified micro-dissected cells. Ninety-eight picograms of the mIPEP product were used to recover nearly complete COFiler® (Figure 62A) and Profiler Plus® (Figure 62B) profiles. Allele drop-out at the D7 locus was observed in the Profiler Plus® profile and a complete locus drop-out of the D7 locus in the COFiler® profile was also observed (Figure 62). For a majority of the mIPEP pre-amplified samples, allele or locus drop-out at the D7 locus was observed. A nearly complete Yfiler® profile, with one locus drop-out at DYS392, was obtained from 15 mIPEP-amplified micro-dissected sperm cells (Figure 63).

The results of the single source samples indicated that the use of prior mIPEP amplification would not result in the ability to recover STR profiles from smaller numbers of cells. However, it did result in improved sensitivity in that STR profiles could be recovered from the same number of cells using standard conditions (28 amplification cycles, Taq Gold polymerase) rather than increased cycle number (36 cycles) and an alternative polymerase. These are the conditions currently used in operational crime laboratories, thus allowing for an easier incorporation of the developed strategies into casework without additional validation.

Mock Casework Samples

Additional studies were conducted to evaluate the use of prior mIPEP amplification of mock casework samples, including a semen stained t-shirt that had been stored at room temperature for 40 months, a used beverage container lid, and vaginal post coital swabs. Fifteen sperm cells were collected from the 40 month old semen stained t-shirt and were amplified with mIPEP. One nanogram of the mIPEP product was amplified with Profiler Plus® (28 amplification cycles, 5U Taq Gold polymerase) and a full STR profile was obtained (Figure 64). Ten epithelial cells were collected from a beverage container lid that had been used by a female participant and amplified with mIPEP. Four picograms of the mIPEP product was amplified with Profiler Plus® (28 amplification cycles, 5U Taq Gold polymerase) and a full STR profile was obtained (data not shown). Ten and fifteen sperm cells were collected from a 24 hour post coital swab and amplified with mIPEP. Aliquots of the mIPEP product (~860pg and ~2.1ng, respectively) were amplified with Profiler Plus® (28 amplification cycles, 5U Taq Gold polymerase). A partial profile was recovered from the 10 sperm cell sample (data not shown) with a failure to recover an allele at the D18 locus and both alleles at the D7 locus. A nearly full profile was recovered from the 15 sperm cell sample (data not shown) with only one allele not recovered at the D7 locus.

Reproducibility Studies

Multiple amplifications of the same low template sample can be performed in order to determine if an artifact is consistently observed or is due to stochastic effects. However, often there is in sufficient quantities of low template samples to permit multiple amplifications. When a direct lysis approach is used for a small number of micro-dissected cells, the entire lysate is used in a single amplification reaction and therefore could not be amplified more than once. A potential advantage of the use of whole genome amplification methods for low template samples is that sufficient amounts of the sample are produced allowing for multiple amplifications with the same amplification kit or with several different amplification kits.

In order to evaluate the reproducibility of profiles obtained from mIPEP amplification products two sets of experiments were conducted. The first was to collect multiple samples containing the same number of cells (10 epithelial and 25 sperm cells) from single source samples. These samples were amplified in separate mIPEP amplifications and similar quantities of mIPEP product were amplified in subsequent STR amplifications to ensure that relatively consistent profiles would be recovered. The profiles recovered from these separate mIPEP amplifications were relatively consistent (data not shown). However, some differences in peak balance and allele drop-out were observed between samples due to the low-template nature of the original sample (data not shown).

The second type of experiment was to perform multiple amplifications from the same mIPEP product to ensure that consistent profiles would be obtained. The multiple amplifications included the use of the same multiplex system multiple times or different multiplex systems. An example of multiple amplifications from the same mIPEP product (two aliquots of the same mIPEP product from 25 sperm cells amplified in separate Profiler Plus® reactions) can be seen in Figure 65. As can be seen from these profiles, two full profiles were obtained with relatively similar allelic signal intensities and imbalances. An example of multiple amplifications from the same mIPEP product using different multiplex systems can be seen in Figure 66. The use of these two multiplex systems allowed for additional genetic material to be recovered than if a single multiplex system was used and also allows for a comparison of the genotypes recovered at two loci, D3 and D7, since they are contained in both systems. The same allele was not recovered at the D7 locus in both systems indicating a possible failure to pre-amplify this allele during the mIPEP amplification (Figure 66).

Development of Novel Y-STR Multiplex Systems

While the developed lysis and amplification strategies allowed for a greater sensitivity and reproducibility than other low template sample analysis methods, difficulties in profile interpretations still arose, including allele drop out and peak imbalance. As mentioned previously, Y-chromosome STRs are hemizygous in nature with only one allele present at most loci. Therefore, an allele drop out would result in

failure to recover a genotype at a particular locus rather than give the appearance of a false homozygous genotype as would be the case with autosomal STR loci. Peak imbalances are heterozygous autosomal STR loci can often incorrectly indicate the presence of a mixture, with the less intense allele attributed to a minor component. If multiple alleles are present at an individual Y-STR locus, this would more clearly indicate the number of male donors present in the sample.

While there are significant advantages to using Y-STRs for low template sample analysis, Y-STRs do not afford the same degree of discrimination as compared to autosomal STRs. Most of the Y chromosome is inherited paternally as a block of linked haplotype markers from generation to generation. Therefore, Y-STR loci are not inherited independently and the individual discriminatory potential of each locus cannot be combined using the product rule in order to achieve a high level of discrimination. The frequency of a Y-STR profile therefore can only be determined through the use of the counting method (i.e. how many times a particular profile is observed in a database). The discrimination potential of Y-STRs is therefore limited by the size of the database and the number of included loci.

Initially, a set of nine loci ("minimal haplotype" or MHL) were suggested for use in forensic casework [108]. Subsequently, the MHL set was expanded to include three additional loci in an attempt to improve discriminatory potential [109]. This set of twelve Y-STR loci, known as the SWGDAM "core" loci have been incorporated into commercially available Y-STR multiplexes (Promega's PowerPlex® Y and Applied Biosystems' AmpF*l*STR® Yfiler®) and are currently being used in forensic casework.

However, coincidental matches between unrelated males still occur using these multiplex systems. Therefore, there was still a need to develop new multiplex systems that could assist in the resolution of coincidental Y-STR matches between unrelated males.

While the commercially available Y-STR multiplexes incorporate 12-17 loci, over 400 loci have been identified on the human Y chromosome with most of these loci not well characterized [110,111]. Therefore, it is possible that more highly discriminating loci exist than those that are currently being used. In order to begin a more systematic analysis of novel Y-STR loci, a comprehensive STR physical map of the human Y chromosome was created which sequentially positioned the over 400 loci along the Y chromosome (Figure 67) [110]. Through the developed physical map, numerous duplicate loci were identified (i.e. sequences that had been deposited into the Human Genome Database multiple times with different DYS designations). This information was particularly useful when attempting to design novel Y-STR multiplexes to avoid the inclusion of duplicated loci.

An extensive evaluation of approximately 33% of all known Y-STR loci (133 loci) was performed in order to identify novel highly discriminating loci. Each locus was evaluated based on its amplification efficiency, ability to be included into a multiplex system, and its discriminatory potential. Numerous loci were rejected due to poor amplification efficiencies or due to poor diversity values. The remaining loci were incorporated into novel multiplex systems (MPIII – MPIX) in order to evaluate the suitability of use of these multiplexes with forensic samples [96-99]. The diversity values of each of the incorporated loci was determined and is provided in Figure 68, with the

loci ranked from highest to lowest discrimination potential within each multiplex system. It was apparent from this data that each multiplex system contained loci with diverse ranges of discriminatory potential with several loci in each system with very poor discriminatory potential. It is unlikely that operational crime laboratories would utilize all eight multiplex systems for the analysis of individual samples due to budgetary limitations and due to the limited quantity of genetic material often recovered from forensic samples. Therefore attempts were made to incorporate a sub-set of the highly discriminating loci into a single multiplex system, an ultra-high discrimination (UHD) multiplex. The purpose of this multiplex was not to replace the currently used commercially available multiplexes, but to improve the significance of Y-STR data in forensic investigations. As a result, any locus selected for inclusion into the UHD multiplex needed to be highly discriminating on its own but also demonstrate the ability to increase the discriminatory potential of the SWGDAM core loci.

In order to determine which of the highly discriminating loci would provide the highest support to the SWGDAM core loci, the potential increase in haplotype diversity of the SWGDAM loci with the additional of one highly discriminating locus was determined [100]. The increase in haplotype diversity for each locus was plotted against its individual diversity values (Figure 69). For some loci, only diversity values from a limited data set (n=100) were available. Therefore these loci were not immediately considered for inclusion into UHD multiplex but were analyzed for future use. For the remaining loci, those that were located in the upper right quadrant of the graph (high diversity value and larger increase in haplotype diversity for the SWGDAM core loci)

were identified as potential candidates for inclusion into the UHD multiplex. The resulting UHD multiplex included 14 highly discriminating loci (Figure 70) and had an overall discriminatory potential of 99.7% [100]. When the UHD multiplex was used in addition to the Applied Biosystems' AmpF*l*STR® Yfiler® kit, 100% discrimination of all individuals within the sample set was achieved [100]. This level of discrimination has not been achieved with any other Y-STR multiplex system. Through the application of the mIPEP strategy to low template samples, sufficient amounts of genetic material could be obtained from low template samples to permit the recovery of both autosomal and Y-chromosome STR data from an individual sample. This combined data could result in an improvement in the amount of genetic data obtain (i.e. discriminatory potential) but could also result in an improvement in the interpretation of challenging low template samples.

CHAPTER SIX: DISCUSSION

In this report we have demonstrated the ability to obtain standard and novel genetic information from low template samples, including a determination of the time since deposition of dried bloodstains using spectrophotometric analysis of hemoglobin and a progressive decline in enzyme activity, an identification of the body fluid of origin using miRNA profiling, and a determination of the genetic profile of the donor of a small number of micro-dissected cells using standard and novel DNA biomarkers. Collectively these findings constitute the basis for the development of a "genetic eyewitness" profiling system for low template biological samples.

Hemoglobin UV-Visible spectrophotometric profiles were successfully obtained from dried bloodstains. Upon examination of the characteristic peaks in the visible absorption spectral data from aged bloodstains, a hypsochromic shift (shift to shorter wavelength) of the Soret band was observed as the age of the stain increased. A significant correlation between the age of the stain and the $\Delta\lambda$Soret (hypsochromic shift) was demonstrated ($R^2 > 0.9$ in most cases). The hypsochromic shift measurements resulted in the highest resolution of any previously developed TSD method enabling bloodstains differing in age by minutes, days, weeks and months to be distinguished. Additionally, it was demonstrated that determined that hypsochromic shift measurements could be obtained from sub-microliter quantities of blood from stains as small as 1 μl. To our knowledge, this is the first strategy that permits the determination of the time since deposition of low template samples with this level of sensitivity. The potential to perform this analysis "on-site" at crime scenes was also demonstrated through the use of a

portable "point-of-use" spectrophotometer allowing crime scene technicians to identify the presence of a bloodstain (through a characteristic UV-VIS spectral profile) and also determine the time since deposition of that bloodstain. This information, therefore, could immediately provide investigators with a molecular estimation of when a crime occurred and could assist in the determination of what evidence to collect for further analysis.

While the hypsochromic shift assay permitted a determination of the time since deposition of bloodstains, the molecular basis for the shift is theorized to be the result of oxidation to the central Fe^{2+} ion in heme. If this hypothesis is correct, there are numerous environmental factors that could influence the rate of oxidation and therefore affect the accuracy of the time since deposition measurements. It was determined that the rate and extent of the hypsochromic shift was increased at higher temperatures and reduced at higher humidity levels. Despite the changes in the rate of the shift, the correlation between the hypsochromic shift and the age of the stain was still significant. Therefore with prior knowledge of a reasonable estimate of storage conditions, it may be possible to still obtain accurate estimations of the time since deposition. For samples exposed to relatively constant temperatures and humidity levels that could be more accurately measured (i.e. indoor environments), reference curves established from samples stored at similar conditions could be used to determine the time since deposition. However, it is more difficult to perform such an analysis or obtain reference samples for samples found in variable environments (i.e. outdoor environments). In outdoor settings, there are fluxuations in temperature, humidity and level of precipitation that may not be easily recorded. During our analysis of bloodstains that had been stored outside, we had to rely

on reported high and low temperatures and humidity levels since it was not possible to continuously monitor environmental changes. Upon comparison of the hypsochromic shift to reference samples closest to the approximated temperature, it was determined that the samples had been likely exposed to much higher temperatures than previously thought. This data, therefore, reflects the danger in relying on reported environmental conditions and indicates a necessity for constant monitoring of environmental conditions before time since deposition determinations can be made. This would not be feasible or practical with the current capabilities of and demands on operational forensic laboratories. However, these challenges represent technological obstacles and are not indicative of a failure of the developed strategy. If proper methods for the determination of the precise environmental conditions to which a sample was exposed can be developed, then accurate estimations of the time since deposition could be made.

Despite the ability of the hypsochromic shift to provide high resolution determinations of the time since deposition, it is limited to the analysis of bloodstains. Since other biological fluids are frequently encountered in forensic investigations, additional strategies needed to be developed to allow for a determination of the time since deposition of other forensically relevant fluids. We hypothesized that it could be possible to identify fluid-specific enzyme candidates and that the progressive loss of activity of the enzymes could provide an indication of the time since deposition of biological fluids. We successfully demonstrated that enzyme activity could be detected in dried bloodstains. A linear correlation between the age of the stain and the loss of enzyme activity was observed for six enzyme candidates (lactate dehydrogenase, malate

dehydrogenase, alcohol dehydrogenase, isocitrate dehydrogenase, phosphogluconate dehydrogenase, and glycerate dehydrogenase). While month differences in stain age were needed, the resolution of this method could be improved with the identification of additional enzyme candidates. While only bloodstains were used in initial testing as a proof-of concept, our findings support the potential future use of enzyme activity changes for the determination of the time since deposition of other forensically relevant biological fluids as well.

Currently, the methods routinely used in forensic casework for the identification of biological fluids in evidentiary items are costly in terms of time and sample and have varying degrees of sensitivity and specificity. Recently the use of molecular based body fluid identification methods, such as messenger RNA (mRNA) profiling based on tissue-specific gene expression, has been proposed to supplant conventional methods for body fluid identification [8-10,112-114]. While the advantages of mRNA profiling compared to conventional methods include greater specificity, improved timeliness, and the ability to perform simultaneous and semi-automatic analyses, the size of the amplification products used in these assays (~200-300 nt) and the significant amount of input RNA required for analysis (~50 ng) may not make this method well-suited for the analysis of low template forensic specimens. Recently, there has been increased scrutiny of a newly identified class of small non-coding RNAs, microRNAs (~20-25 nt in length) with numerous published studies reporting an identification of potential tissue-specific candidates. In this report, we demonstrated that miRNAs are present in total RNA isolates from body fluid stains in sufficient quantity for analysis and also provided the

first comprehensive evaluation of miRNA expression in forensically relevant biological fluids (blood, semen, saliva, vaginal secretions and menstrual blood) in an attempt to identify potentially body-fluid specific miRNAs. While no truly fluid-specific candidates were identified (in the sense of being present in one body fluid but completely absent in the others), we developed a panel of 9 differentially expressed miRNAs for the identification of the body fluid origin of biological stains. The normalized expression of each of the miRNA pairs exhibited a body fluid-specific expression pattern which allowed for an identification of the body fluid of interest.

The miRNA body fluid identification assays successfully detected the presence of biological material in aged and environmentally compromised samples as well as in simulated casework samples that included admixed body fluid samples, post coital samples and trace body fluid samples. While the results of this study support the potential future use of the miRNA profiling assays to identify the body fluid origin of forensic biological samples, it is recognized that additional work is needed prior to the utilization of miRNA profiling in forensic casework. Additional miRNA candidates for use in the body fluid identification assays need to be identified. From our initial screen of the 452 miRNAs, only a single strong candidate was identified for vaginal secretions and menstrual blood and no strong candidates for semen were identified. While the candidate used in the assays for each of these fluids still provide the ability to distinguish the body fluid of interest, the inclusion of stronger candidates would only serve to enhance our ability to do so. Since the initial evaluation of the 452 miRNAs, an additional ~300 miRNAs have been added to the miRNA database [115] and it is possible that better

candidates for each body fluid may be identified through an evaluation of these new miRNAs.

Due to the significantly smaller size of miRNAs compared to mRNAs, we hypothesized that miRNAs may be less susceptible to degradative processes (i.e. RNase digestion) and therefore more stable in aged, degraded or environmentally compromised samples. In order to test this hypothesis, total RNA extracts degraded with various RNase enzymes would need to be assessed using both miRNA and miRNA profiling assays in order to determine if stability differences can be observed. In additional to an evaluation of the stability differences between the difference classes of RNAs, a comprehensive evaluation of all currently available body fluid identification methods (serological, immunological, mRNA profiling, and miRNA profiling) would need to be conducted on compromised biological stains in order to fully determine the most suitable approach to body fluid identification of forensic specimens.

A positive body fluid identification using our current miRNA body fluid identification assays is determined by the proximity of the unknown sample to the cluster of known human biological samples. Typically an elliptical boundary was defined around the known body fluid sample clusters. Using this type of simplified approach, in some cases subjective calls for weakly positive samples needed to be made. In order to provide a robust objective approach for declaring the presence of a particular body fluid, more refined analysis interpretation metrics such as those based upon discriminant function analyses [116] will need to be developed.

The development of powerful and robust DNA typing strategies (STR analysis) has made it is possible to ascertain with a high degree of certainty whether a biological stain found at a crime scene originated from a particular individual. However, the standard profiling methods typically will fail to recover suitable genetic profiles from low template samples which contain less than 100 pg of template DNA (equivalent to approximately 15 diploid or 30 haploid cells). If profiles are recovered from these samples, interpretation is often difficult due to the occurrence of allelic drop-out or drop-in and significant peak height imbalance. The frequency of low template samples and the difficulty of interpretation warrant development of additional methodologies to allow for more successful recovery of genetic information. We have developed a "smart" low template sample analysis approach that utilizes laser capture micro-dissection to recover individual and few cells and enhanced amplification strategies to recover full autosomal and Y chromosome STR profiles from 2-5 epithelial cells and 5-10 sperm cells from single and multiple donor samples.

We had anticipated that the use of prior whole genome amplification strategies would allow for the recovery of genetic profiles from a smaller number of cells. However, surprisingly, an increase in sensitivity was not observed. Despite the inability to recover profiles from smaller numbers of cells, several advantages to prior whole genome amplification were observed. To obtain the high level of sensitivity without WGA methods, modified strategies were employed that are not currently utilized by operational crime laboratories. The use of the mIPEP amplification method allowed for subsequent use of standard conditions for downstream typing assays eliminating the need

for additional extensive validations of new methodologies. Without prior WGA amplification, micro-dissected cell lysates could only be used in a single STR amplification reaction thereby limiting the amount of genetic information that could be obtained. Sufficient quantities of template DNA was produced with prior mIPEP amplification to allow for aliquots of the same sample to be analyzed with multiple STR systems. This not only allowed for the recovery of an extended DNA profile (autosomal STRs, Y chromosome STRs), but also allowed for the reproducibility of the profile to be assessed through repeated amplifications. There is an occasional overlap between the loci included in the various multiplex systems and the concordance of genotypes recovered at these loci could therefore be established. Additionally, significant peak imbalance and allele drop in are observed and could incorrectly indicate the presence of a mixture. The presence of a random allele drop in from an adventitious allele could be established through repeated amplification of the same sample. If an additional allele at a particular locus was not observed in each of the multiple amplifications, it would be recognized as an artifact (allele drop-in) rather than a possible indicator of the presence of a minor contributor. Additionally, possible differences in allelic signal intensity within a heterozygous genotype may be observed between multiple amplifications of the same sample. If an allele was found in lower intensity in each of the multiple amplifications that it could suggest the presence of a minor contributor. However if each of the alleles was observed in higher intensity, it could suggest the presence of an imbalanced heterozygous type from a single donor. The resolution of these often challenging interpretations would not be possible without the use of prior WGA strategies.

Currently, there is much debate over the validity of low template sample analysis, with skeptics criticizing the reliability of any results obtained from such samples due to the encountered difficulties in profile interpretation [117-120]. However, rather than viewing potential weakness in low template sample analysis as reasons for its exclusion in forensic casework, we have viewed it as an opportunity for scientific advancement to overcome any perceived limitations. In this work, we have demonstrated the ability to obtain significant probative information (time since deposition, identification of the body fluid of origin, and recovery of genetic profiles) from low template samples. Based on our findings, we believe that, with further advancements, routine and reliable analysis of low template samples in forensic casework will be possible, perhaps even at a true cellular level.

CHAPTER SEVEN: CONCLUSION

In this study, we have identified novel DNA, RNA and protein biomarkers that allowed for the development of a "genetic eyewitness" to provide investigators with the "who", "what", and "when" of criminal offenses. We have identified a novel hypsochromic shift of the Soret band of hemoglobin spectral profiles that allows for a determination of the time since deposition of dried bloodstains. We also demonstrate the possibility of using a decline in enzyme activity to determine the age of biological stains. We have developed a novel strategy for the identification of the source of biological stains utilizing the differential expression of miRNAs. We have developed a "smart" low template sample analysis approach that utilizes laser capture micro-dissection to recover individual and few cells and enhanced amplification strategies to recover full autosomal and Y chromosome STR profiles from 2-5 epithelial cells and 5-10 sperm cells. Additionally, the development of a novel whole genome amplification method ('modified improved primer extension pre-amplification' or mIPEP) to be used prior to the locus specific PCR amplifications resulted in the ability to perform multiple amplifications of the same micro-dissected cell sample and resulted in a greater recovery of heterozygous genotypes at individual loci. The novel biomarkers and profiling strategies described in this report provide the basis for the establishment of a molecular "genetic eyewitness" from low template forensic samples. The strategies presented here not only provide more sensitive and reliable means by which to analyze low template samples, but also provide an indication that with continued progress it may be possible to perform routine forensic analyses on single cells.

APPENDIX A: FIGURES

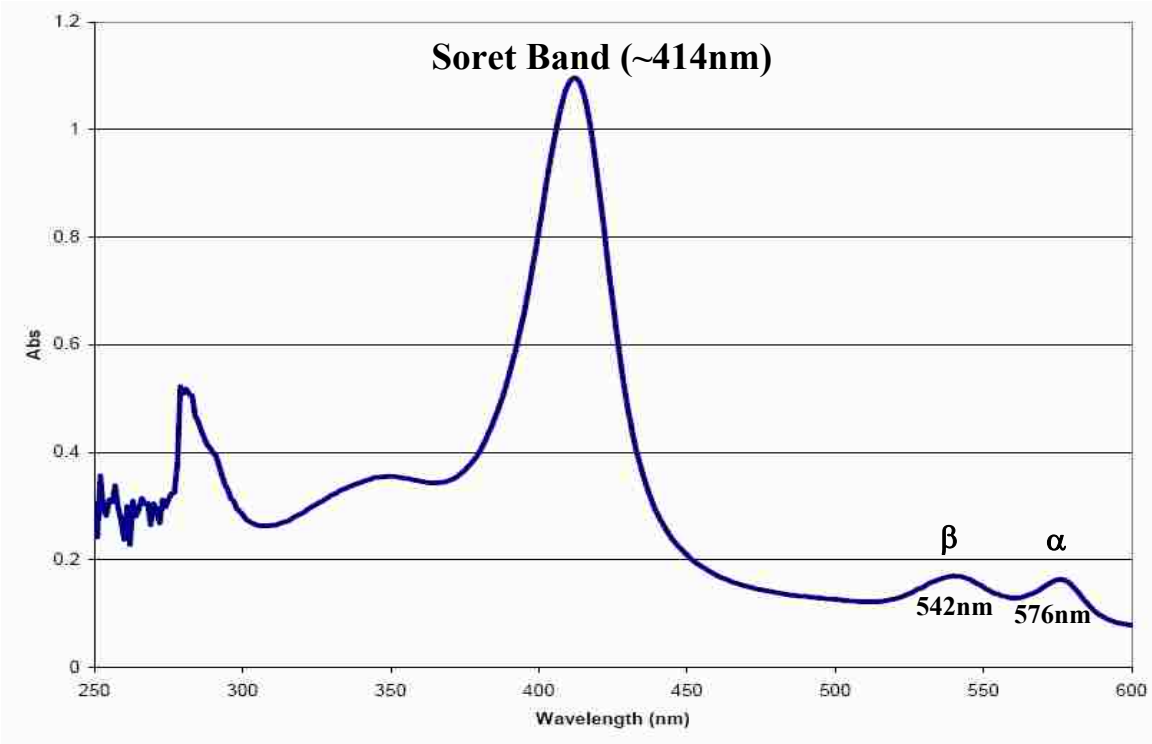

Figure 1. Characteristic UV-VIS Spectral Profile of Hemoglobin

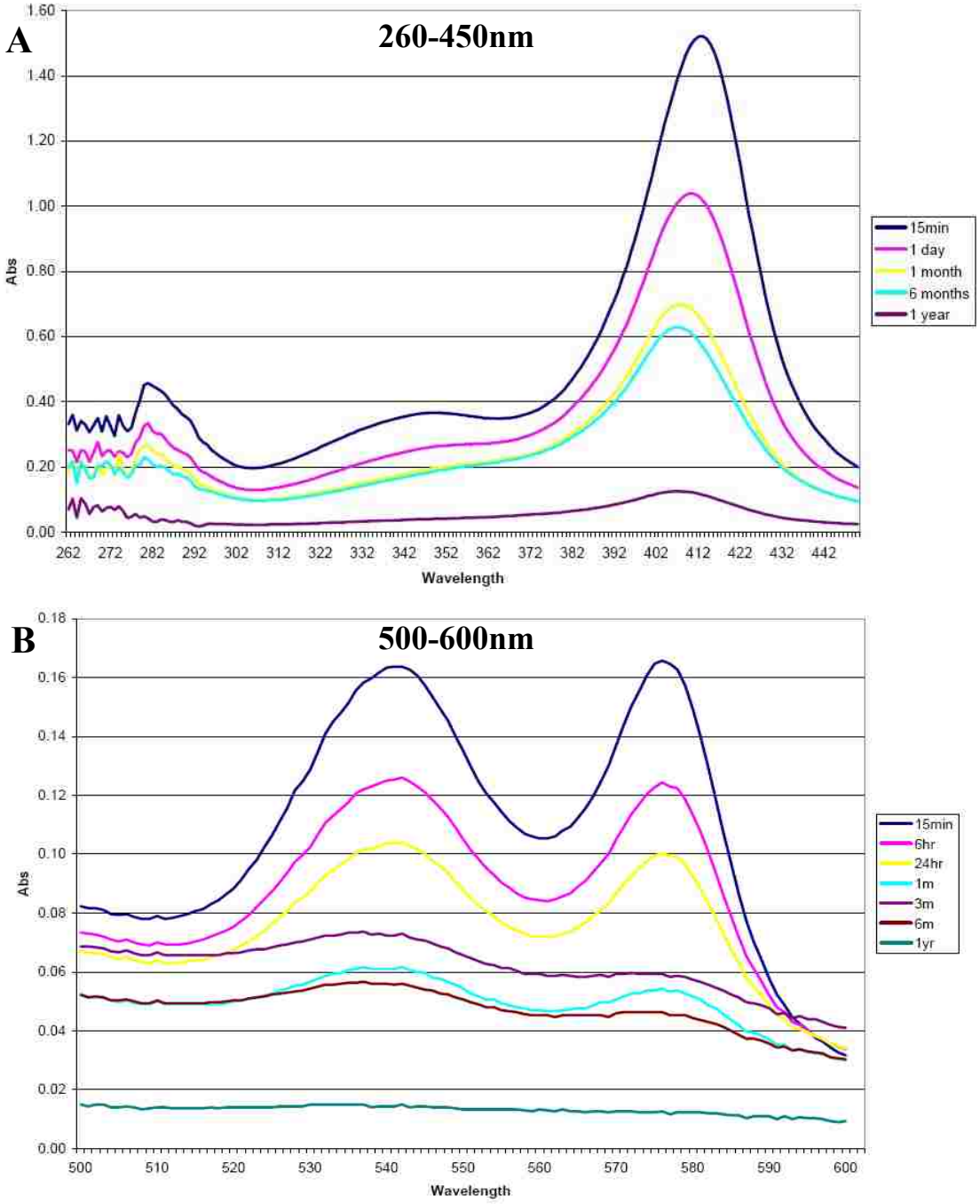

Figure 2. Changes in UV-VIS Spectral Profile of Hemoglobin in Aged Bloodstains

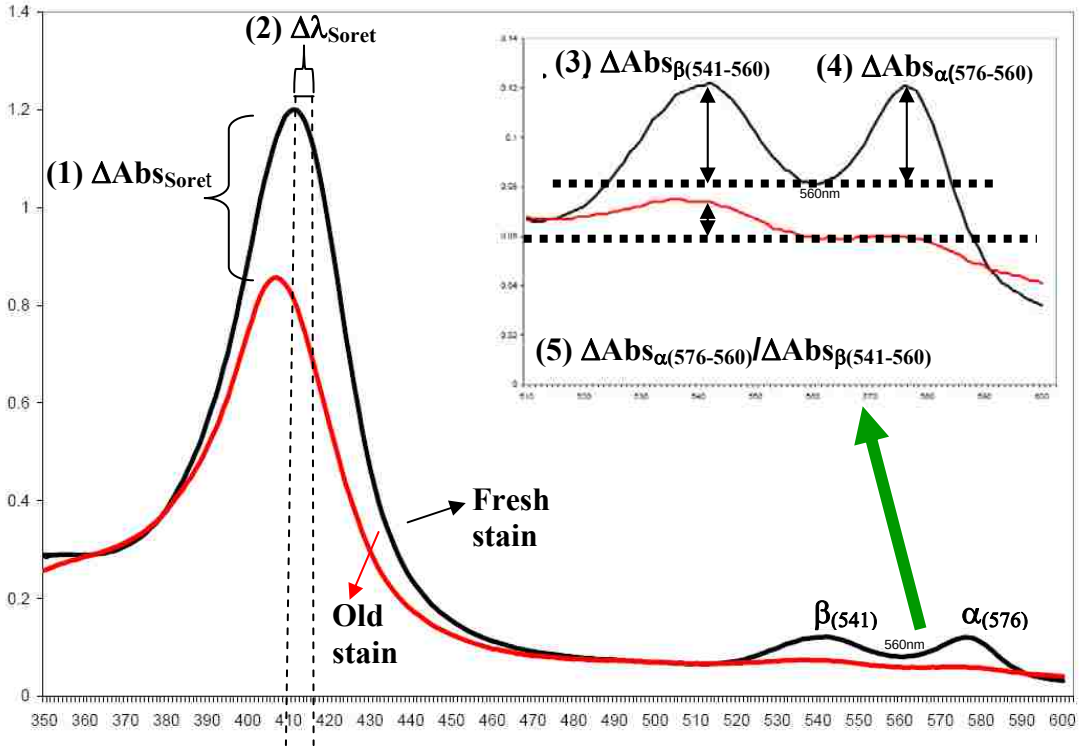

Figure 3. Hemoglobin Spectral Shift Parameters

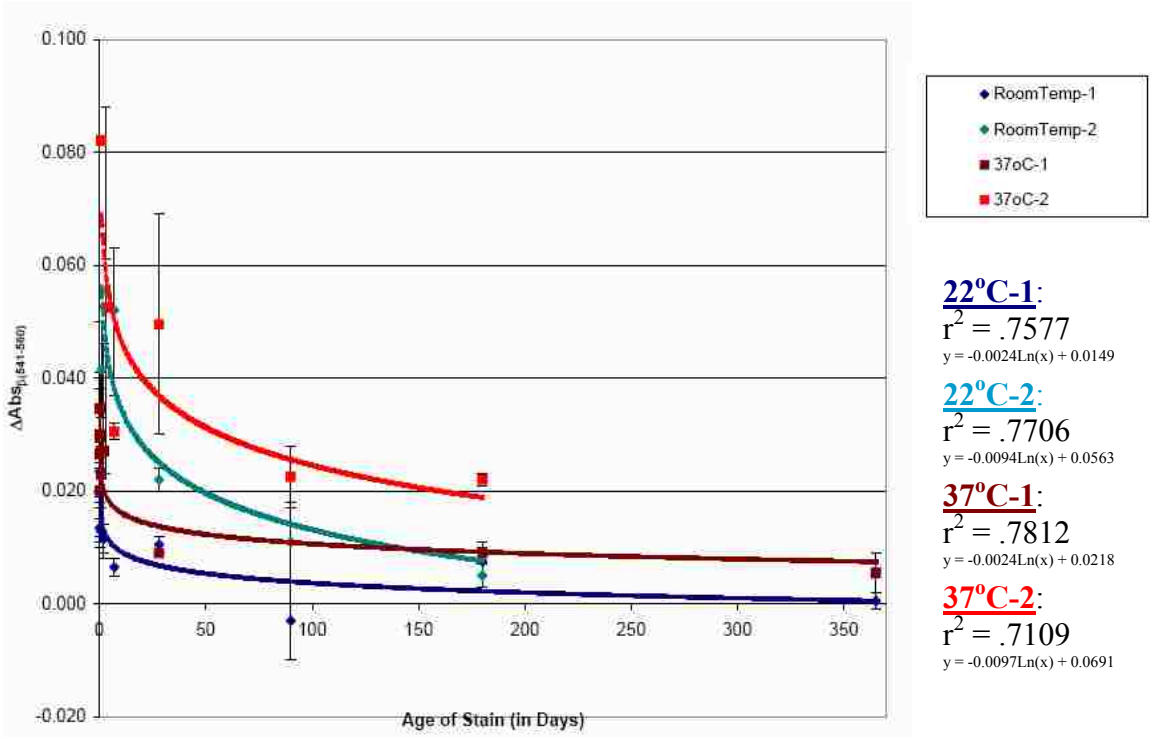

Figure 4. $\Delta Abs_{\beta(541\text{-}560)}$ for Bloodstains Stored at 22°C and 37°C

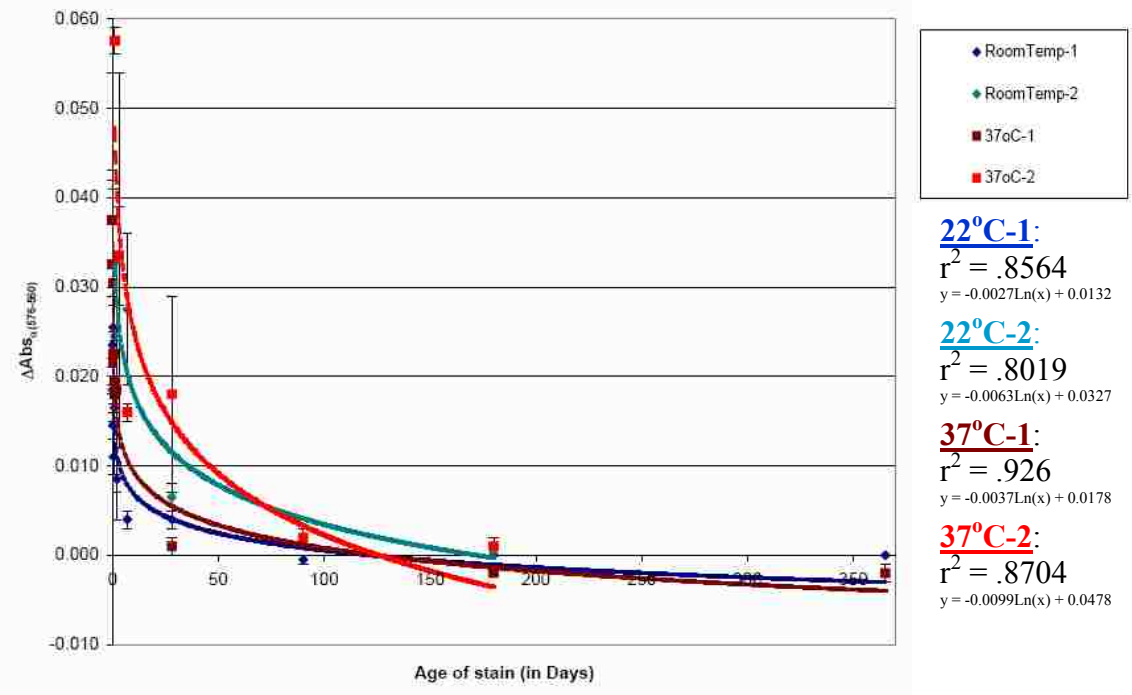

Figure 5. $\Delta Abs_{\alpha(576\text{-}560)}$ for Bloodstains Stored at 22°C and 37°C

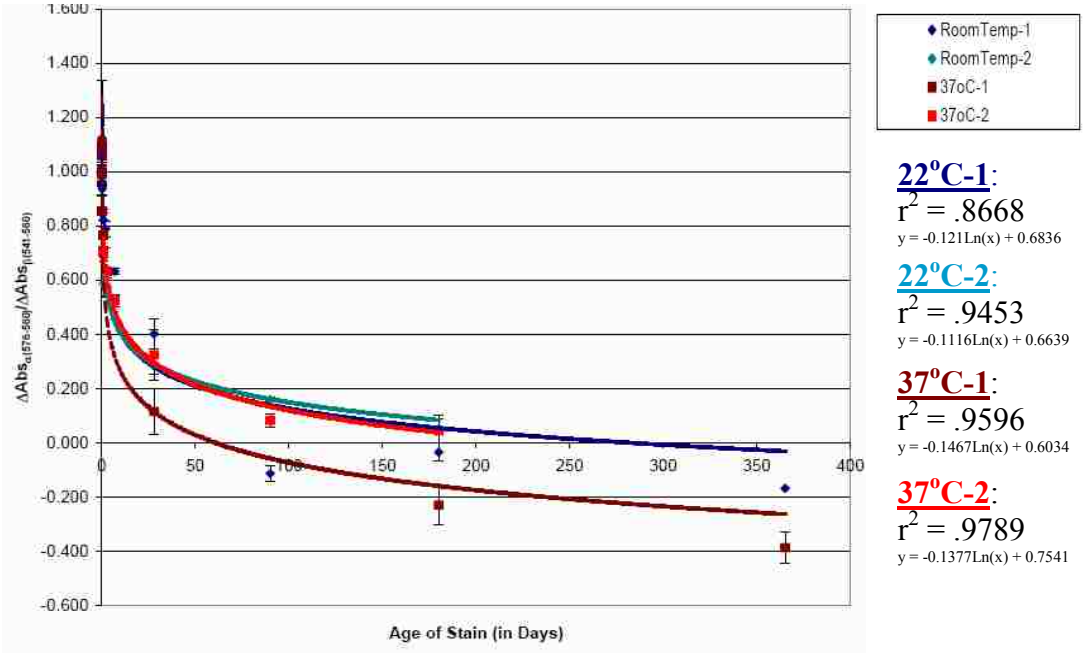

Figure 6. $\Delta Abs_{\alpha(576-560)}/\Delta Abs_{\beta(541-560)}$ for Bloodstains Stored at 22°C and 37°C

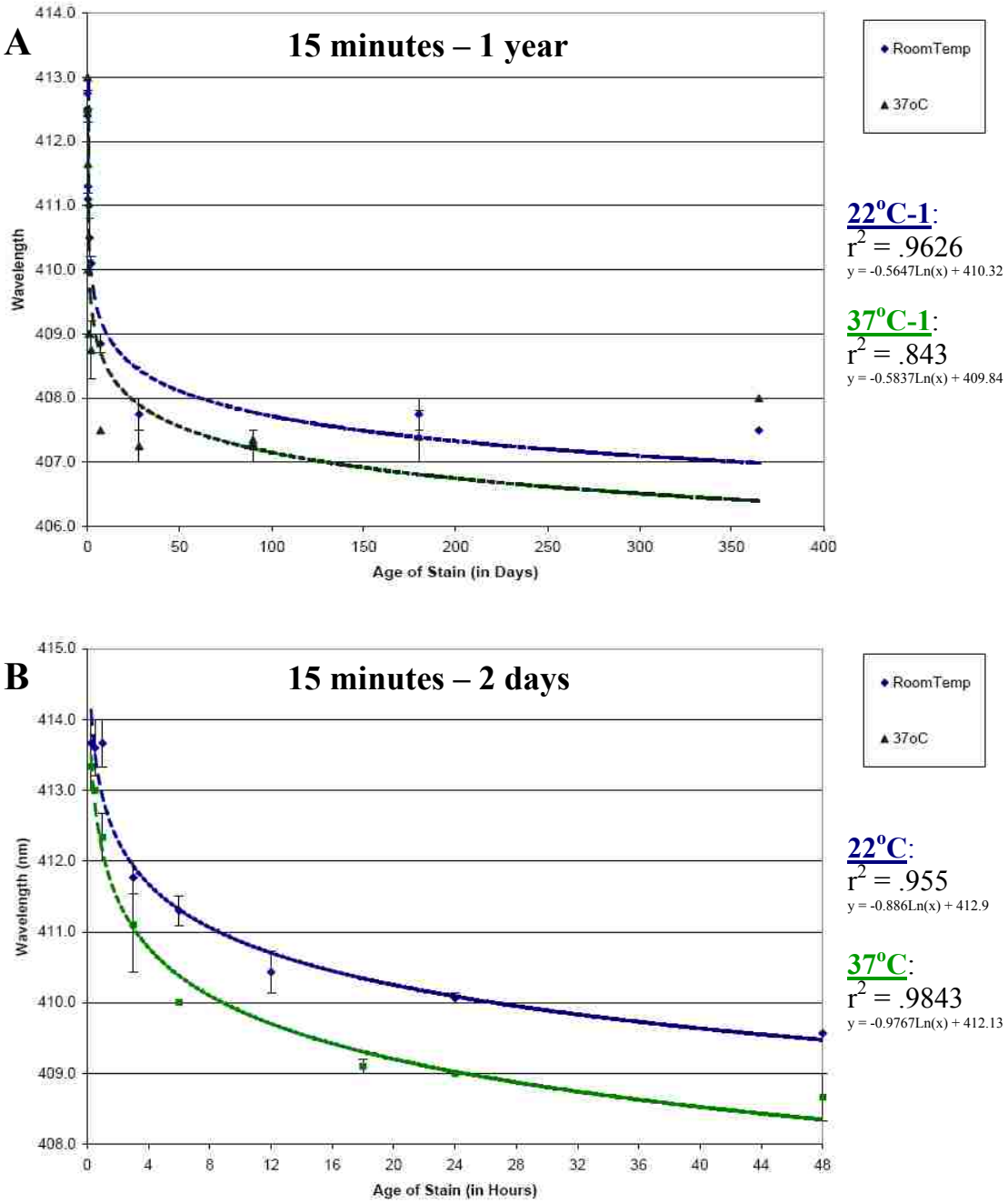

Figure 7. ΔλSoret for Bloodstains Stored at 22°C and 37°C

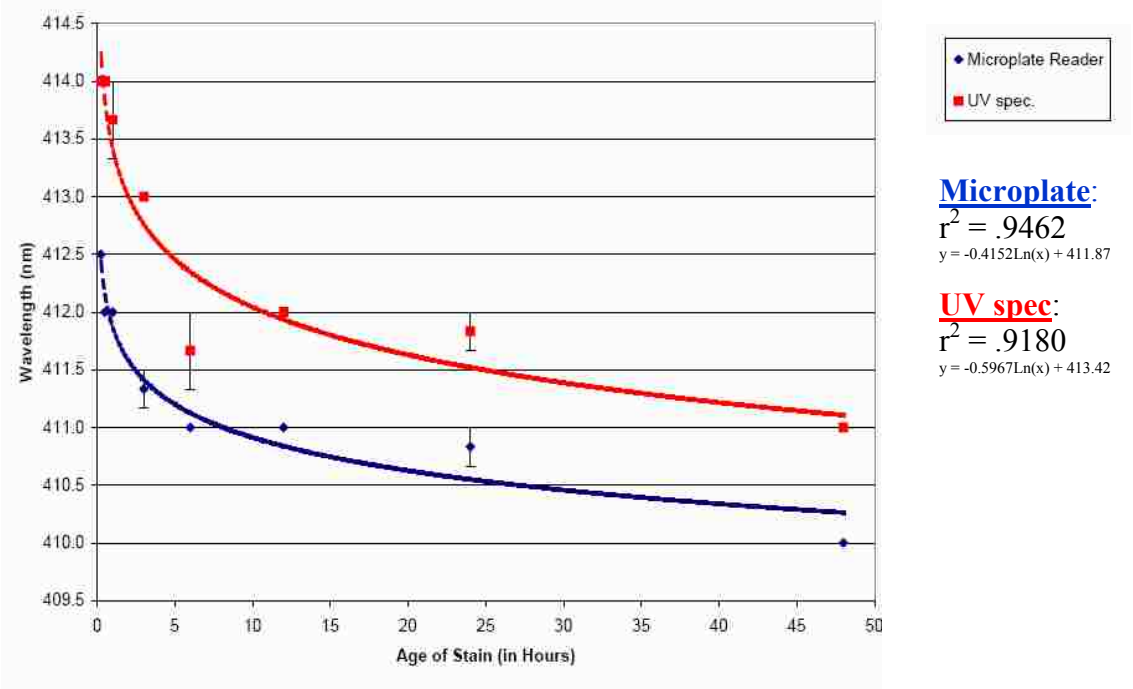

Figure 8. Comparison of ΔλSoret Measurements Using Two Different Spectrophotometers

Figure 9. MicroClimate(R) Humidity Chamber MCH-3

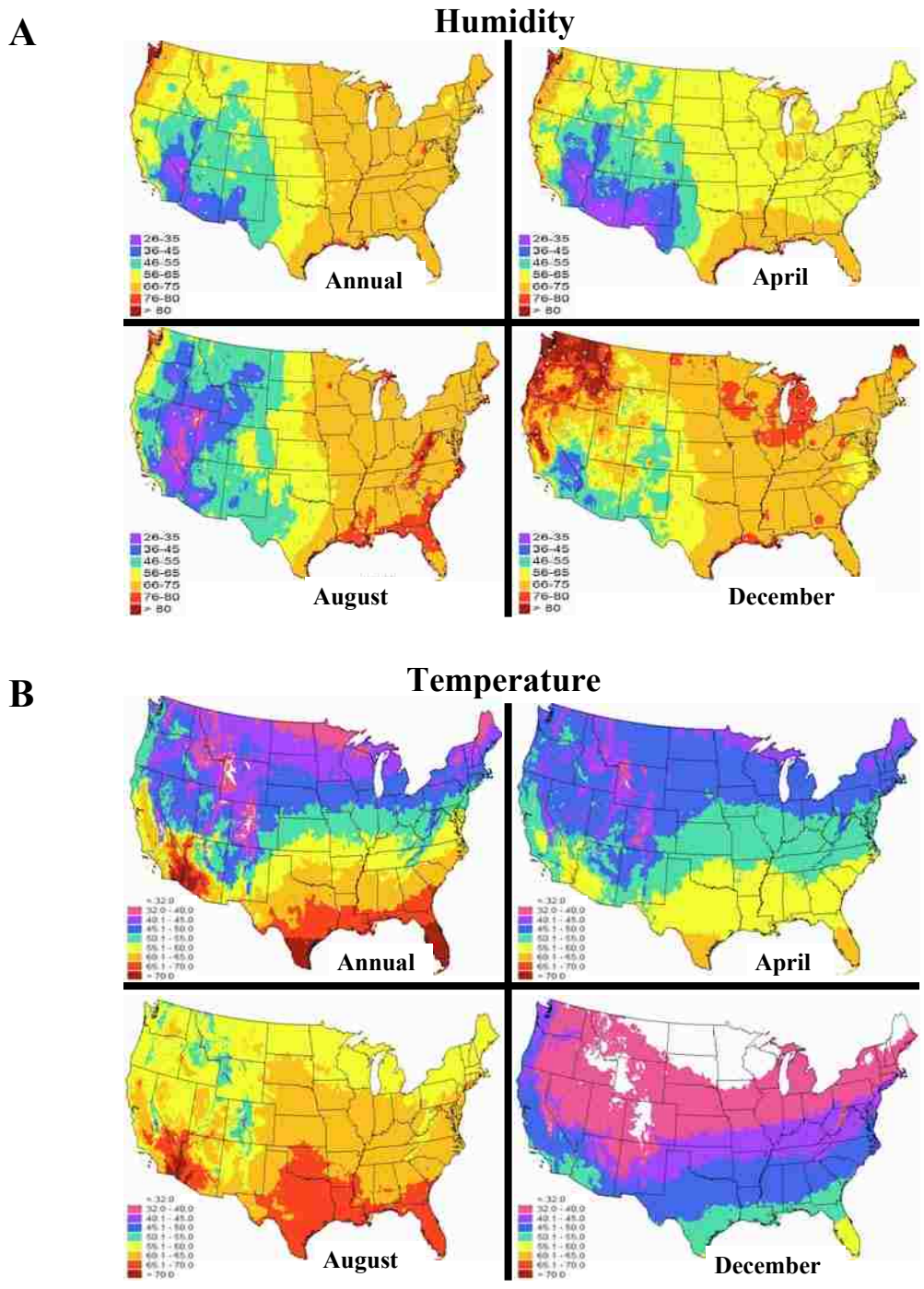

Images generated from public website: http://cdo.ncdc.noaa.gov/cgi-bin/climaps/climaps.pl

Figure 10. National Mean Relative Humidity and Mean Daily Temperature (1961-1990)

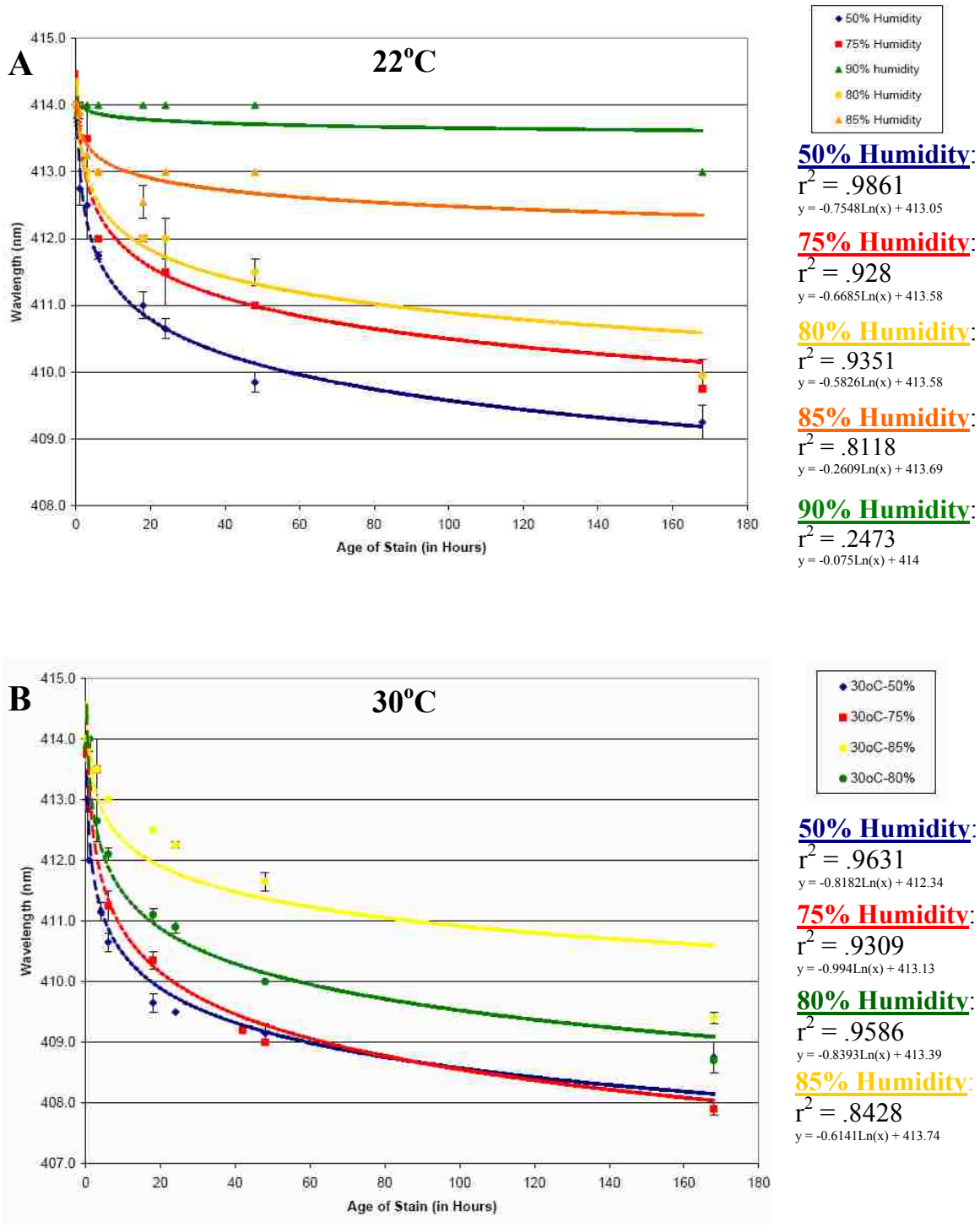

Figure 11. Effects of Humidity on ΔλSoret Measurements for Bloodstains Stored at 22°C and 30°C

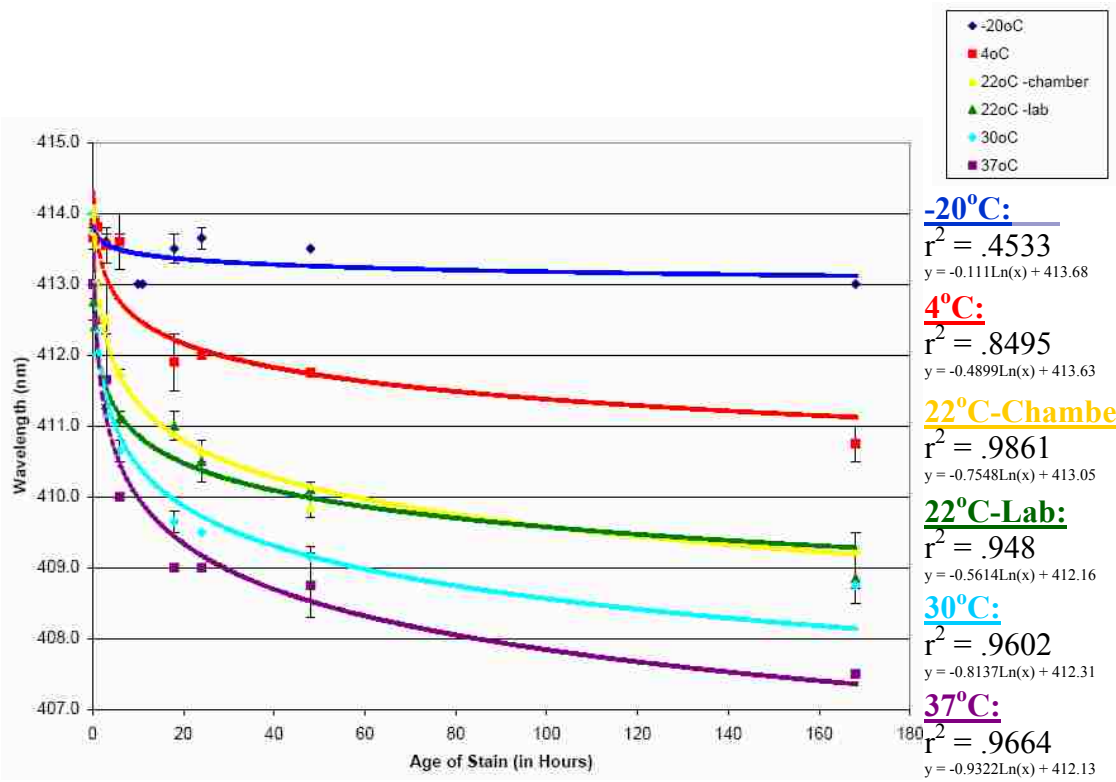

Figure 12. Effects of Temperature on ΔλSoret Measurements for Bloodstains Stored at 50% Humidity

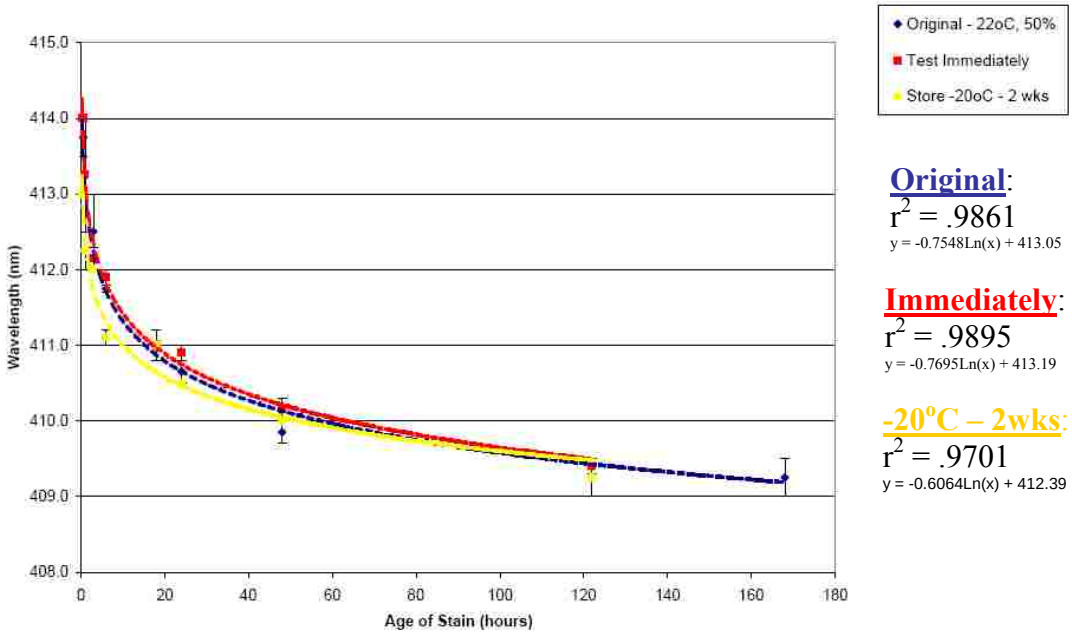

Figure 13. Effects on ΔλSoret from Length of Storage Prior to Analysis

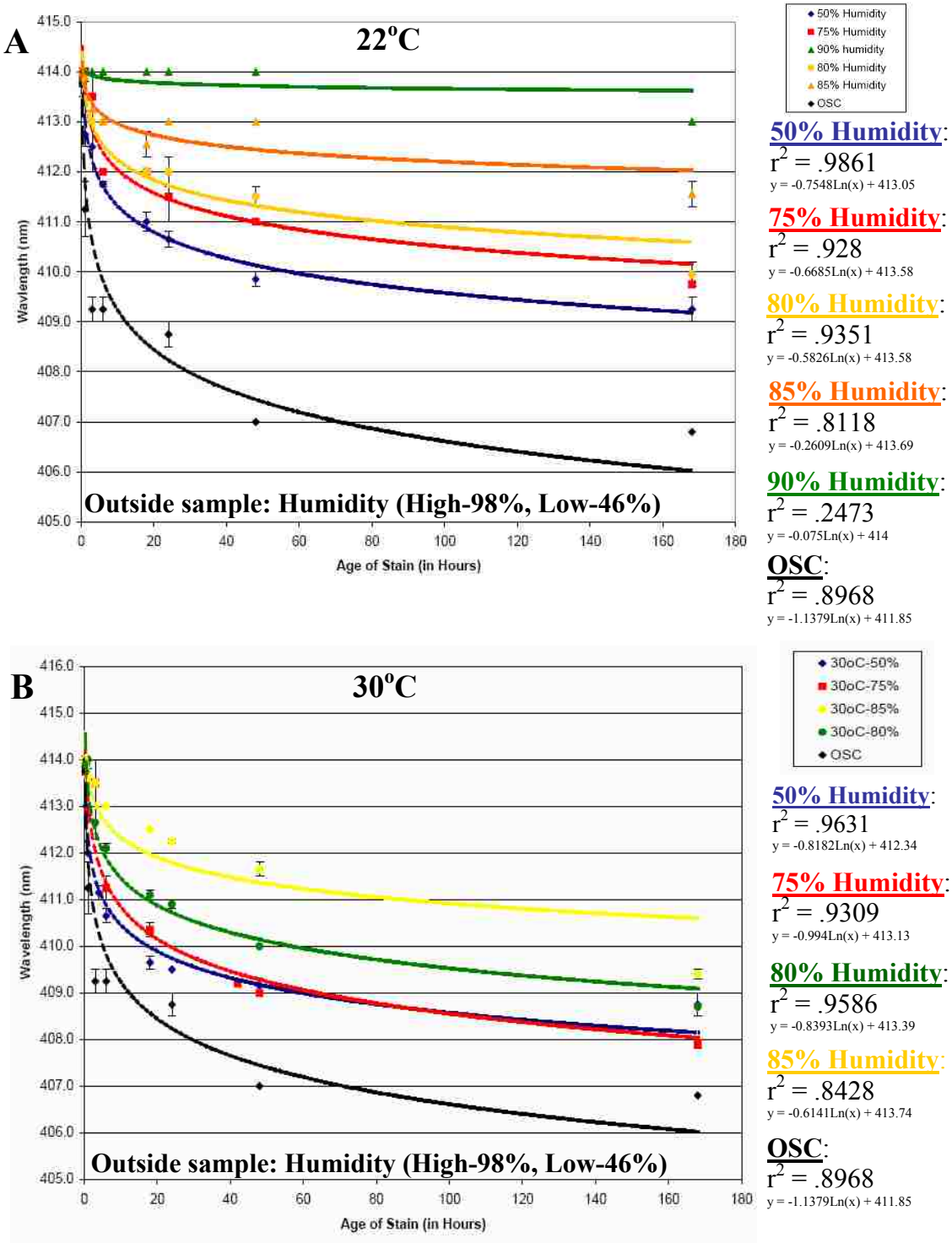

Figure 14. Effects of Outside Storage on ΔλSoret Measurements Compared to Storage at 22°C and 30°C

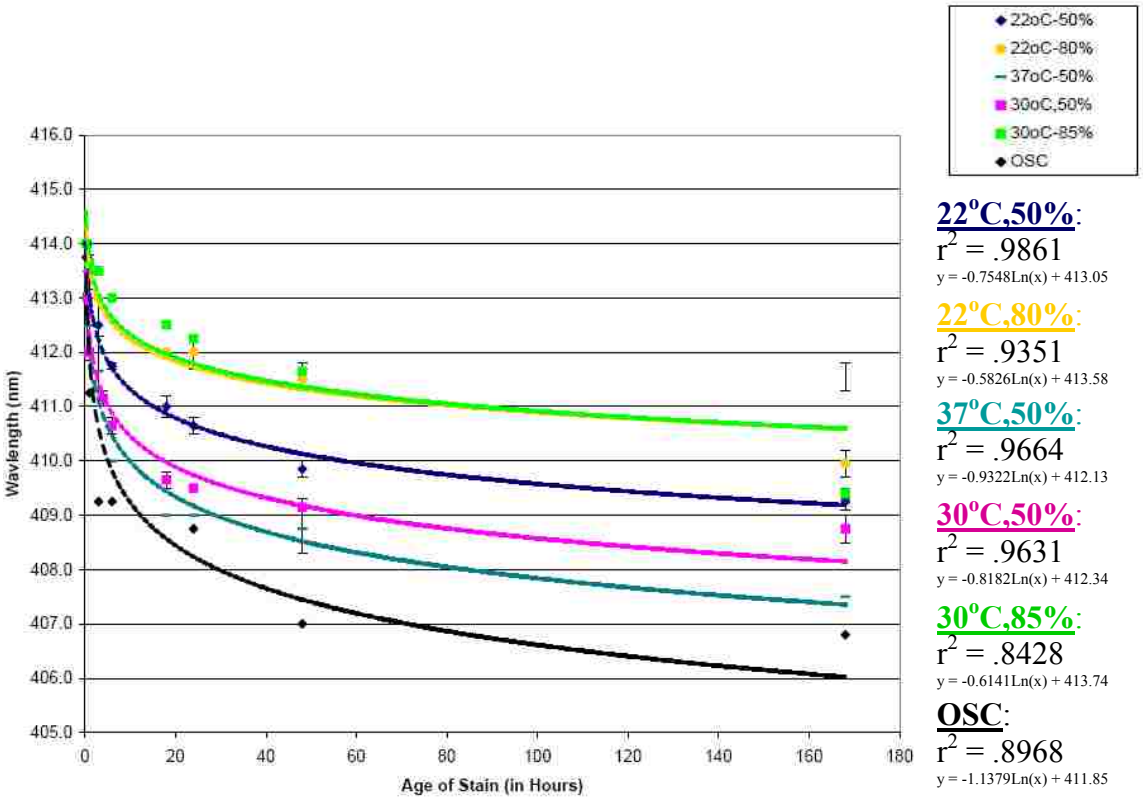

Figure 15. Effects of Outside Storage on ΔλSoret Measurements Compared to Bloodstains Stored at 22°C, 30°C, and 37°C

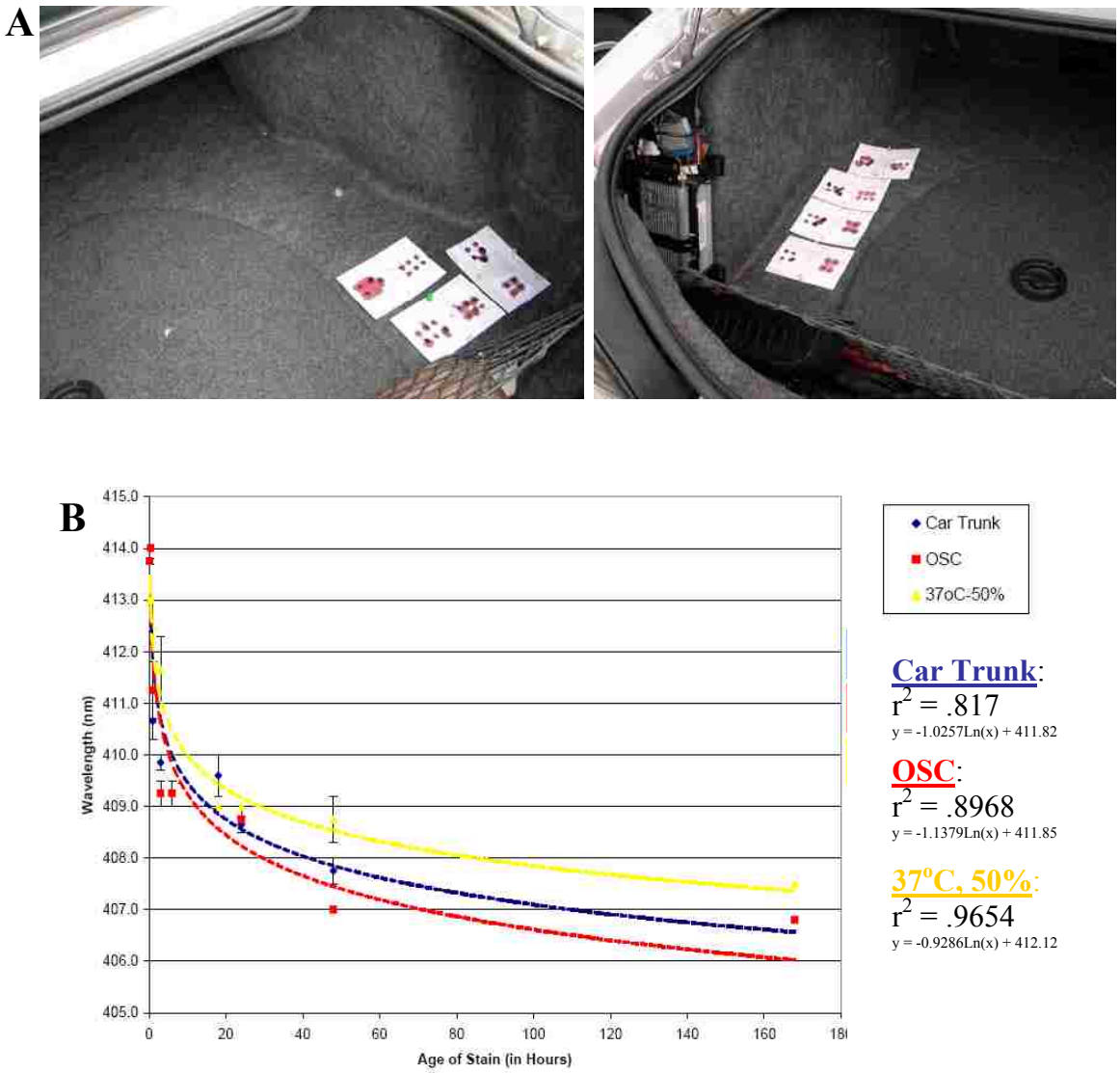

Figure 16. ΔλSoret Measurements from Bloodstains Located in Car Trunk

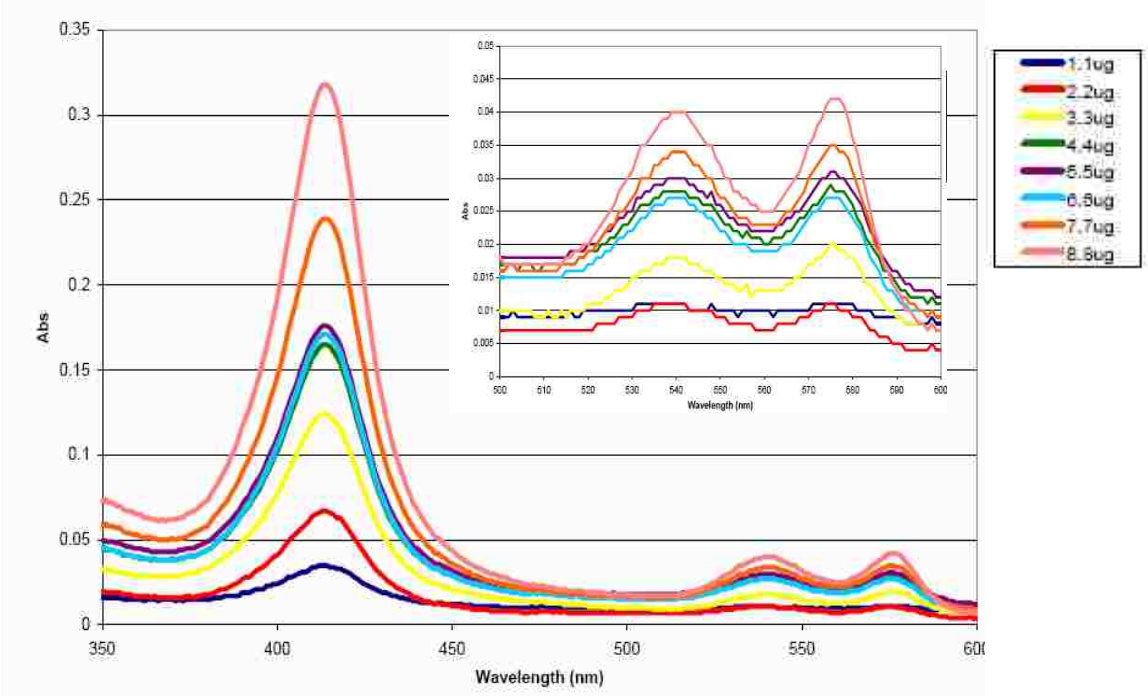

Figure 17. Hb Spectral Profiles Using a Range of Total Protein Input Amounts

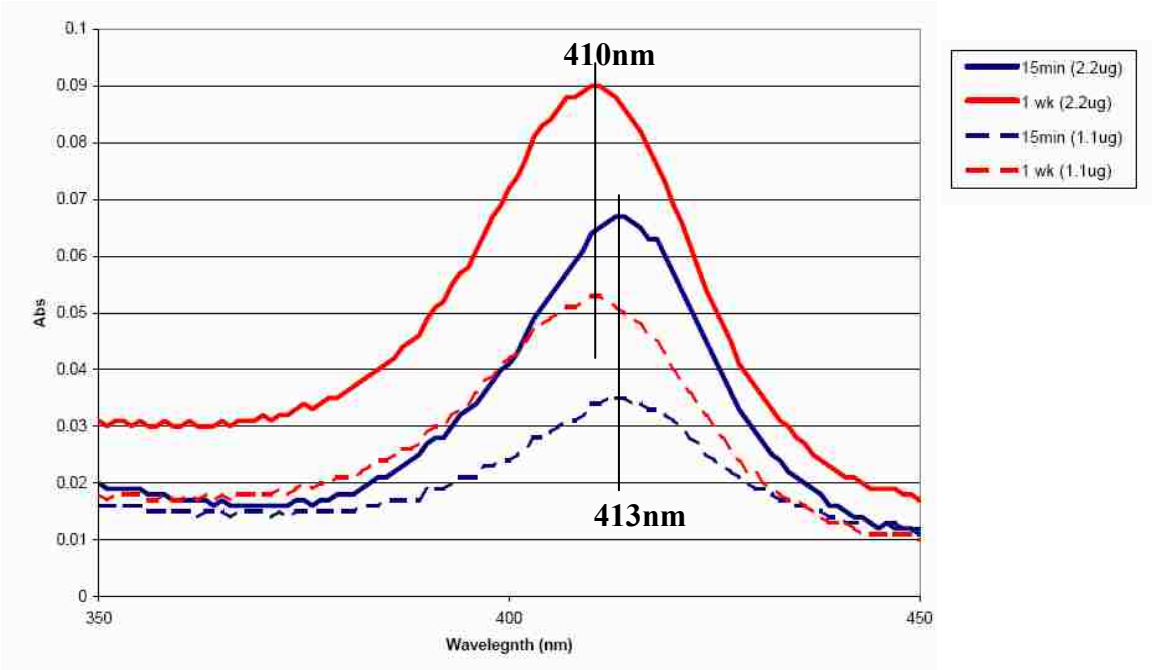

Figure 18. Sensitivity of ΔλSoret Measurements - Total Protein Input

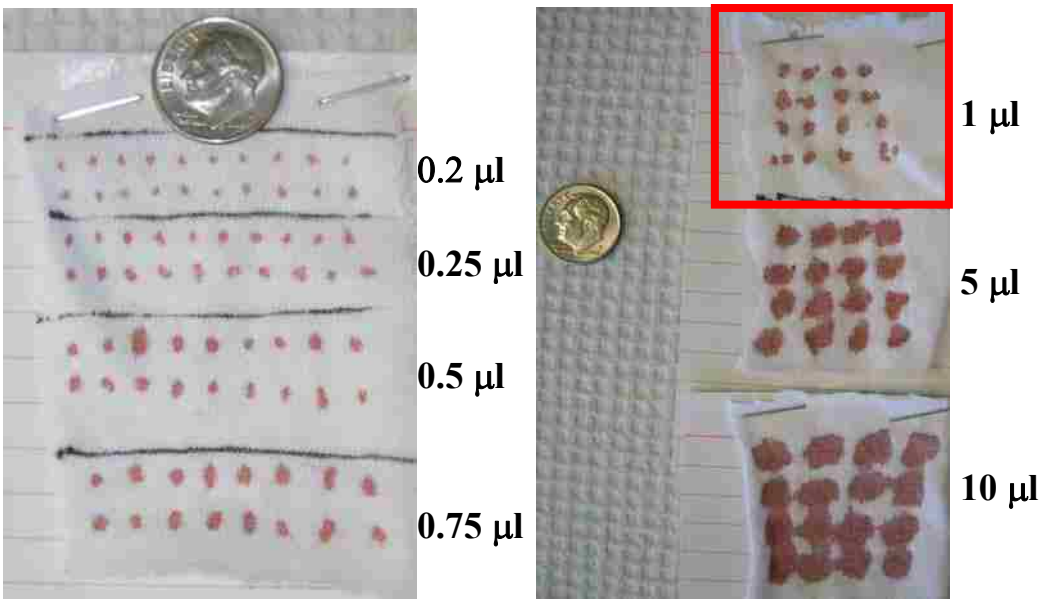

Figure 19. Size of Bloodstains Used to Determine the Sensitivity of the ΔλSoret Assay

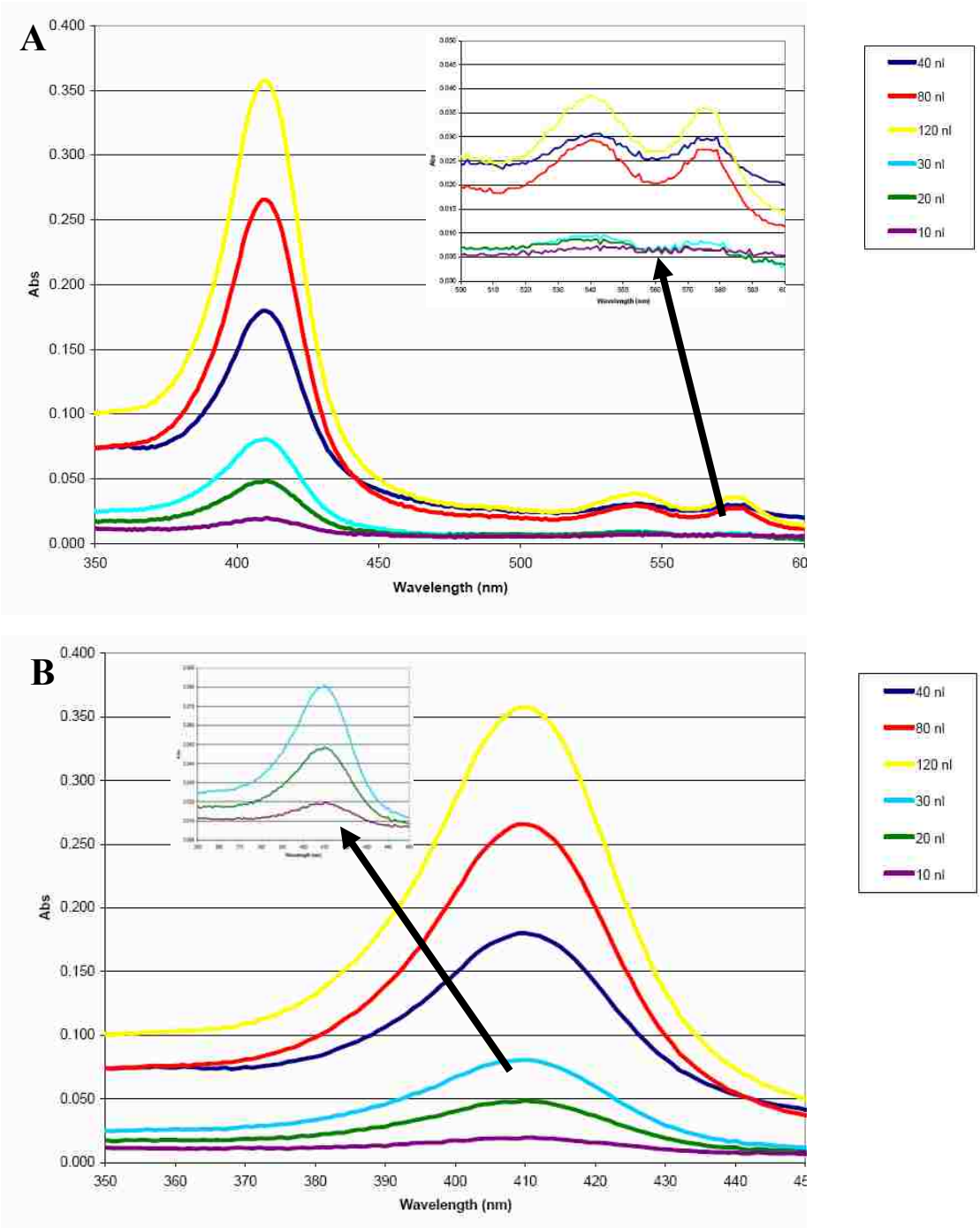

Figure 20. UV-VIS Spectral Profiles from 1 μl Bloodstains Using Nanoliter Input Volumes

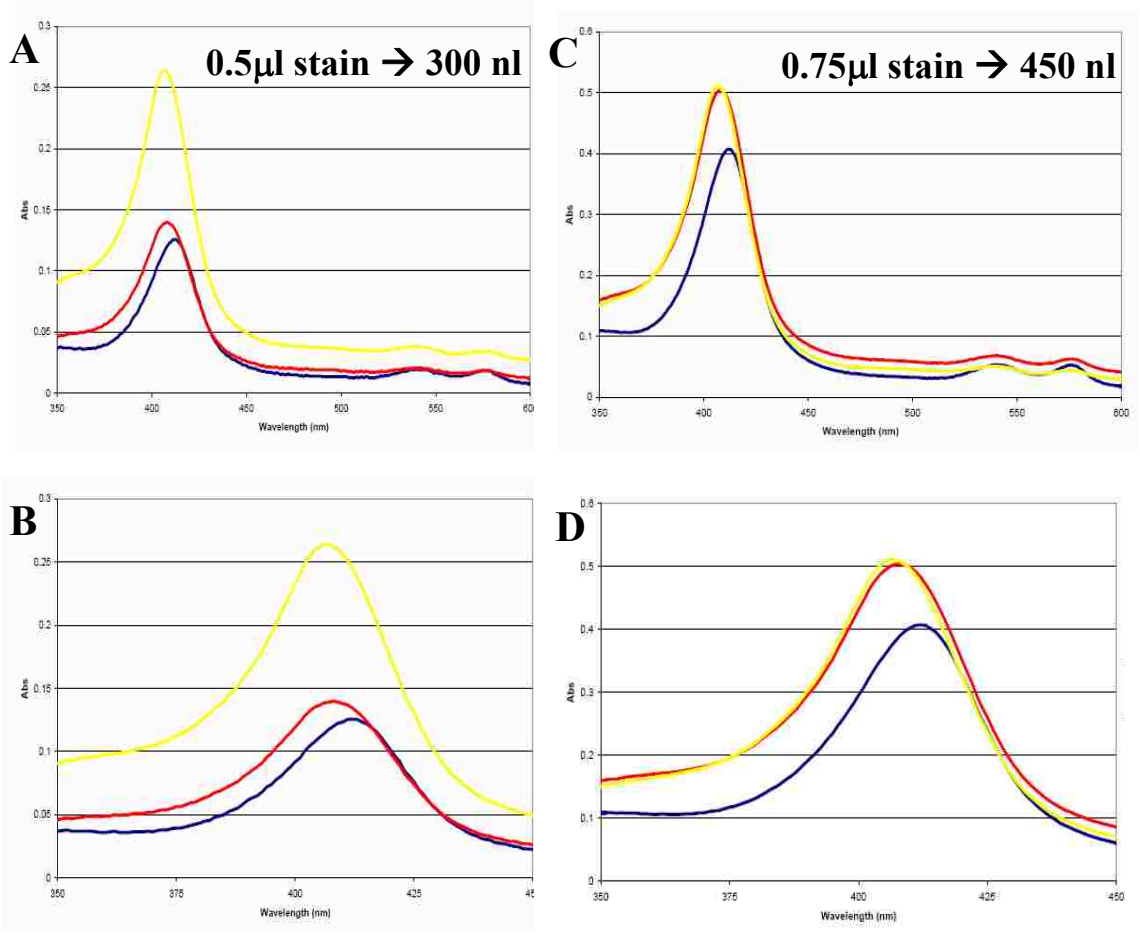

Figure 21. UV-VIS Spectral Profiles from 0.5 and 0.75 µl Bloodstains

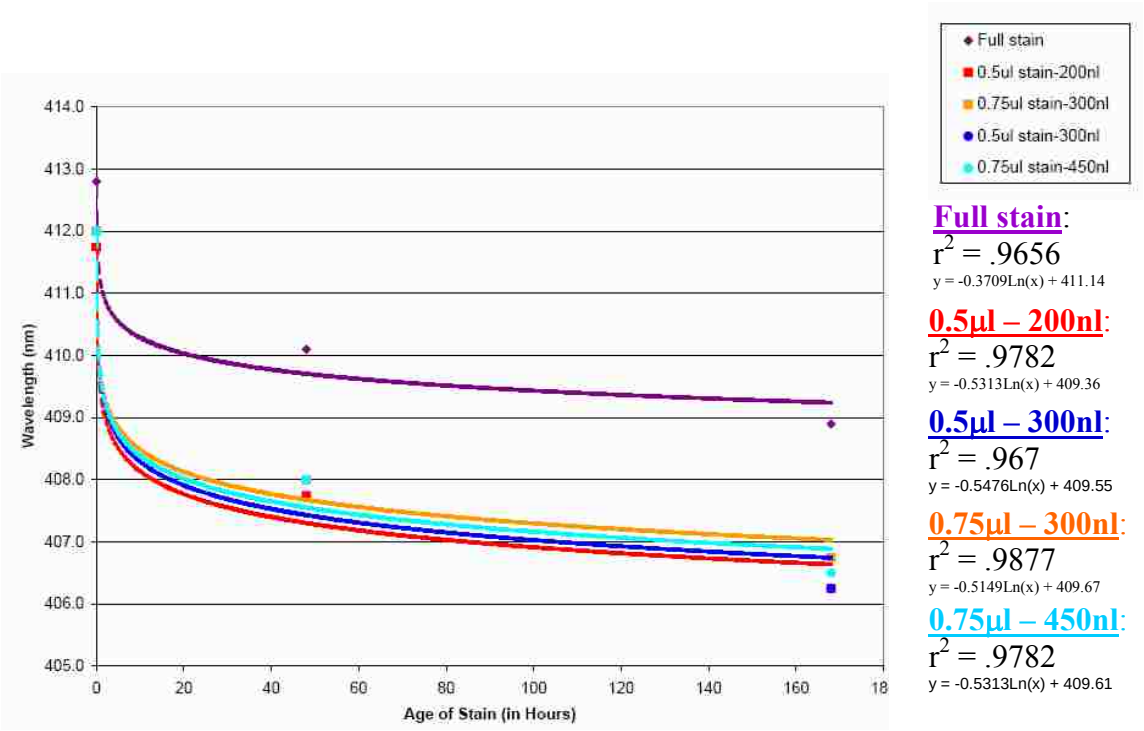

Figure 22. Accuracy of ΔλSoret Measurements from 0.5 and 0.75 µl Bloodstains

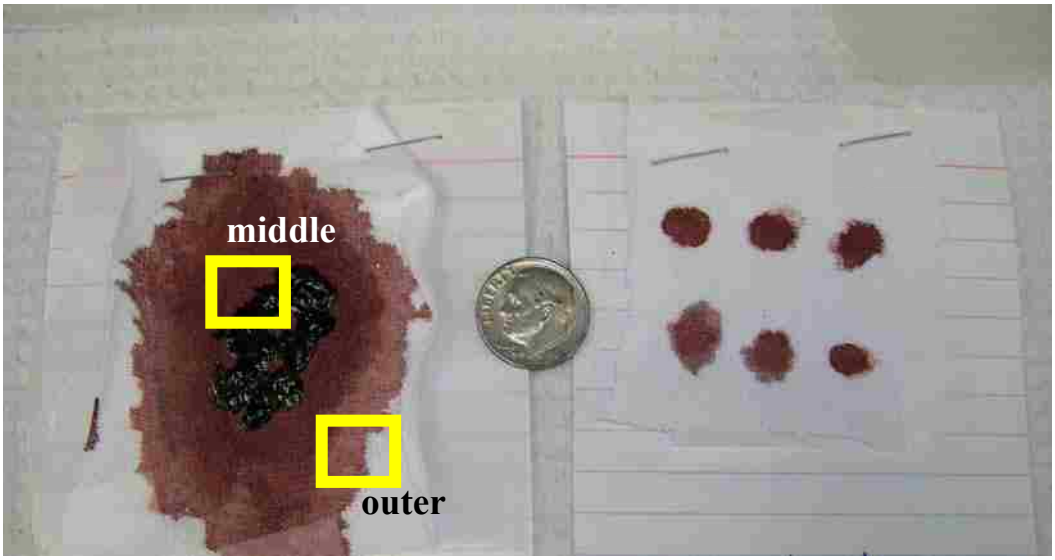

Large = ~600 µl **Small = ~60 µl**

Figure 23. Appearance of Large and Small Bloodstains

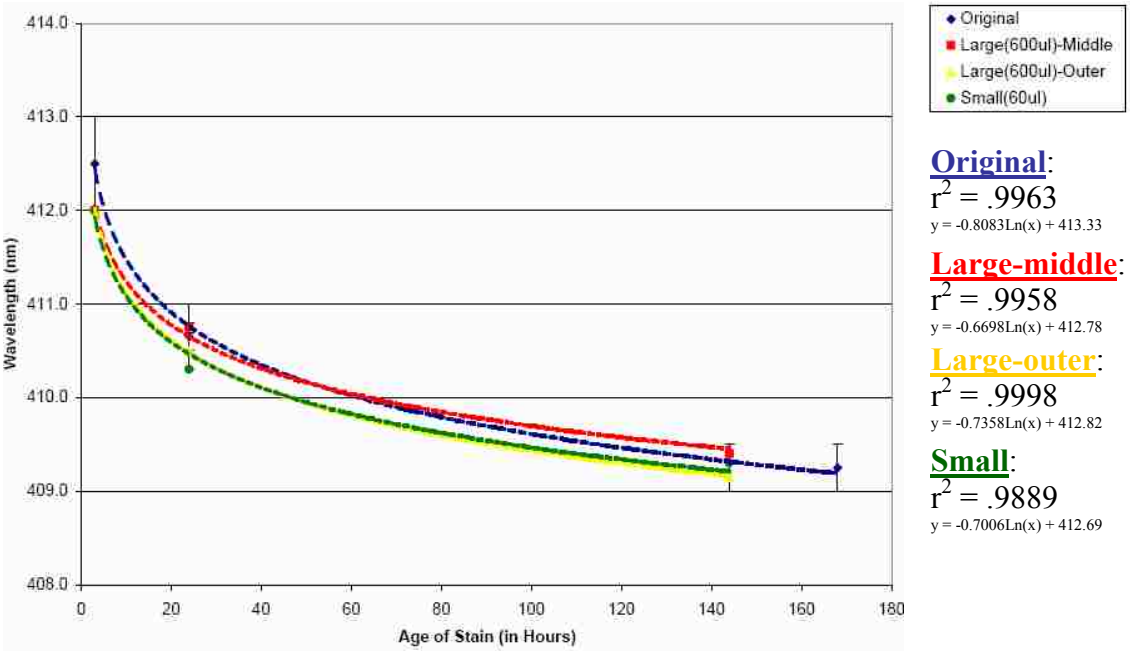

Figure 24. Effects of Bloodstain Size on ΔλSoret Measurements

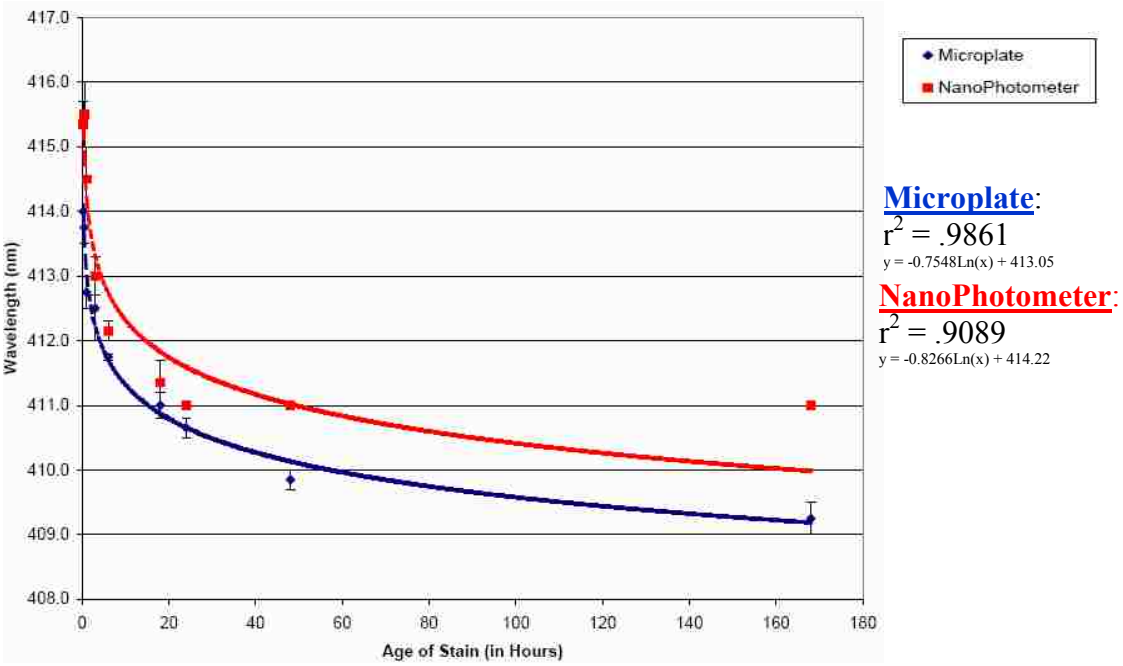

Figure 25. Comparison of the Accuracy of ΔλSoret Measurements Using a Bench-Top and Portable Spectrophotometer

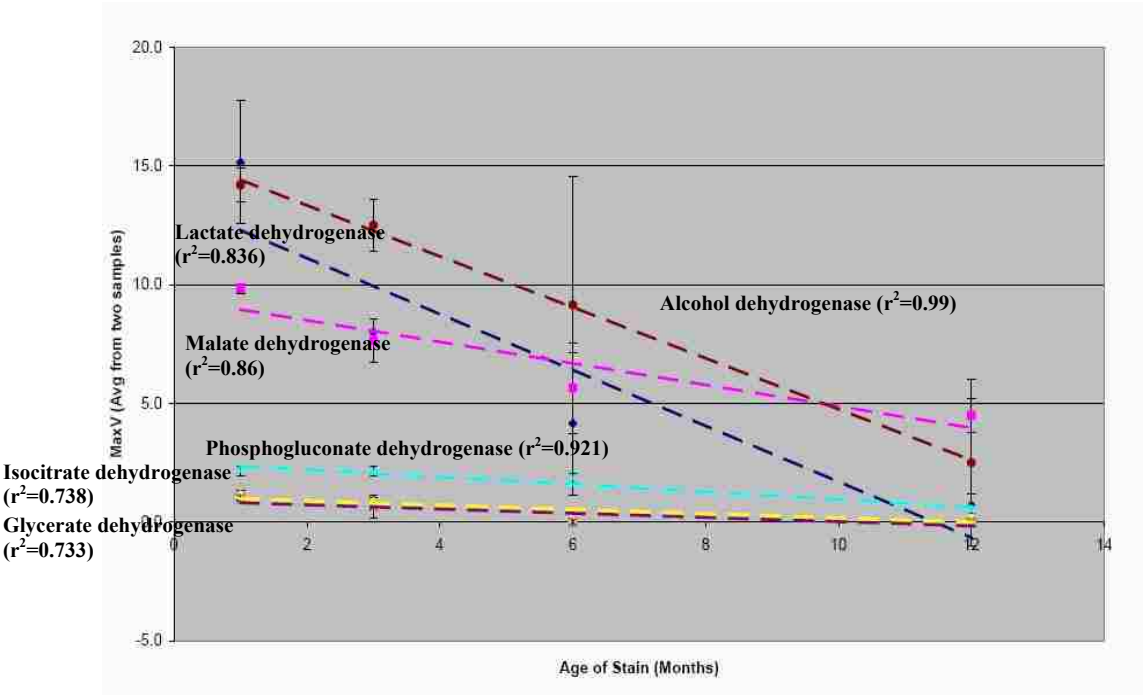

Figure 26. Decline in Enzyme Activity in Aged Bloodstains

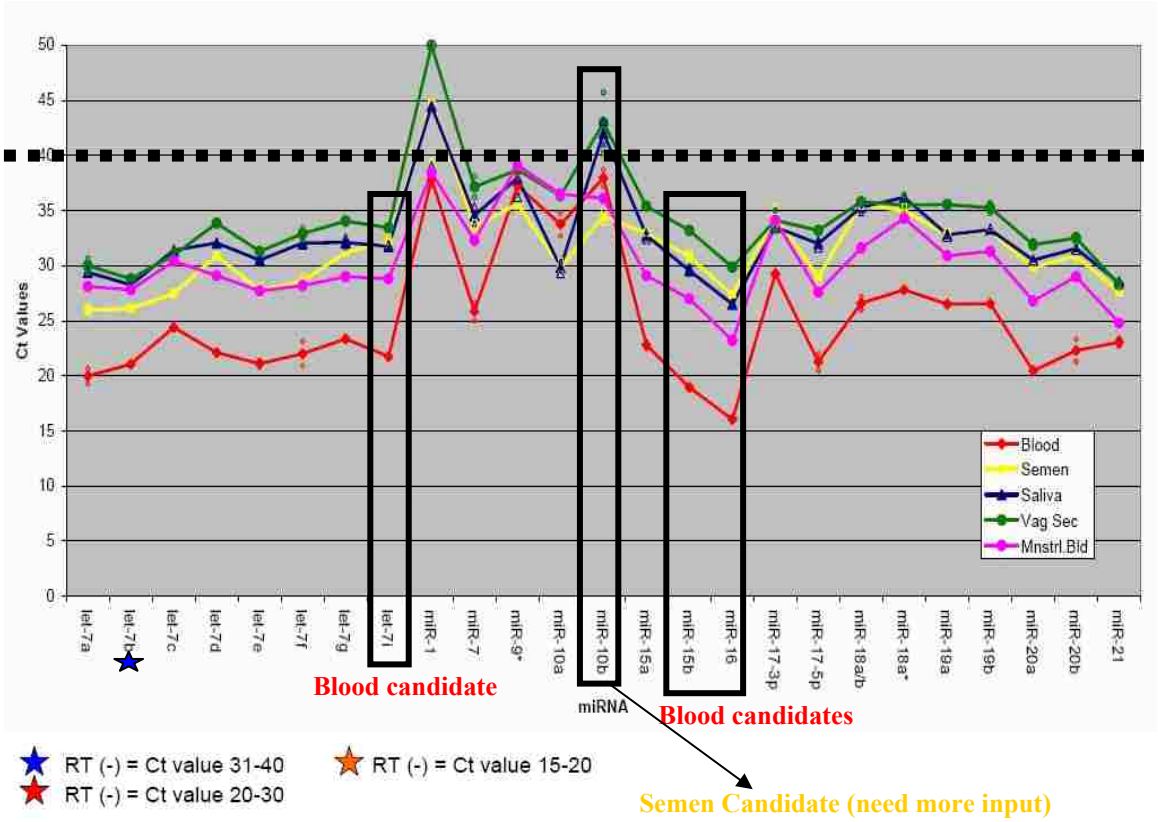

Figure 27. Determination of the Differential Expression of miRNAs in Forensically Relevant Biological Fluids

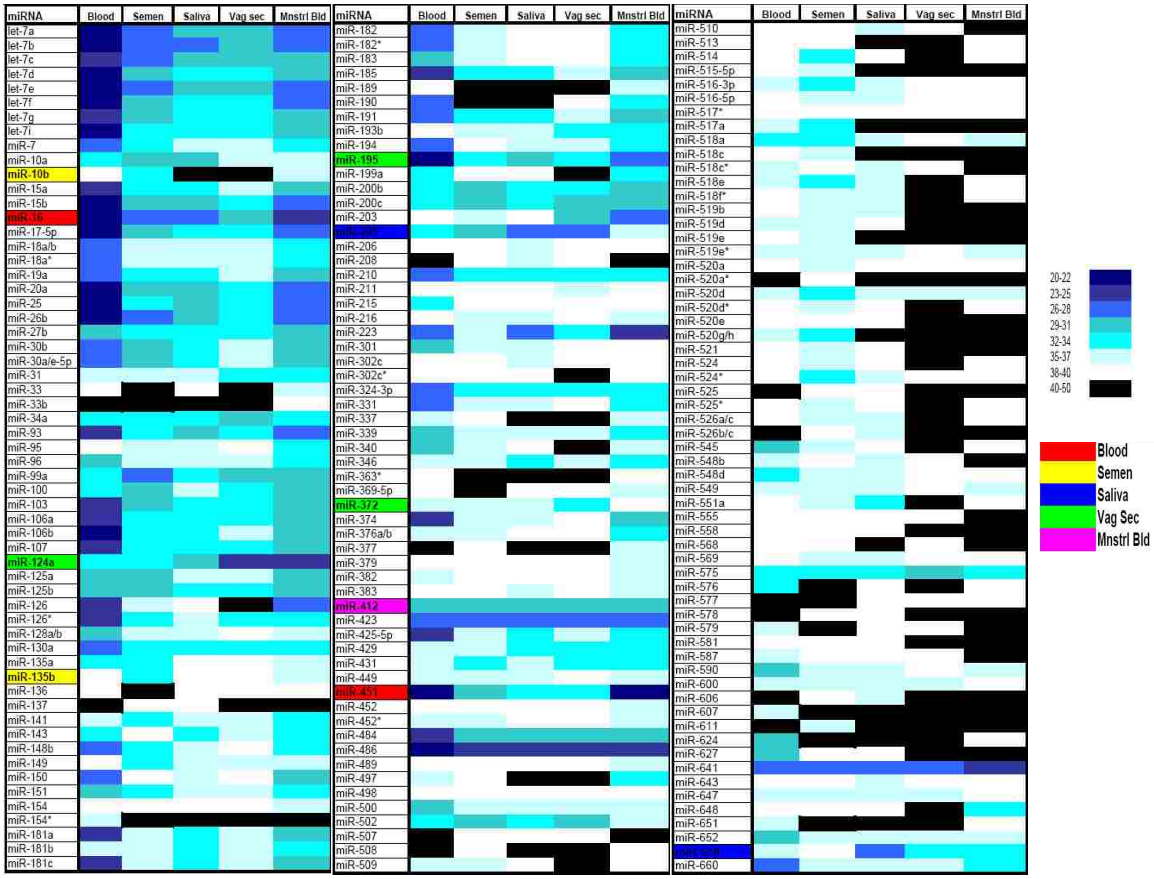

Figure 28. miRNA Expression Heat Map

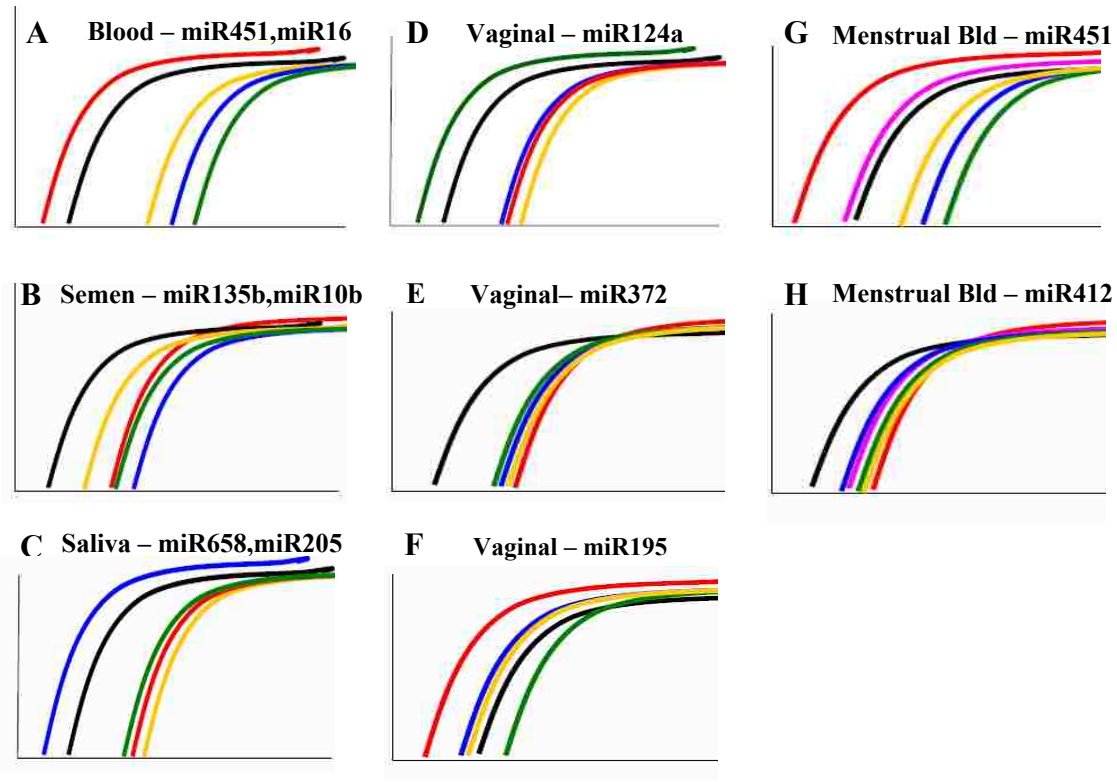

Figure 29. Relative Expression of miRNA Body Fluid Candidates

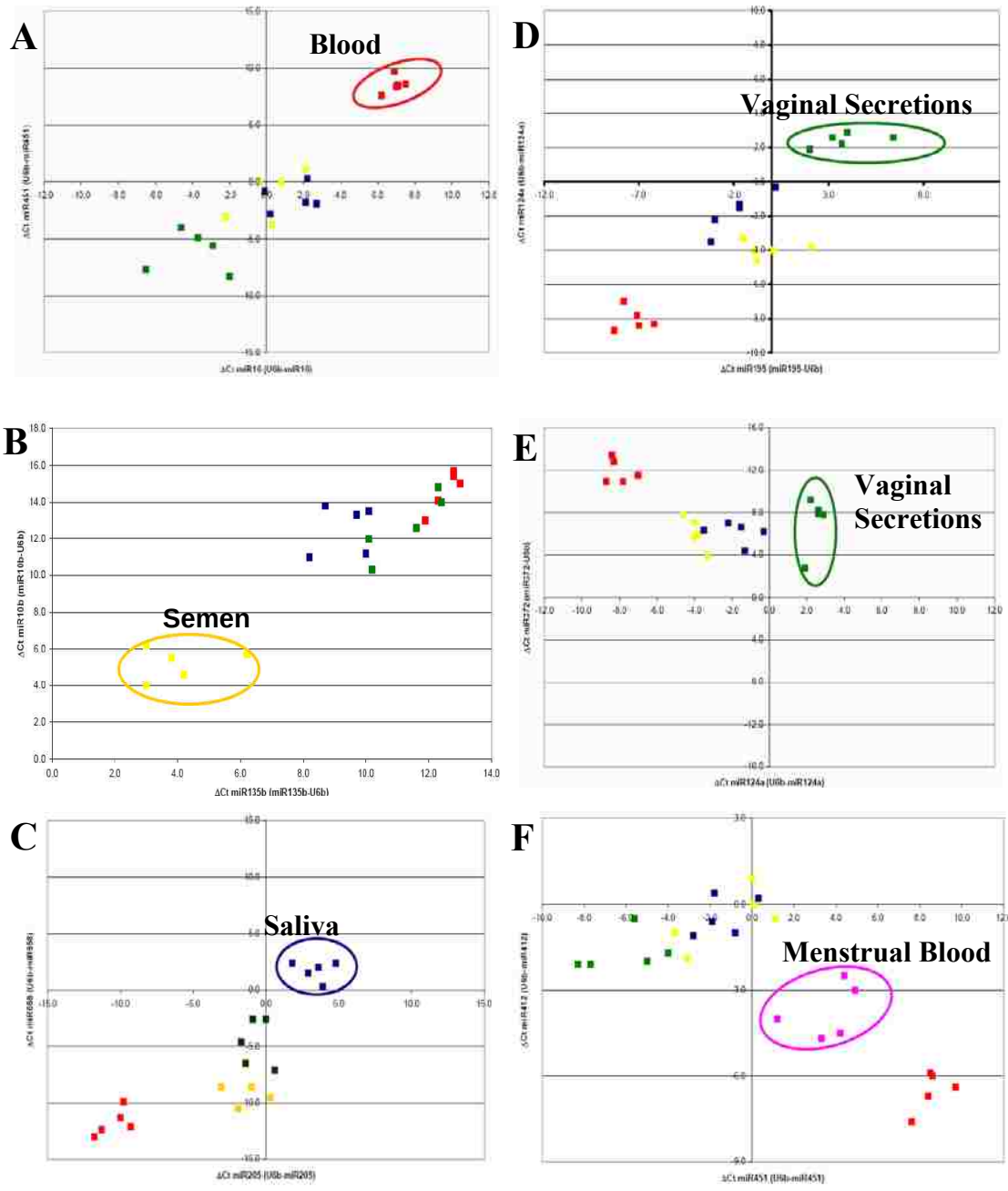

Figure 30. 2D miRNA Body Fluid Identification Assays

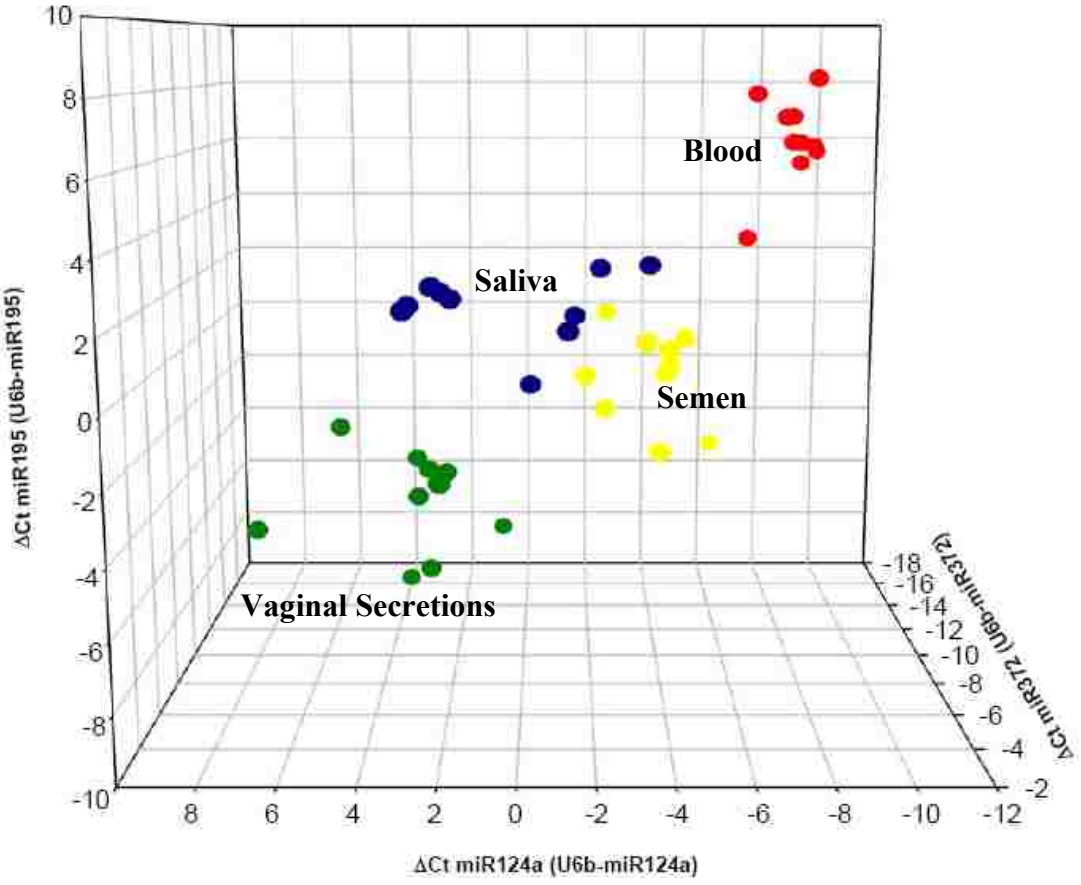

Figure 31. 3D Vaginal Secretion miRNA Assay

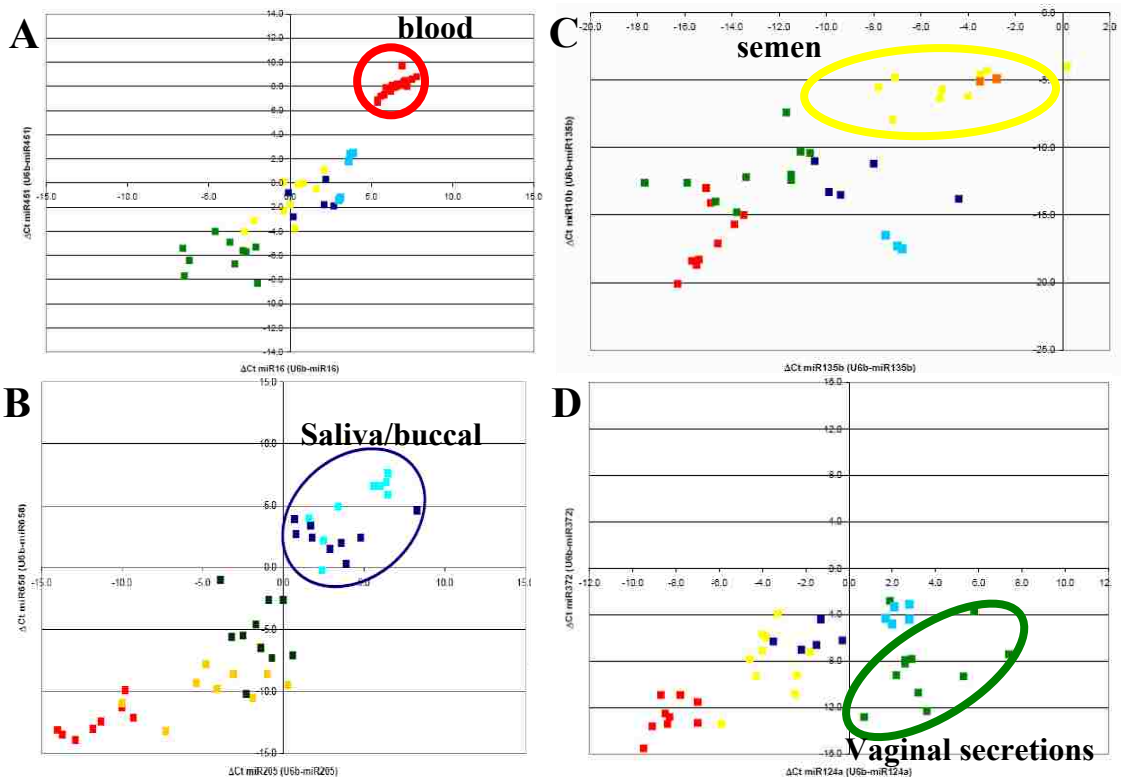

Figure 32. Evaluation of Additional Samples with the miRNA Body Fluid Assays

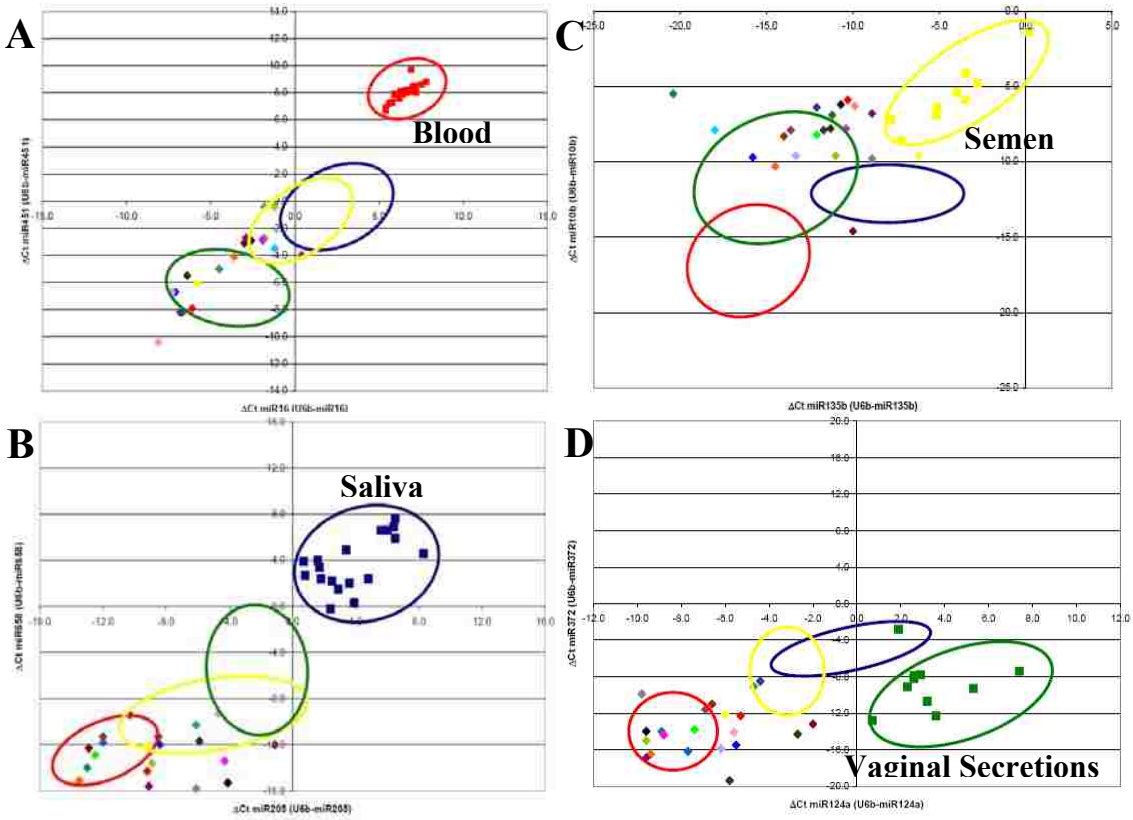

Figure 33. Tissue Specificity of the miRNA Body Fluid Assays

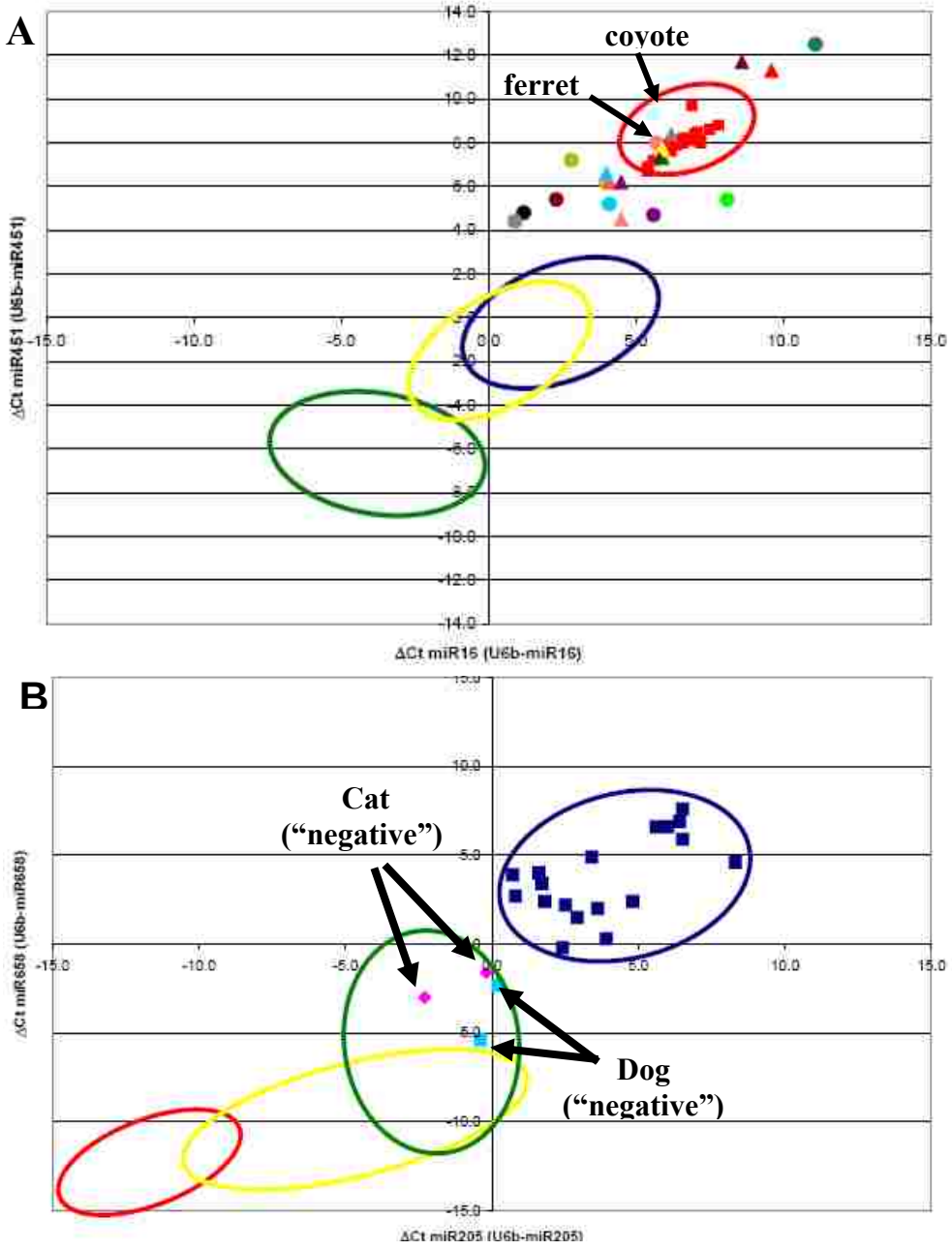

Figure 34. Species Specificity of the Blood and Saliva miRNA Body Assays

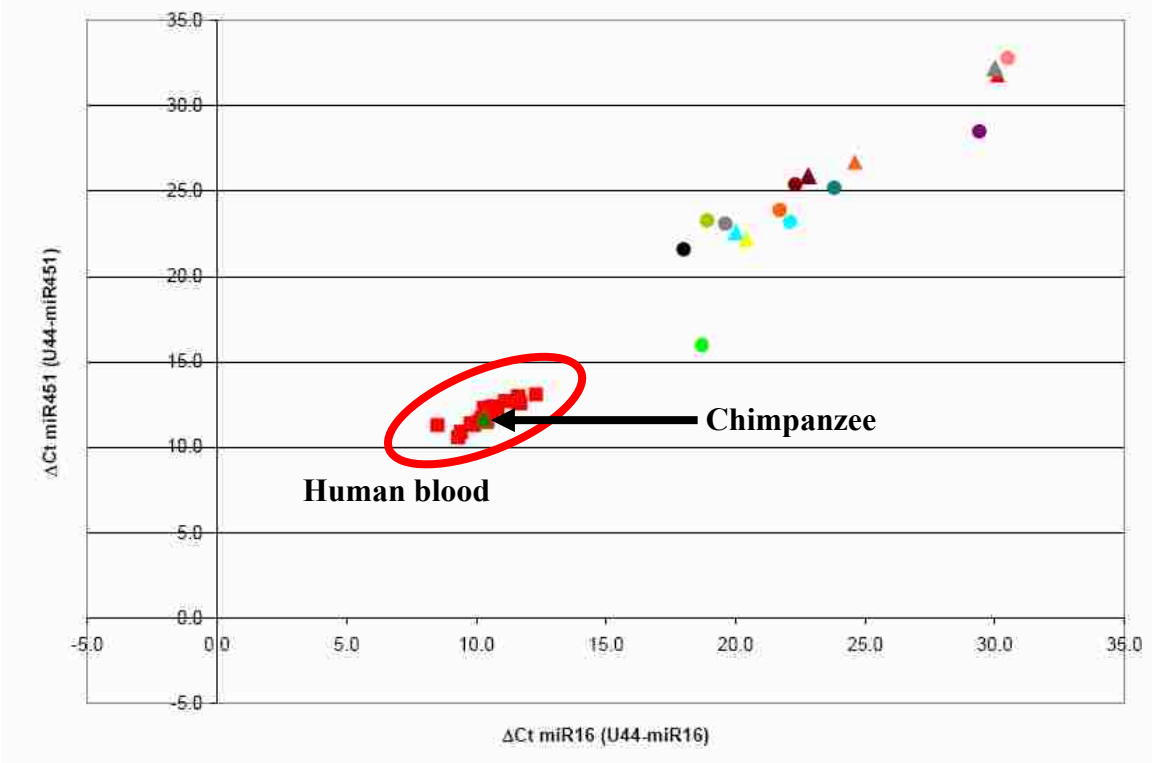

Figure 35. Improved Species Specificity of the U-44 Normalized Blood miRNA Assay

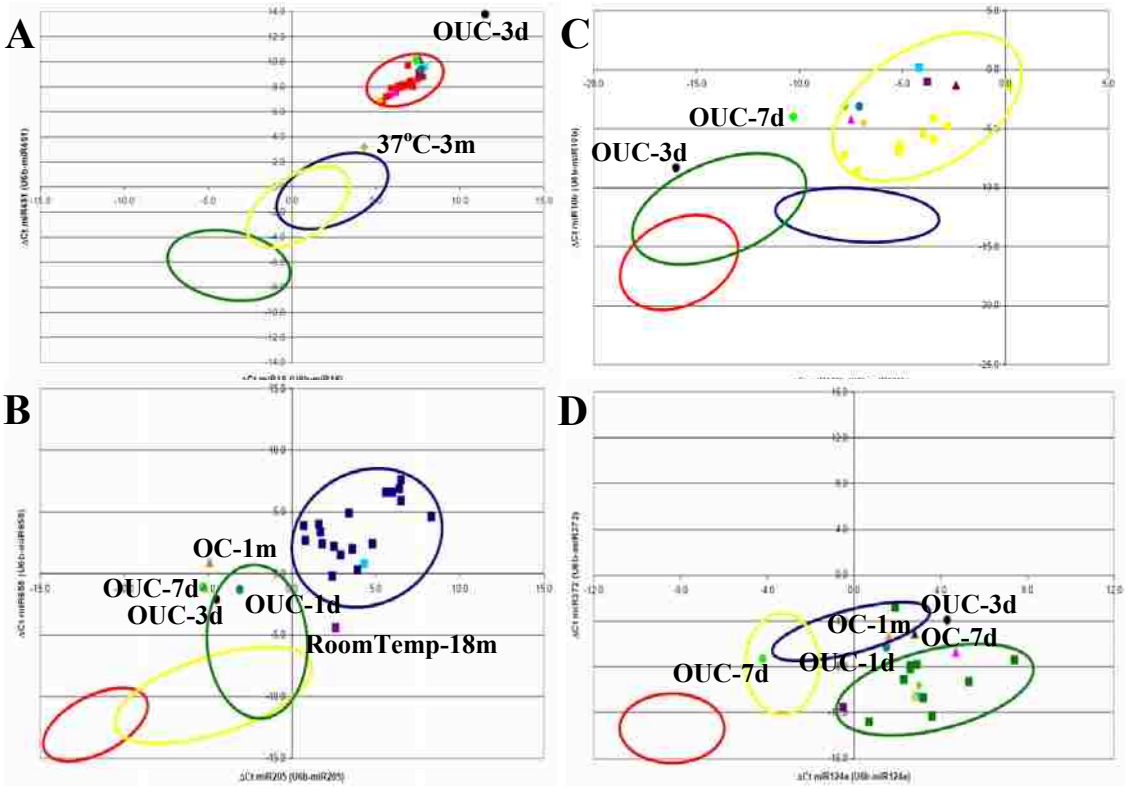

Figure 36. Stability of miRNA in Aged and Environmentally Compromised Body Fluid Samples

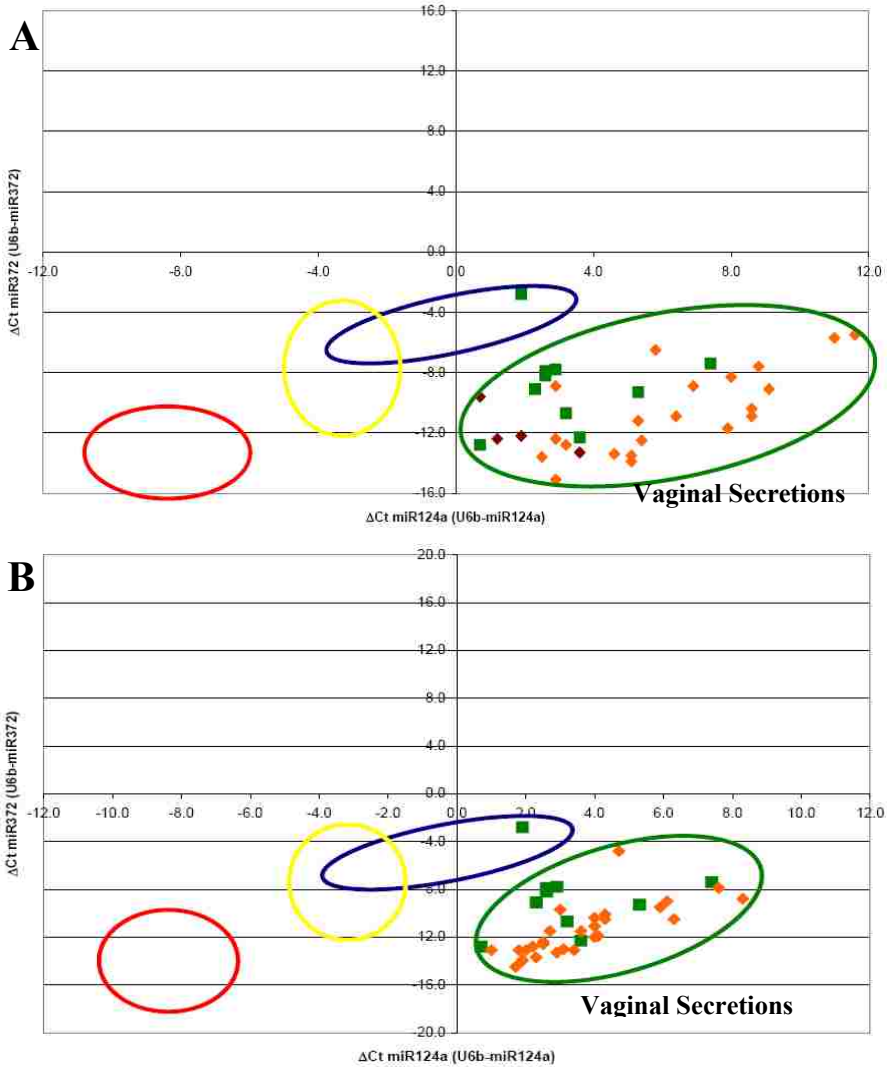

Figure 37. Stability of Vaginal Secretion miRNAs during the Menstrual Cycle

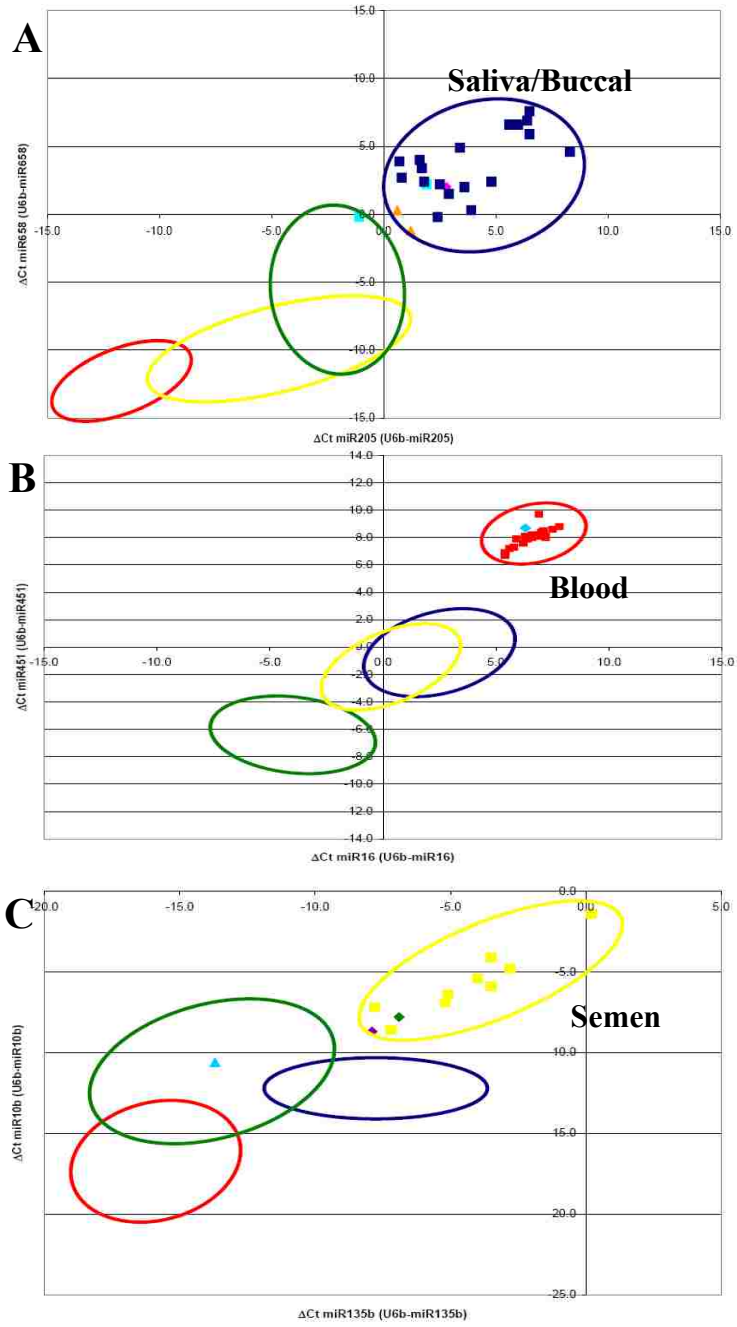

Figure 38. Detection of Body Fluids in Simulated Forensic Casework Samples

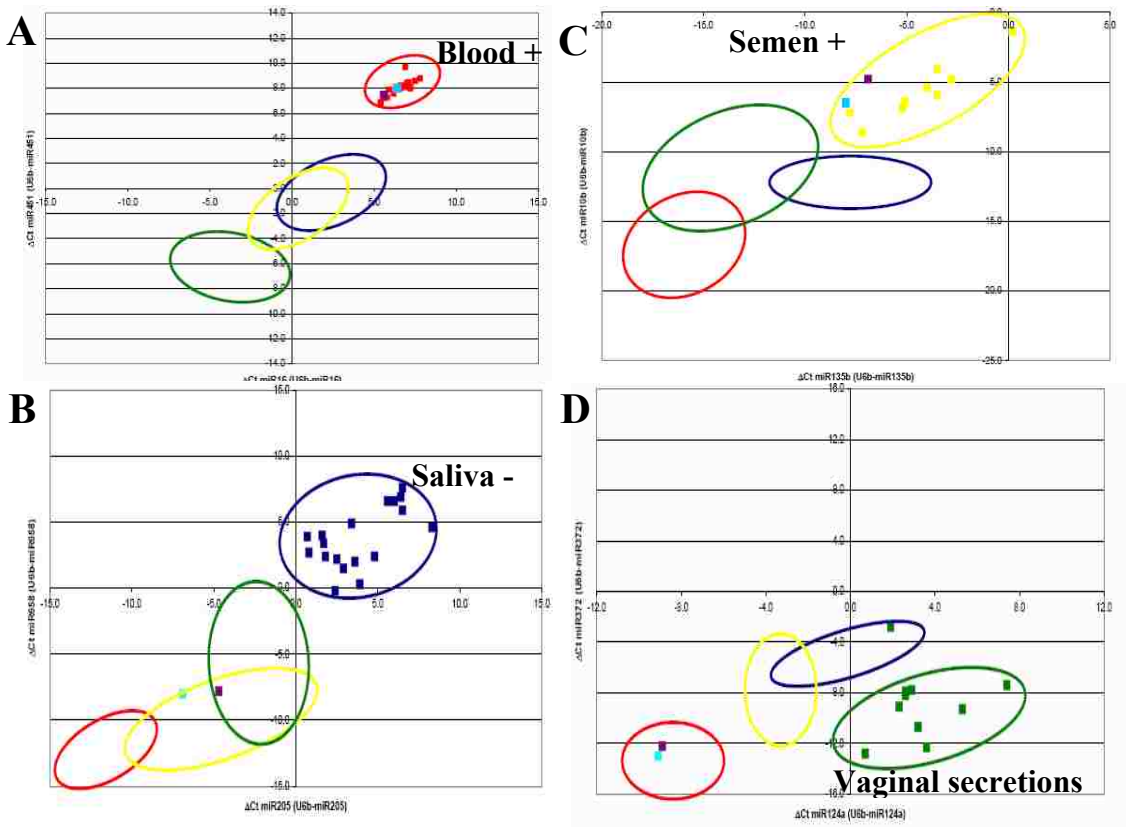

Figure 39. Detection of Blood and Semen in an Admixed Sample

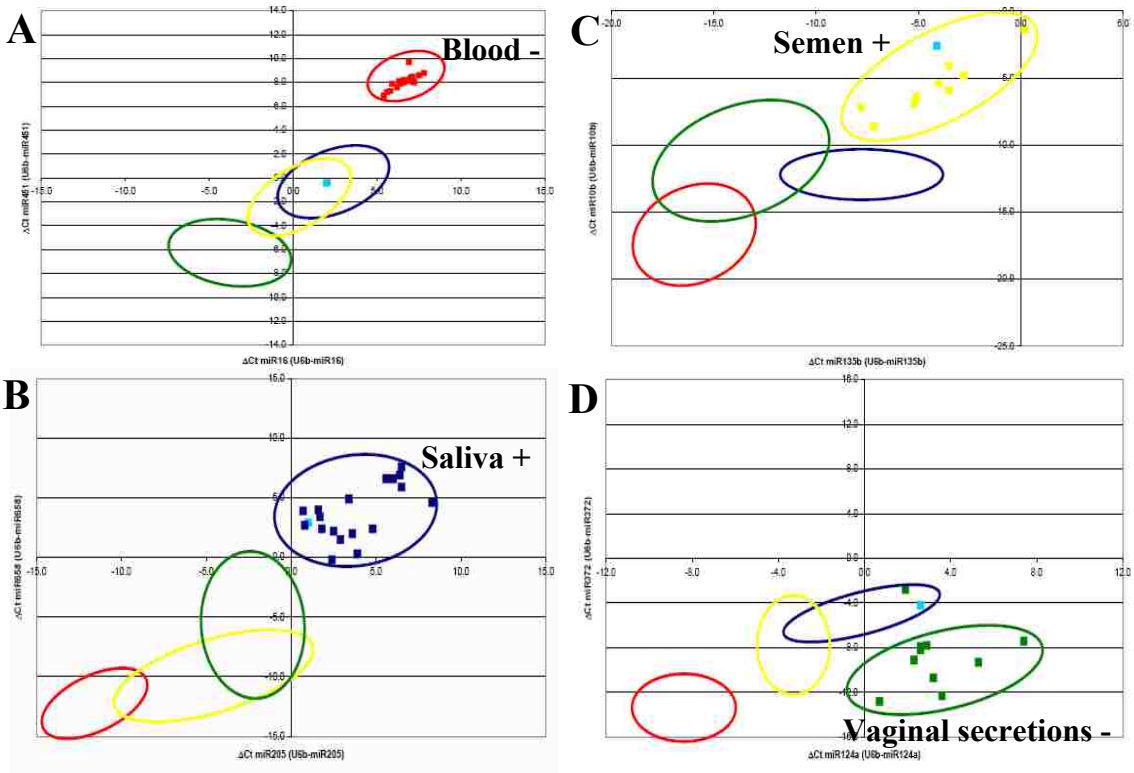

Figure 40. Detection of Semen and Saliva in an Admixed Sample

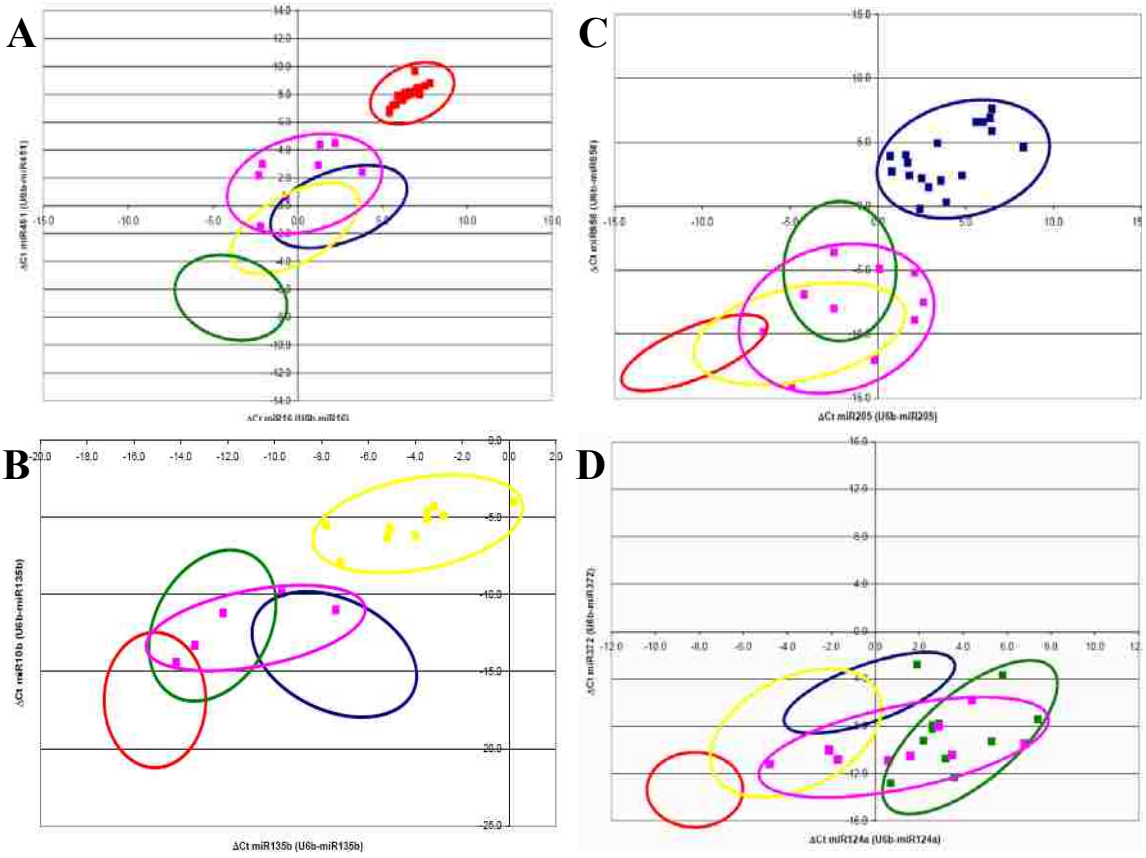

Figure 41. Expression Profile of Menstrual Blood with the miRNA Body Fluid Assays

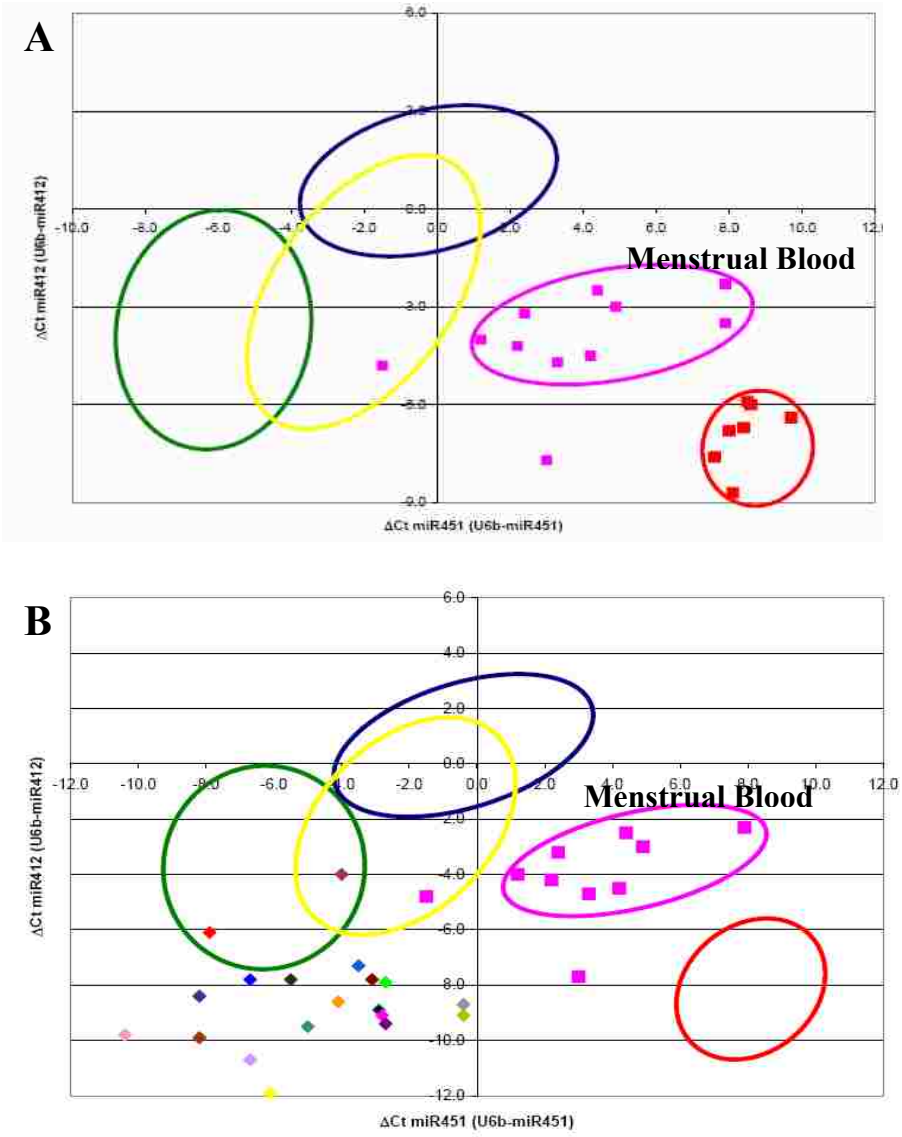

Figure 42. Specificity of the Menstrual Blood miRNA Assay

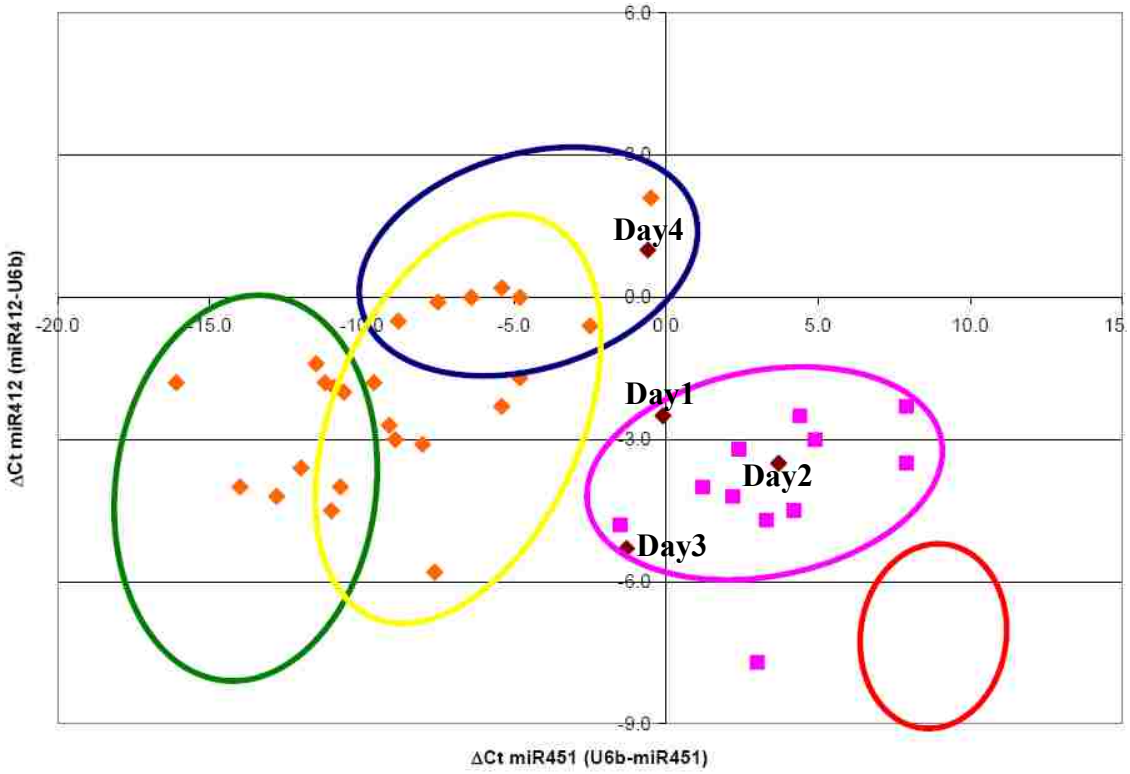

Figure 43. Stability of the Menstrual Blood miRNA Assay during the Menstrual Cycle

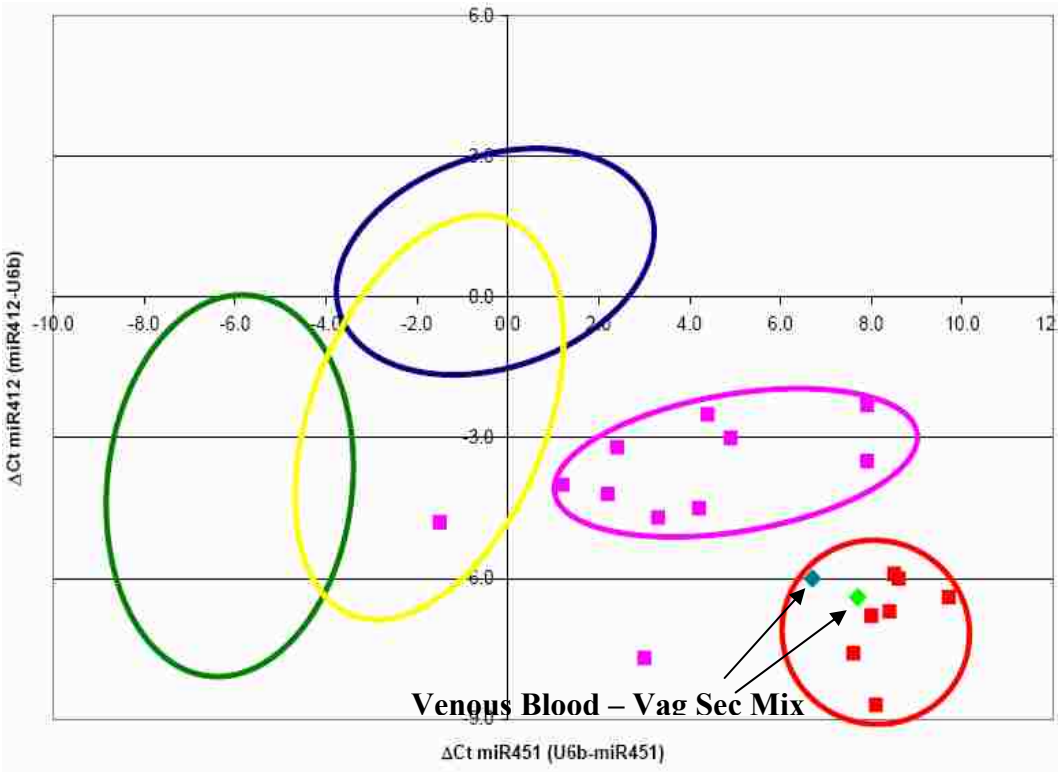

Figure 44. Evaluation of Venous Blood -Vaginal Secretion Mixtures Using the Menstrual Blood miRNA Assay

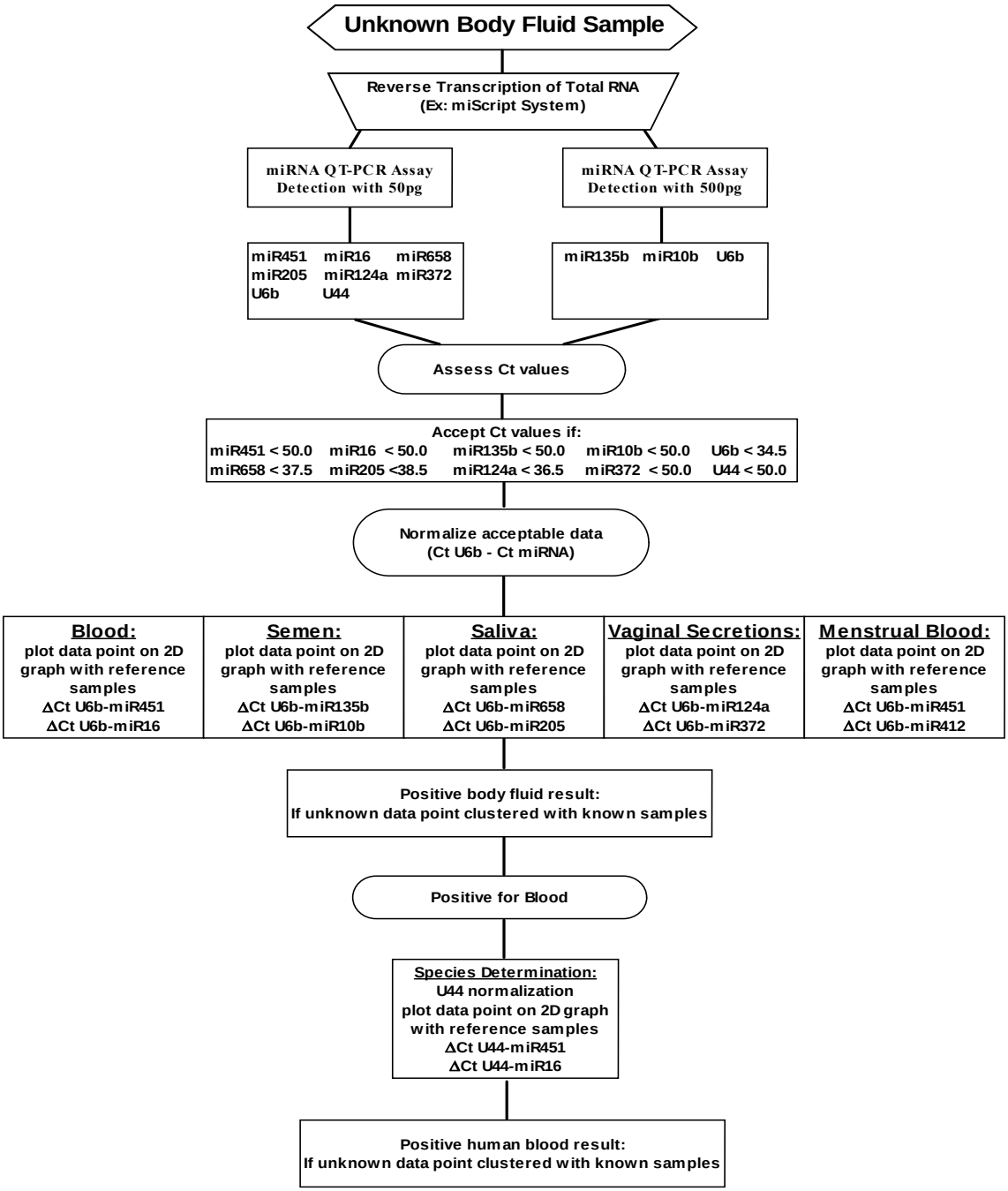

Figure 45. Proposed Schema for the Analysis of Biological Evidence of Unknown Origin using miRNA Body Fluid Profiling

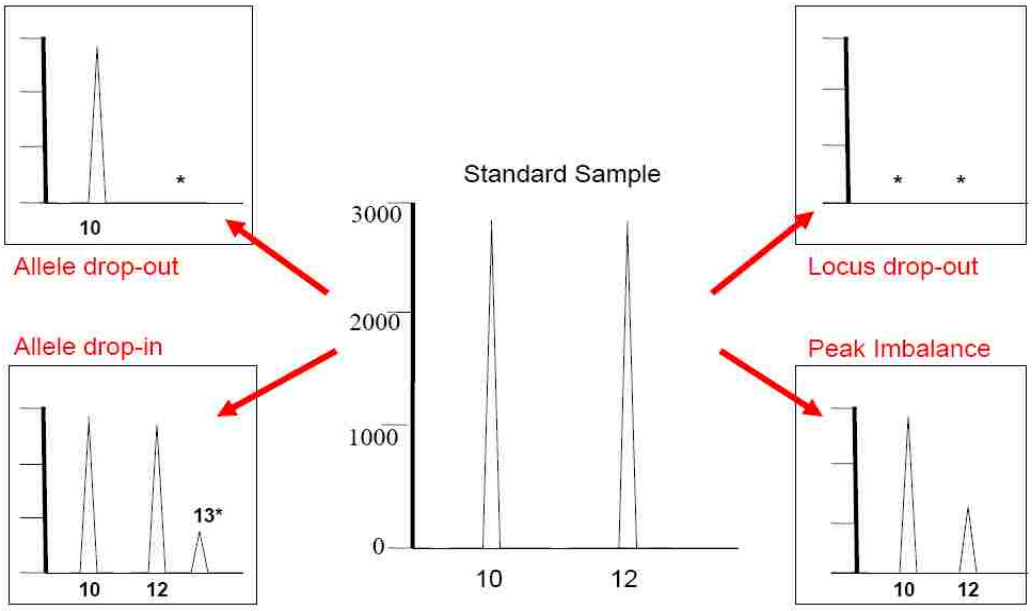

Figure 46. Challenges Associated with Low-Template Sample Analysis

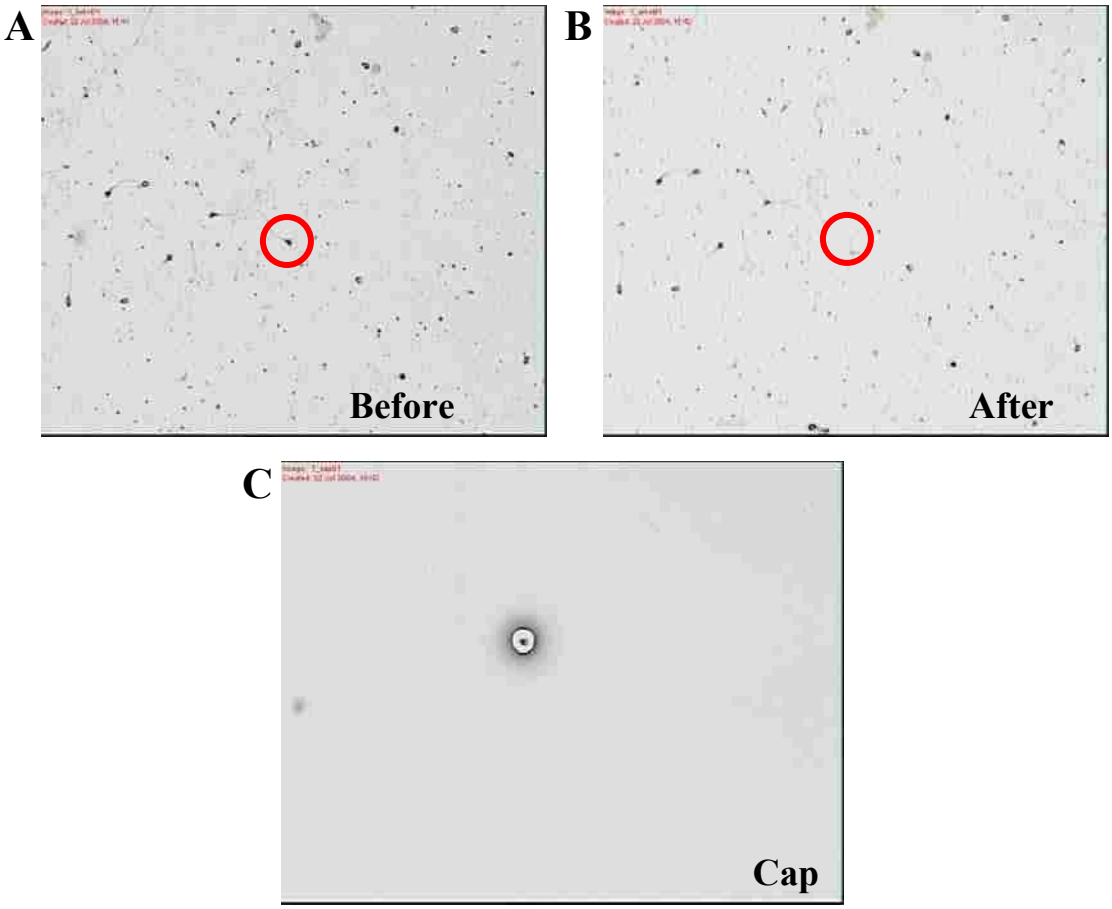

Figure 47. Single Sperm Cell Removal Using the Arcturus PixCell II System

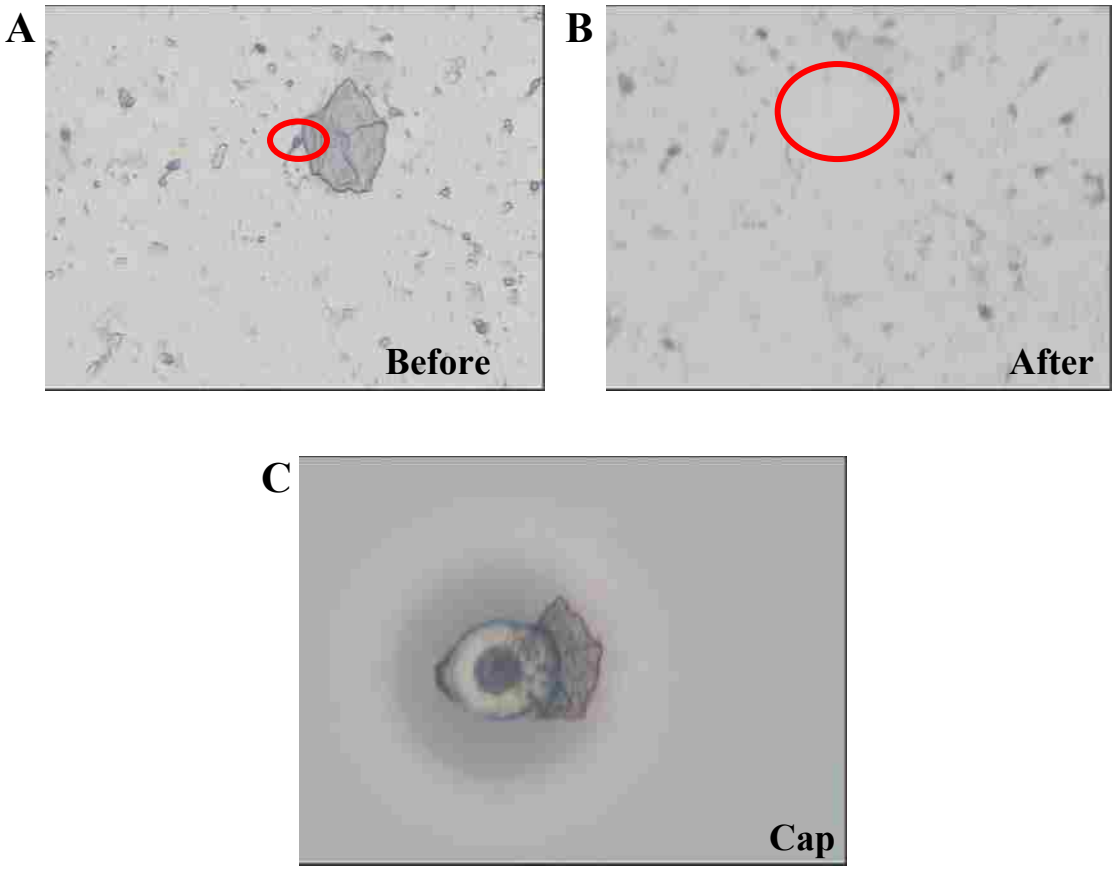

Figure 48. Removal of Sperm Cells Adhering to Epithelial Cells using the Arcturus PixCell System

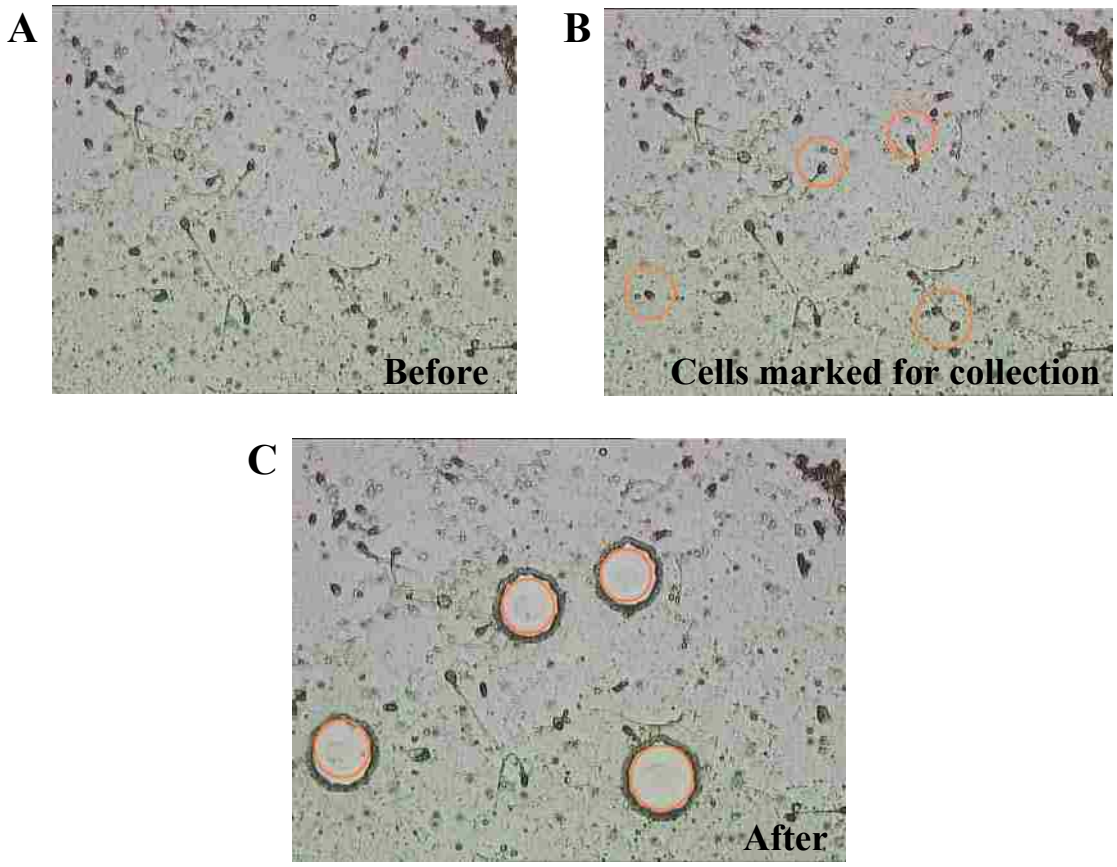

Figure 49. Sperm Cell Removal using the Leica LMD System

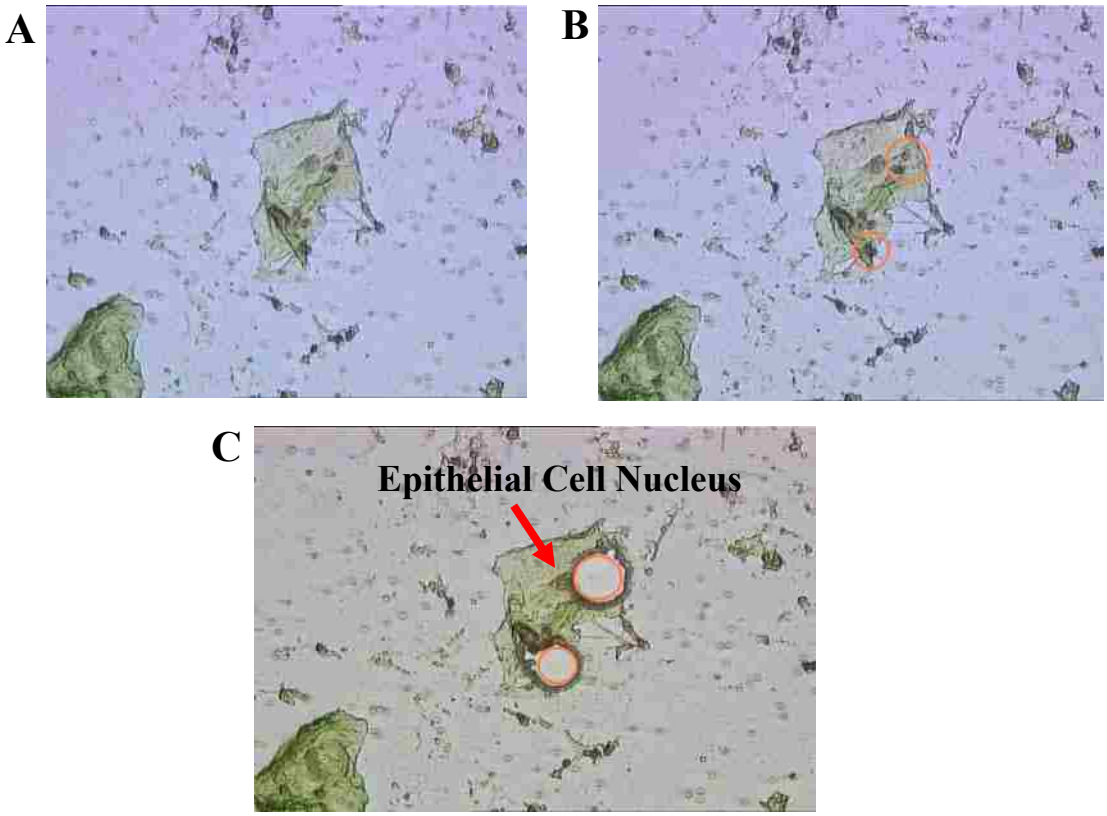

Figure 50. Removal of Sperm Cells Adhering to Epithelial Cells Using the Leica LMD System

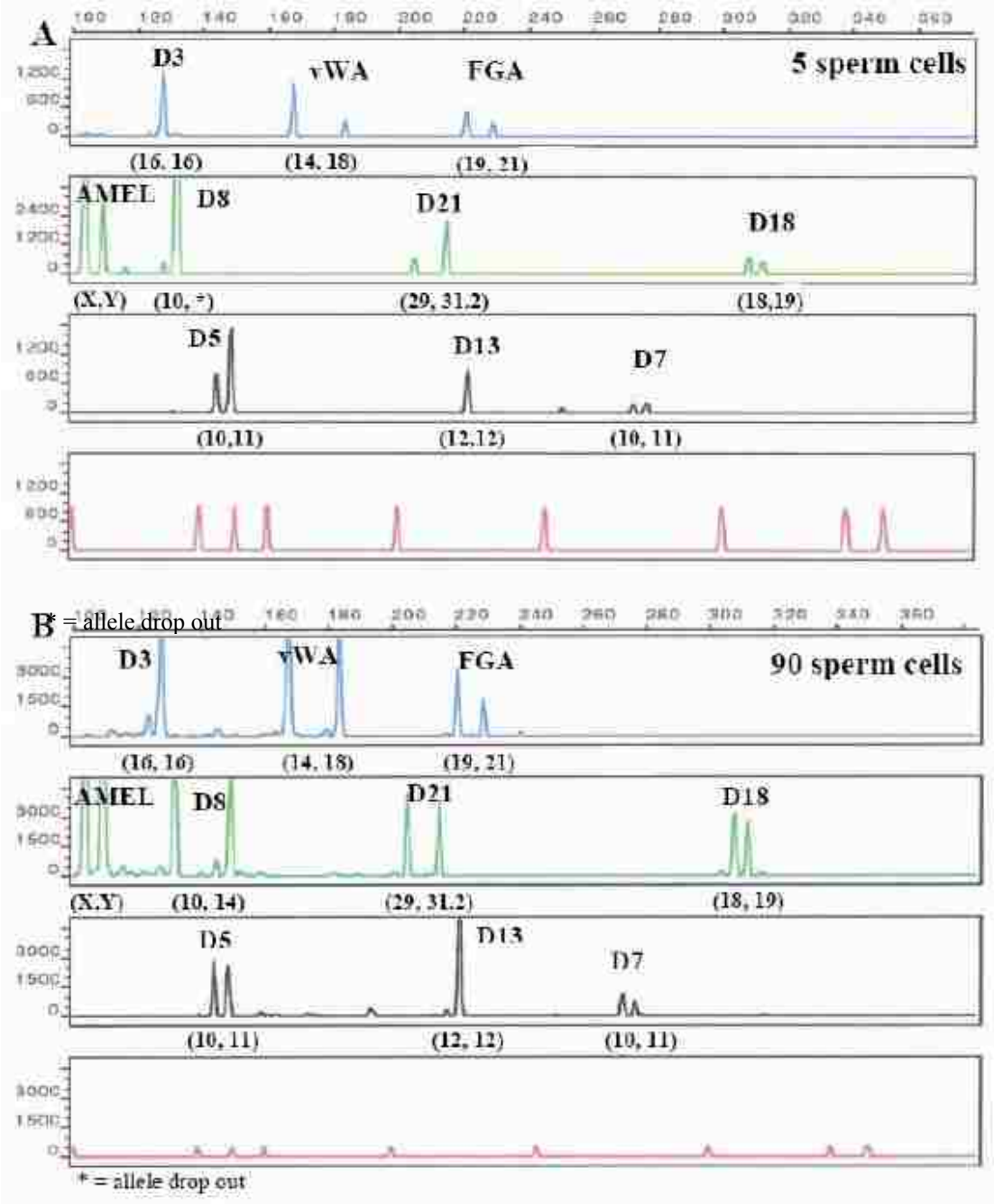

Figure 51. Autosomal STR Profile Recovery from Micro-dissected Sperm Cells

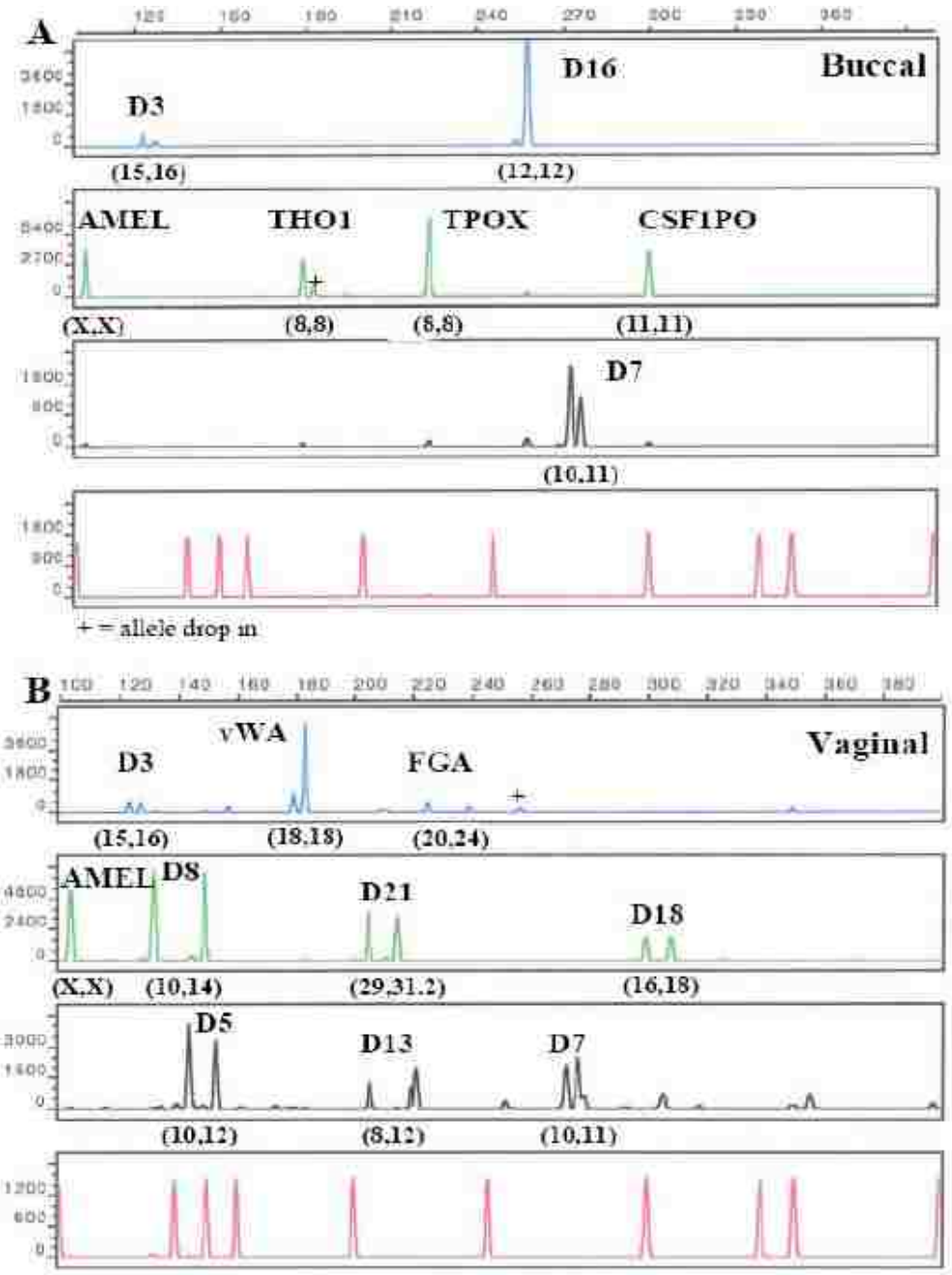

Figure 52. Autosomal STR Profiles Obtained From Single Micro-dissected Epithelial Cells

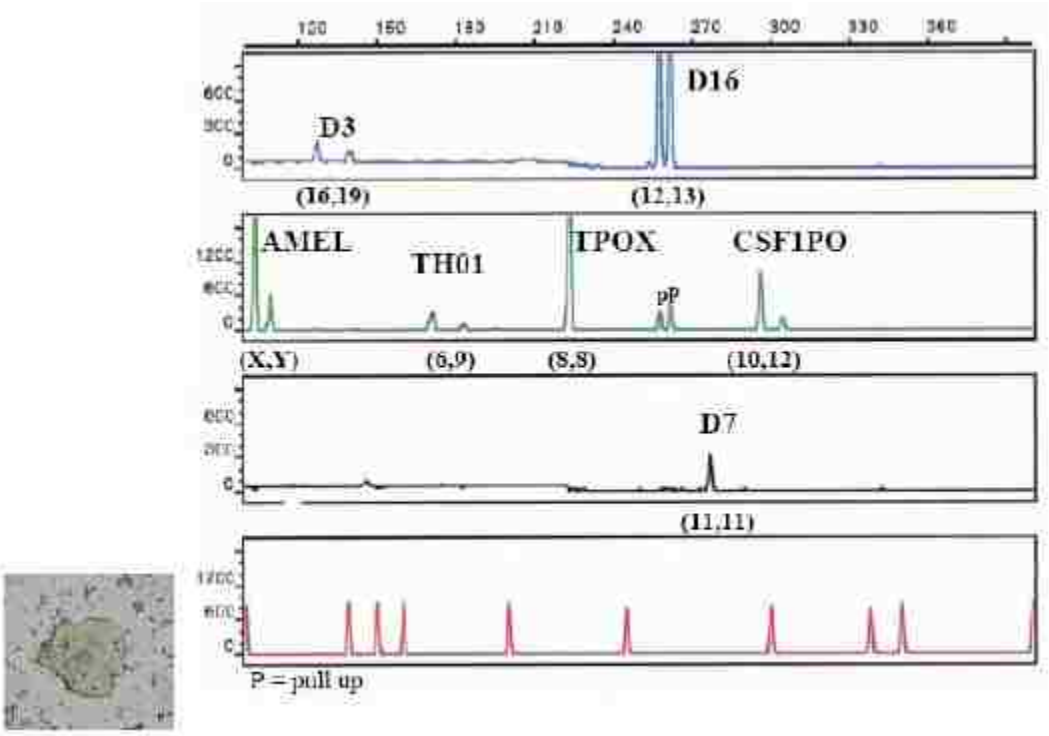

Figure 53. Autosomal STR Profile Recovered From a Single Epithelial Cell from a Vasectomized-Male Semen Sample

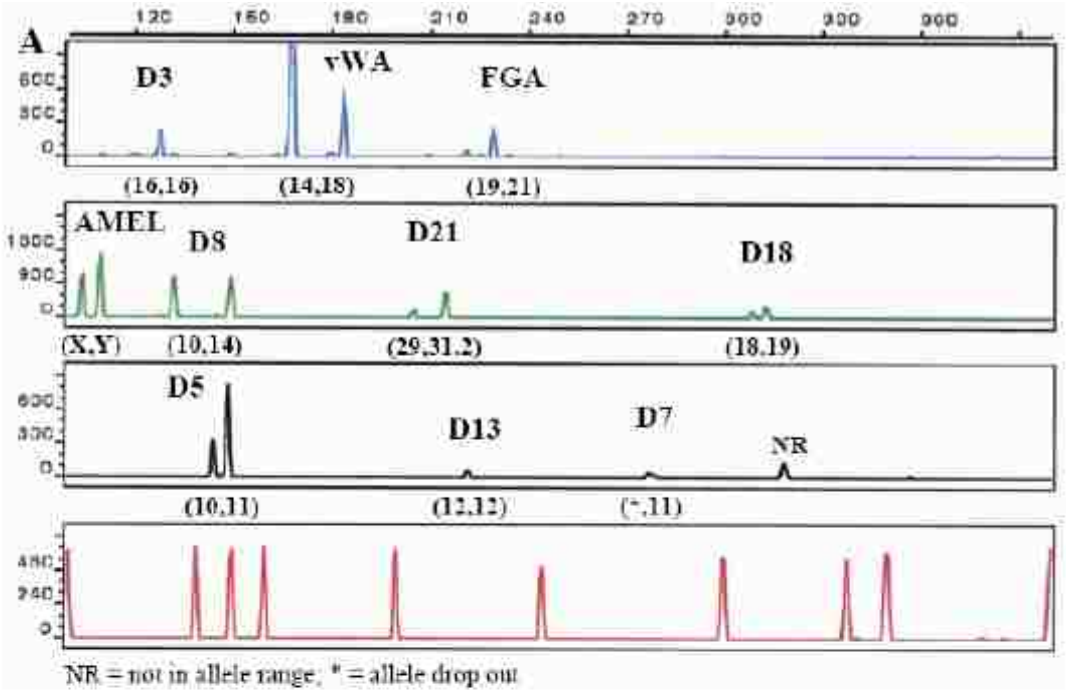

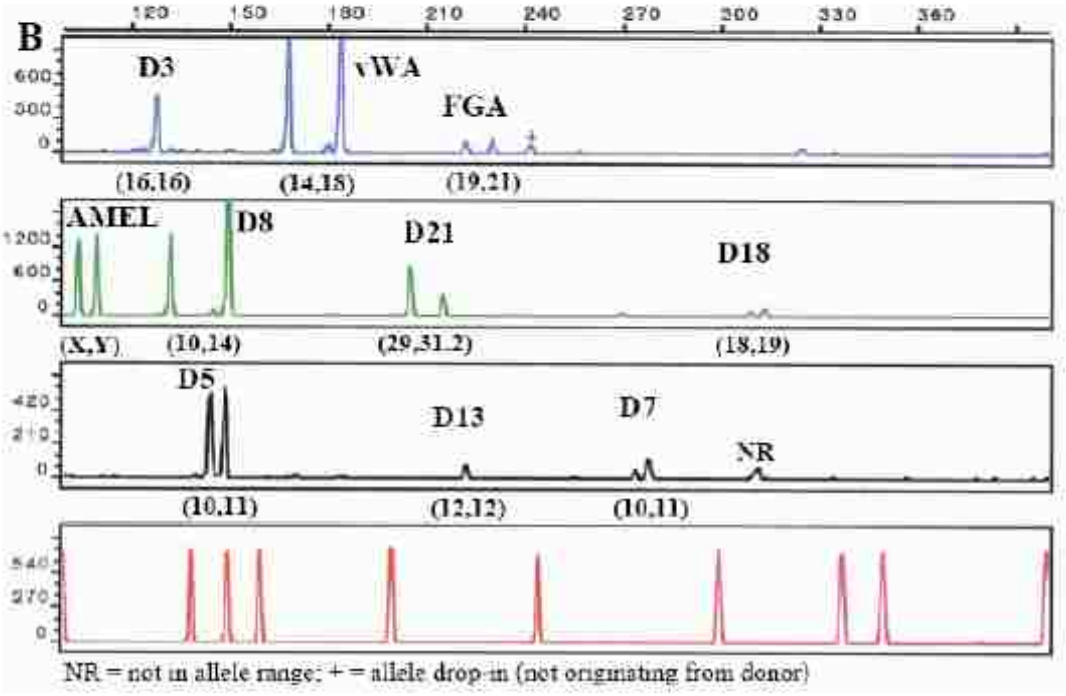

Figure 54. Autosomal STR Profiles Recovered from Epithelial Cells from Beverage Container Lids

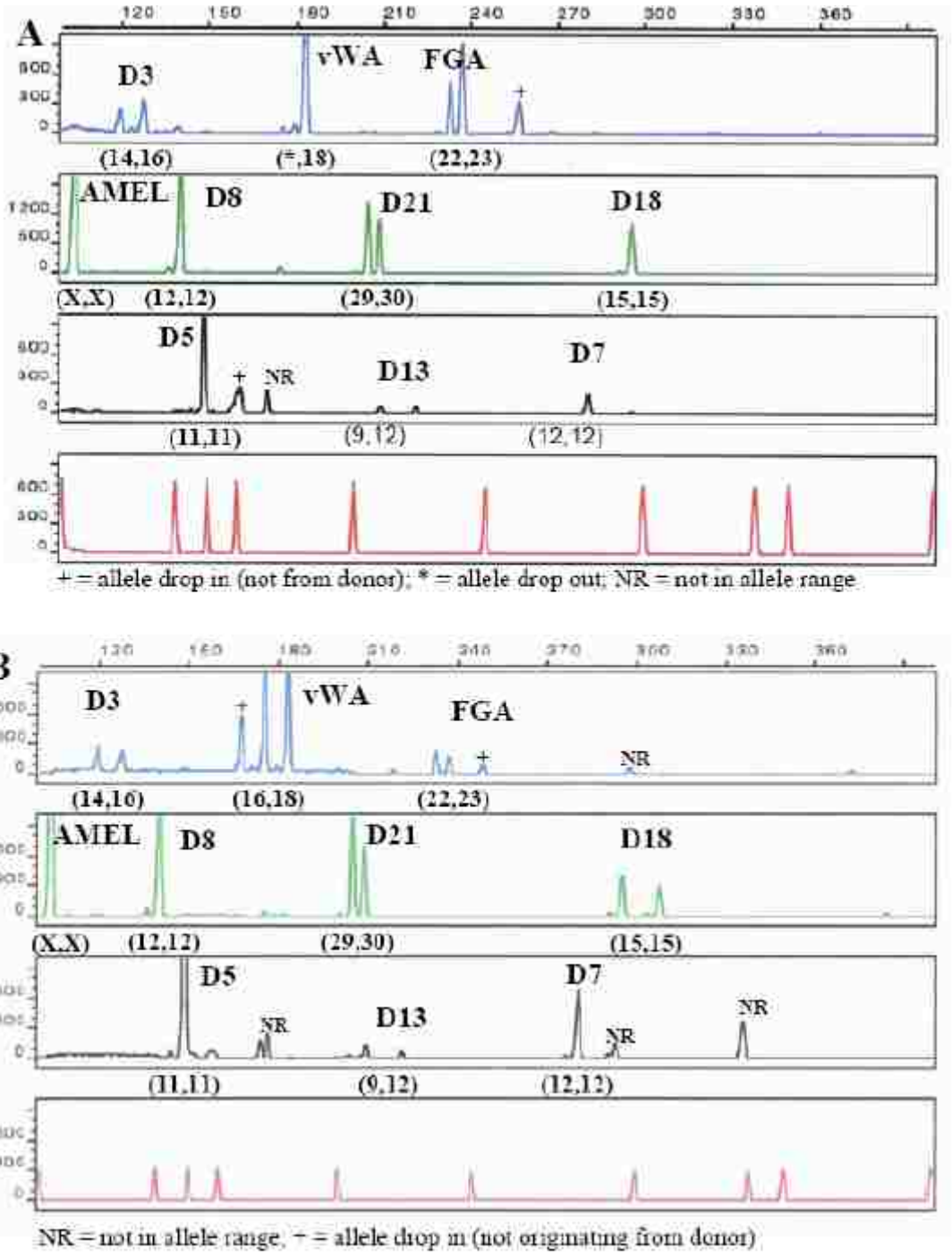

Figure 55. Autosomal STR Profiles Recovered from Epithelial Cells from Menstrual Blood Samples

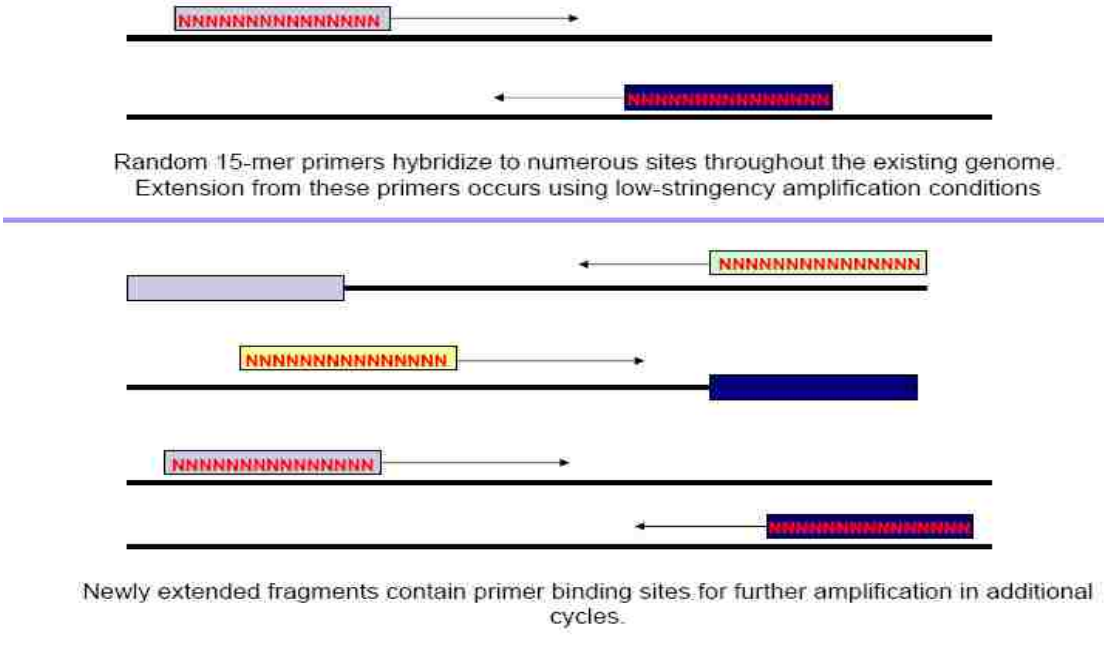

Figure 56. Basic Primer Extension Pre-Amplification Strategy

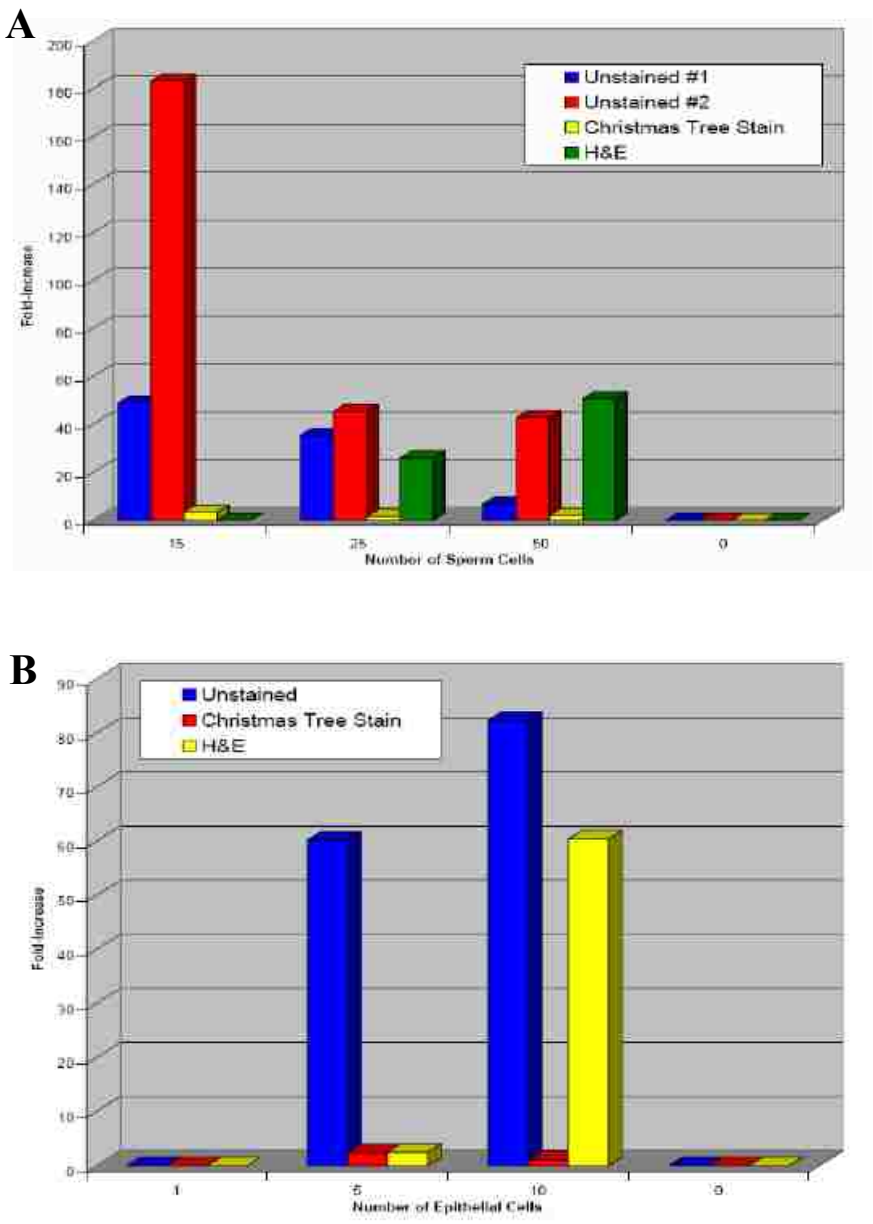

Figure 57. Affects of Cell Staining on Amplification Yield Following mIPEP Amplification

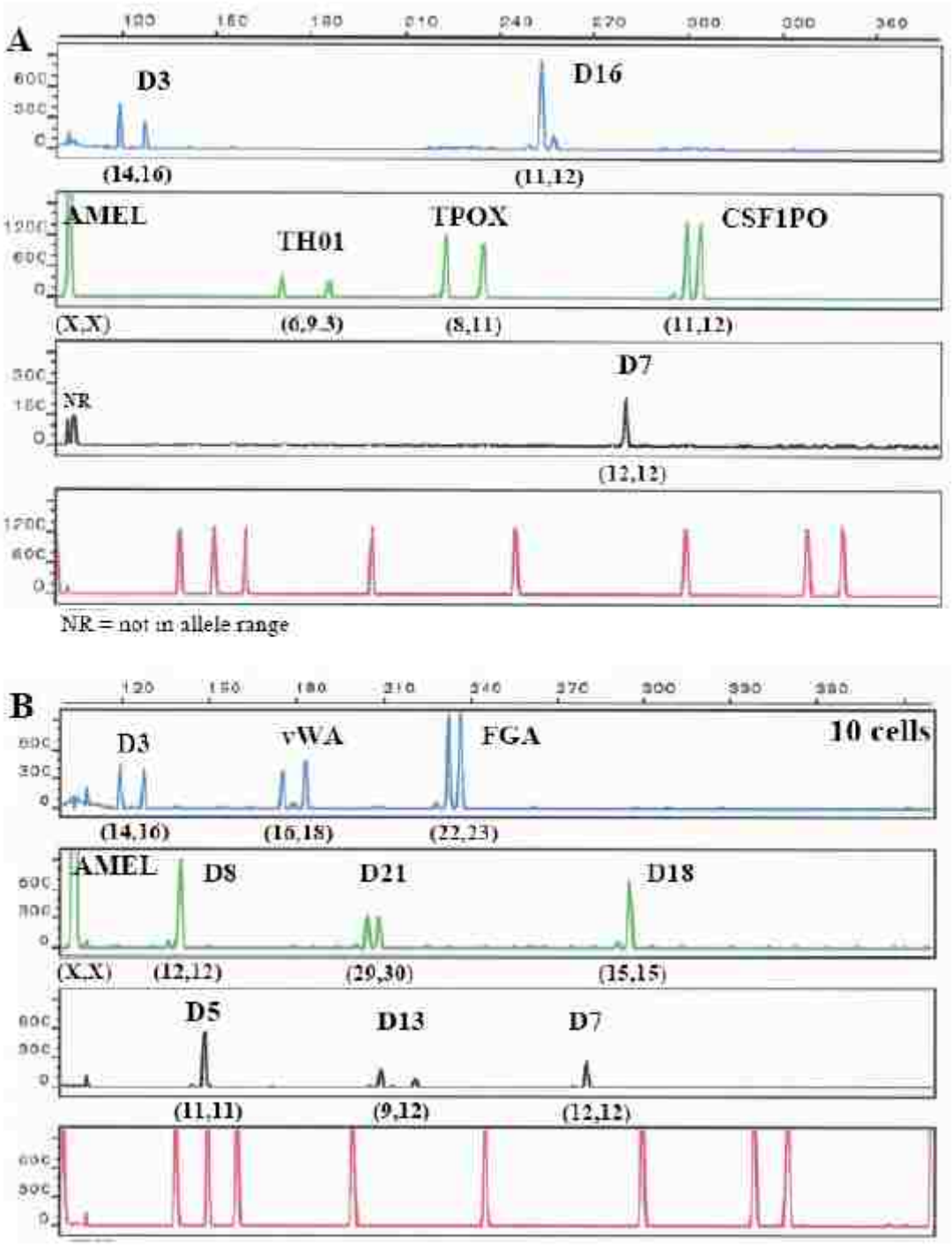

Figure 58. Autosomal STR Profiles Recovered from mIPEP-Amplified Micro-dissected Epithelial Cells After mIPEP Amplification

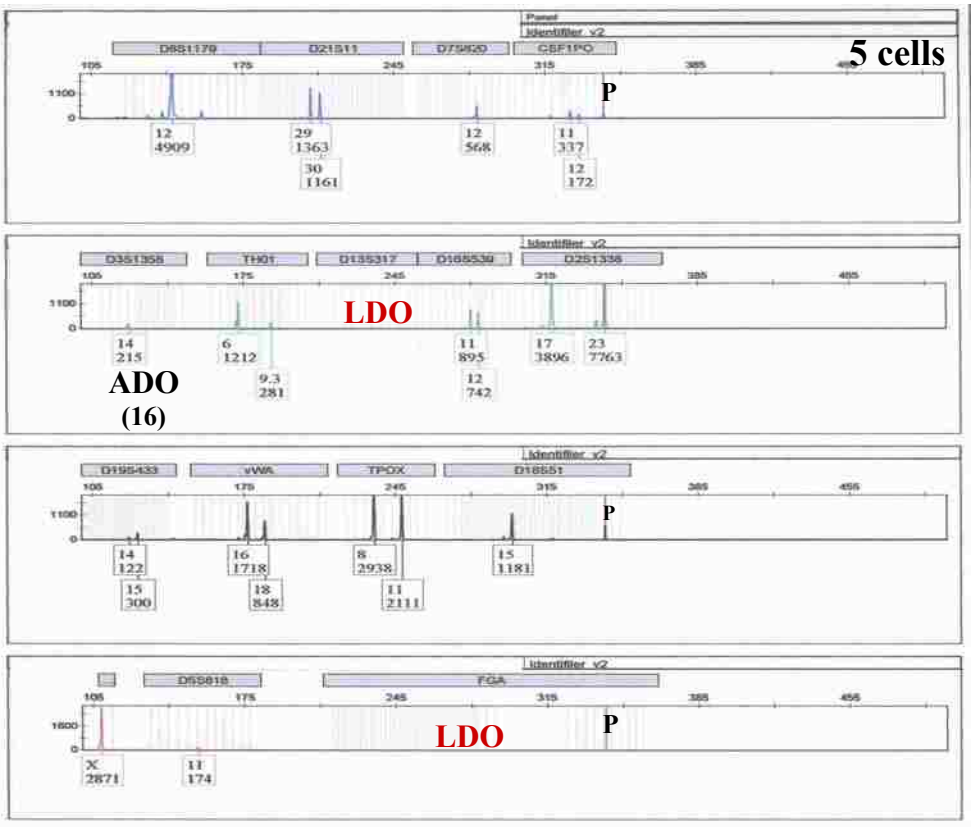

LDO = locus drop out, ADO = allele drop out, P = pull-up

Figure 59. Mega-plex Autosomal STR Profile Recovered from Micro-dissected Epithelial Cells

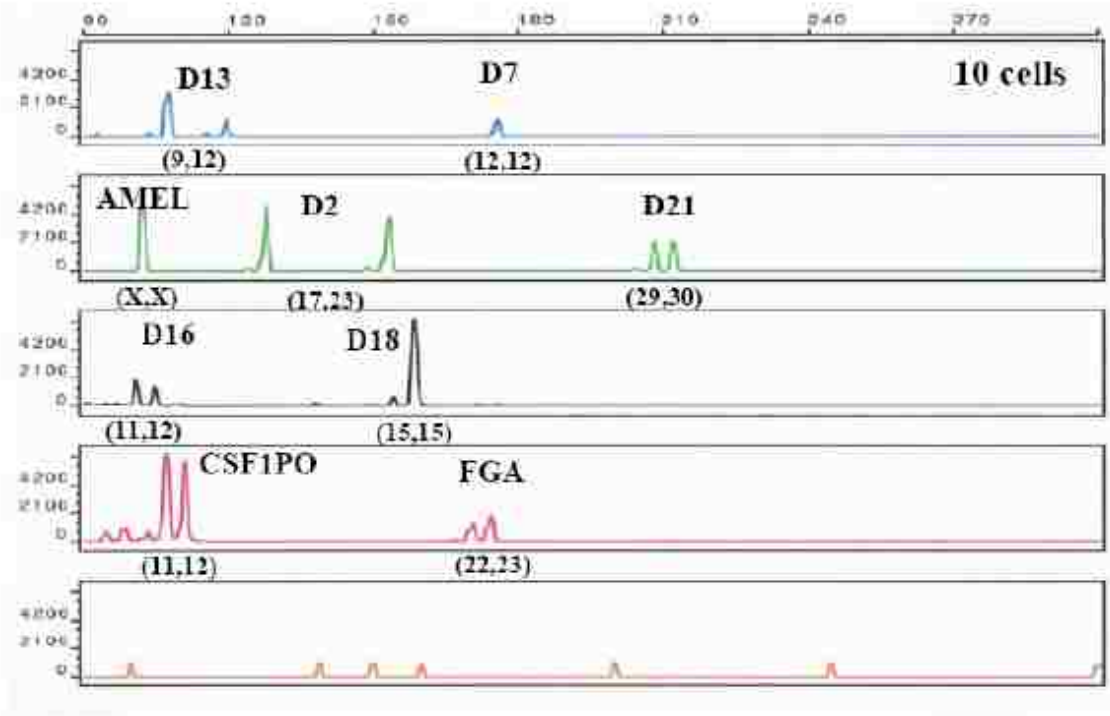

Figure 60. Mini Autosomal STR Profile Recovered from mIPEP-Amplified Micro-dissected Epithelial Cells

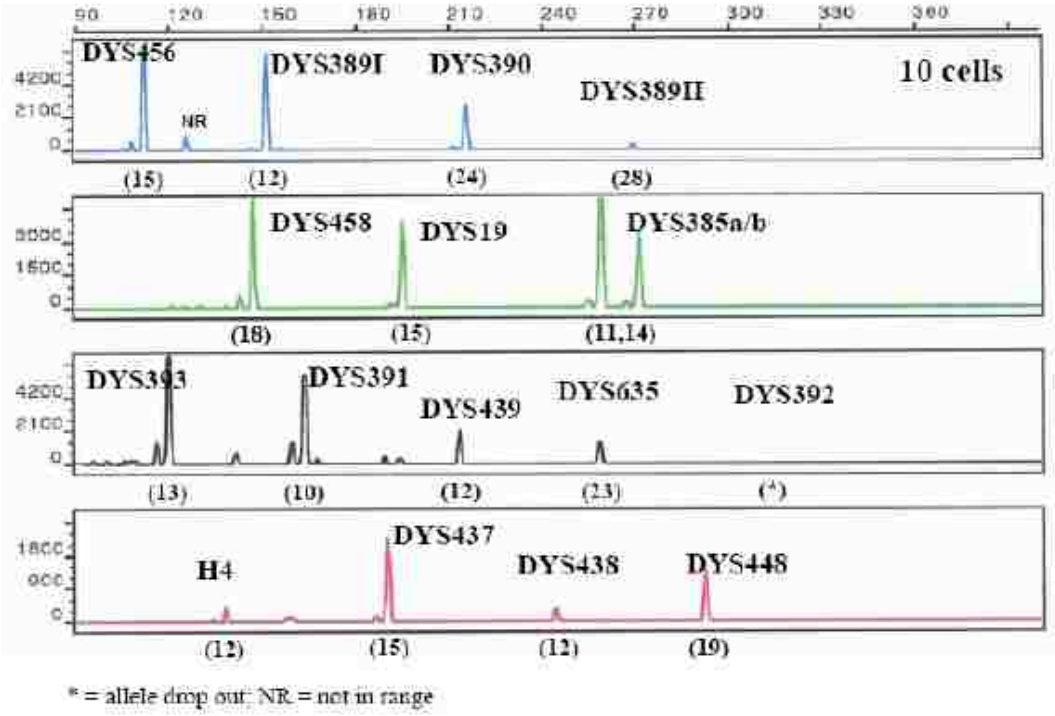

Figure 61. Y-Chromosome STR Profile Recovered from mIPEP-Amplified Micro-dissected Epithelial Cells

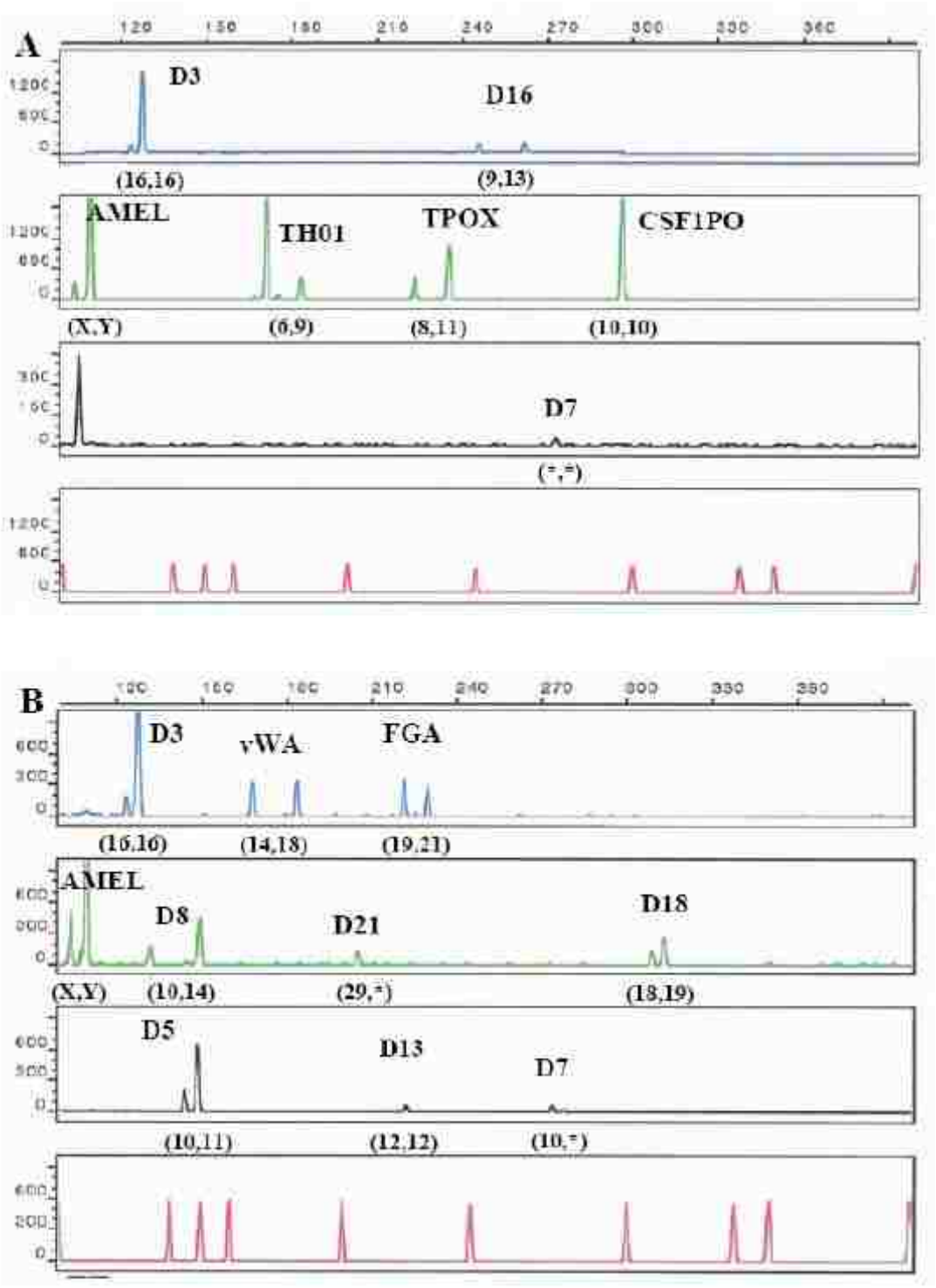

Figure 62. Autosomal STR Profiles Recovered from mIPEP-Amplified Micro-dissected Sperm Cells

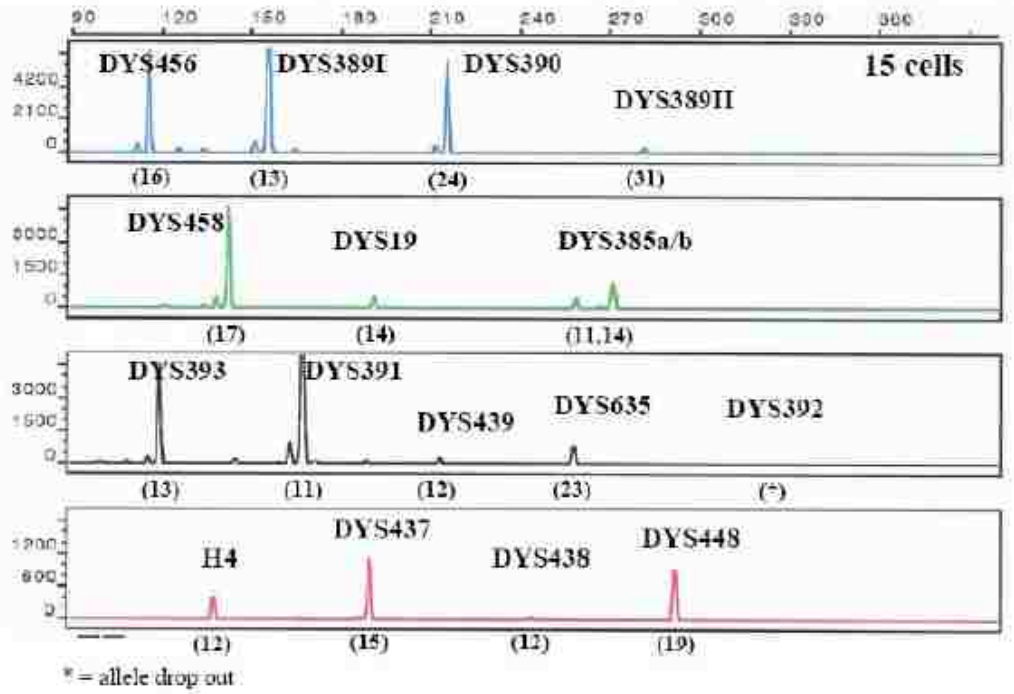

Figure 63. Y-Chromosome STR Profile Recovered from mIPEP-Amplified Micro-dissected Sperm Cells

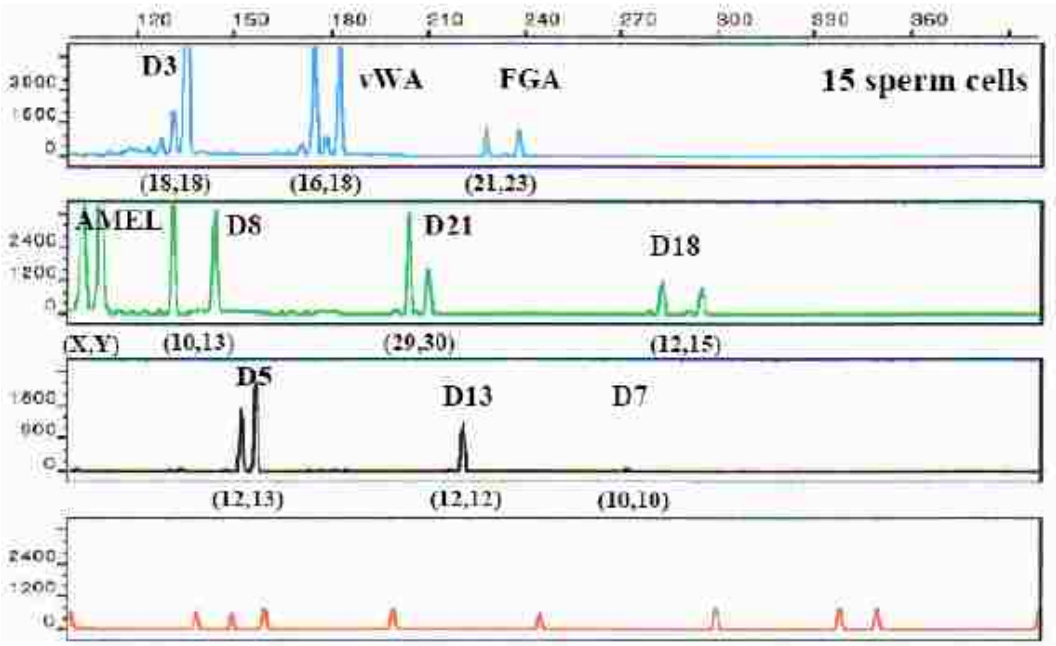

Figure 64. Autosomal STR Profile Recovered from mIPEP-Amplified Sperm Cells Collected from a 40-Month Old Semen-Stained T-Shirt

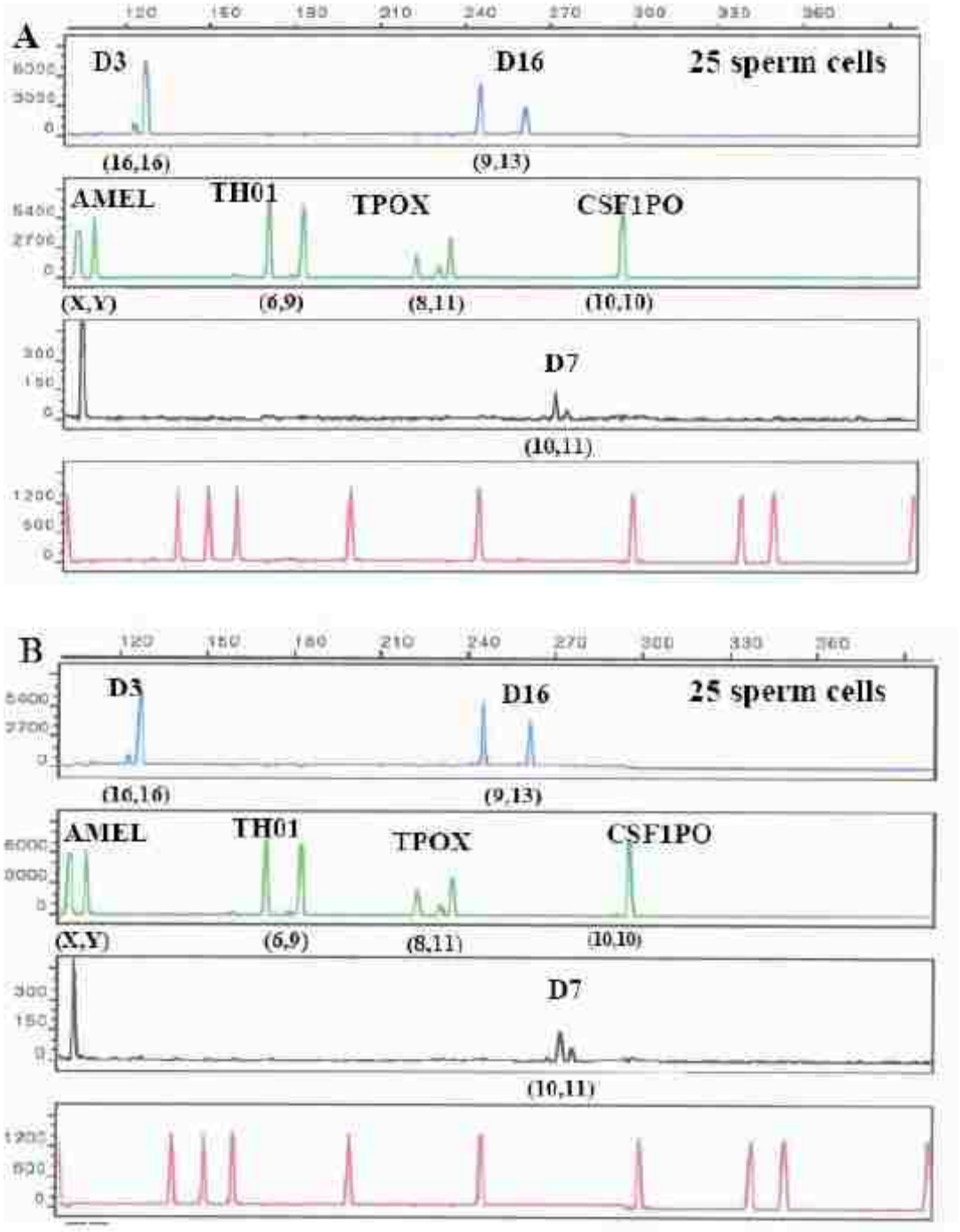

Figure 65. Reproducibility of Profiles Obtained from Multiple Amplifications of the Same mIPEP Product

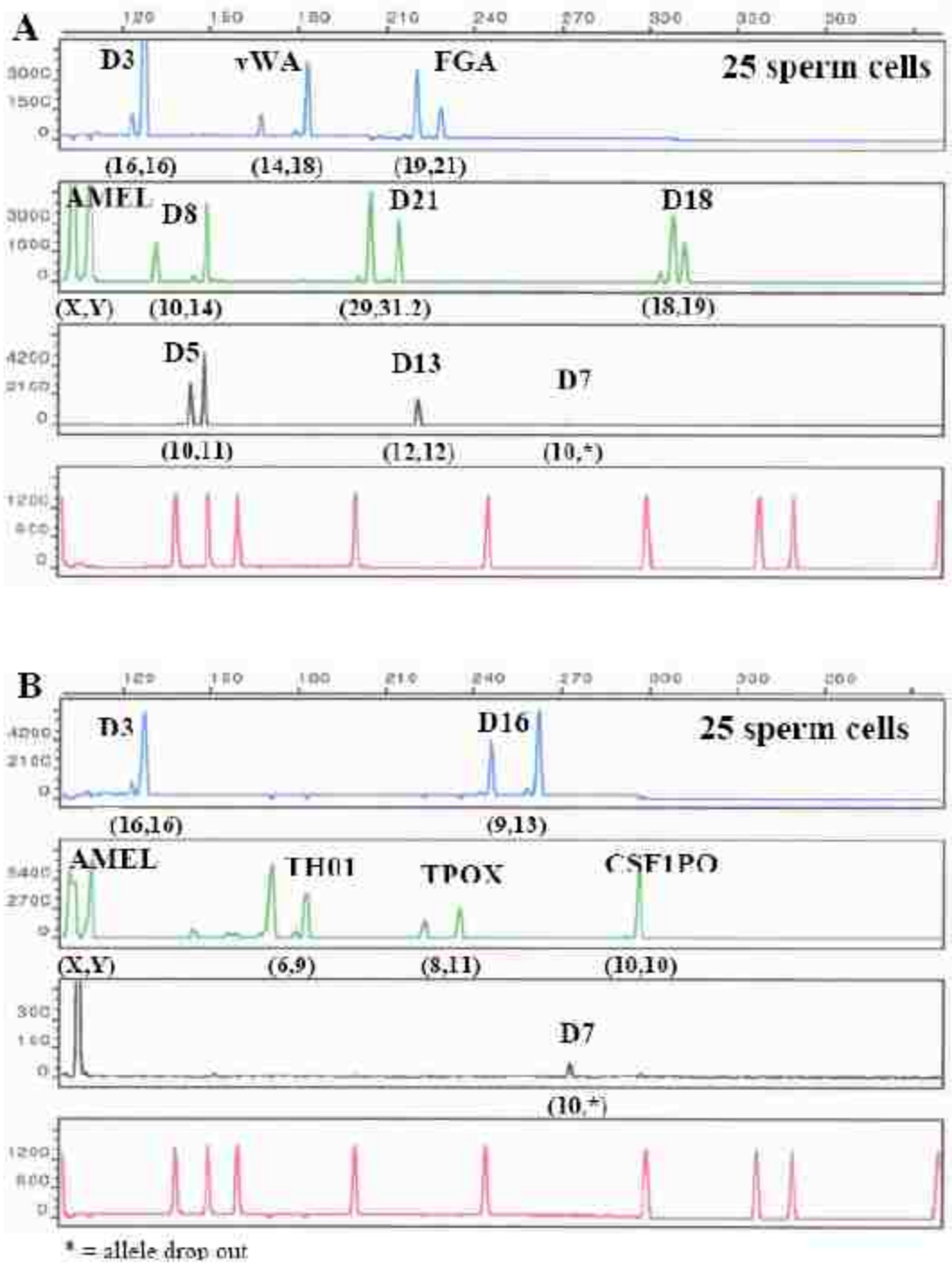

Figure 66. Multiple STR System Profiles Recovered from a Single mIPEP Product

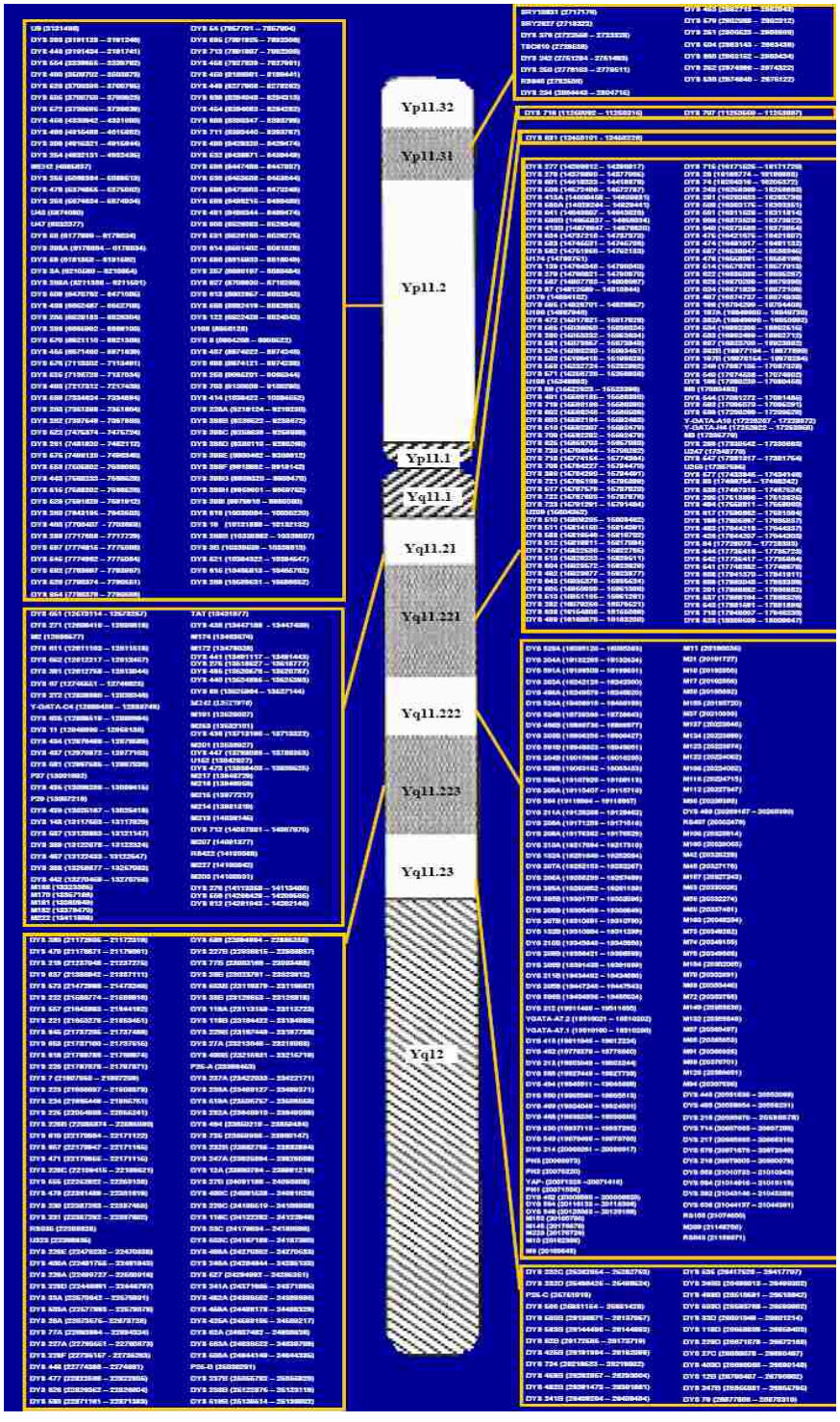

Figure 67. STR Physical Map of the Human Y Chromosome

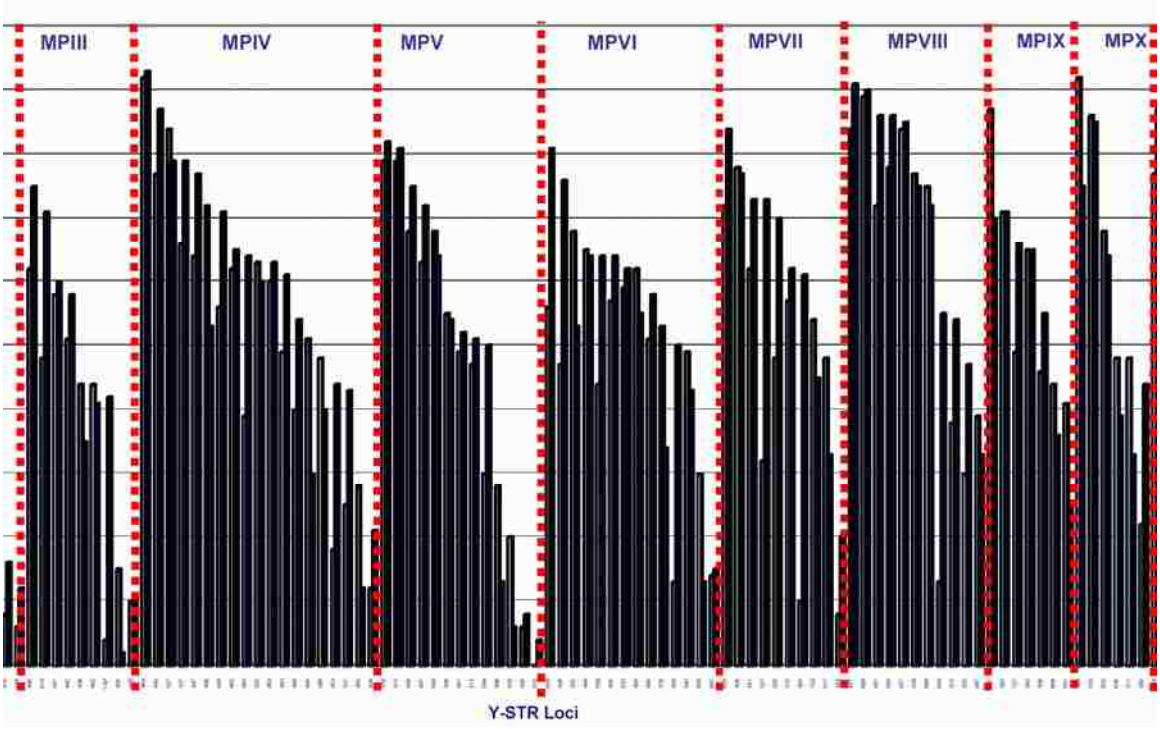

Figure 68. Gene Diversity Values of Loci Contained in Novel Y-STR Multiplexes

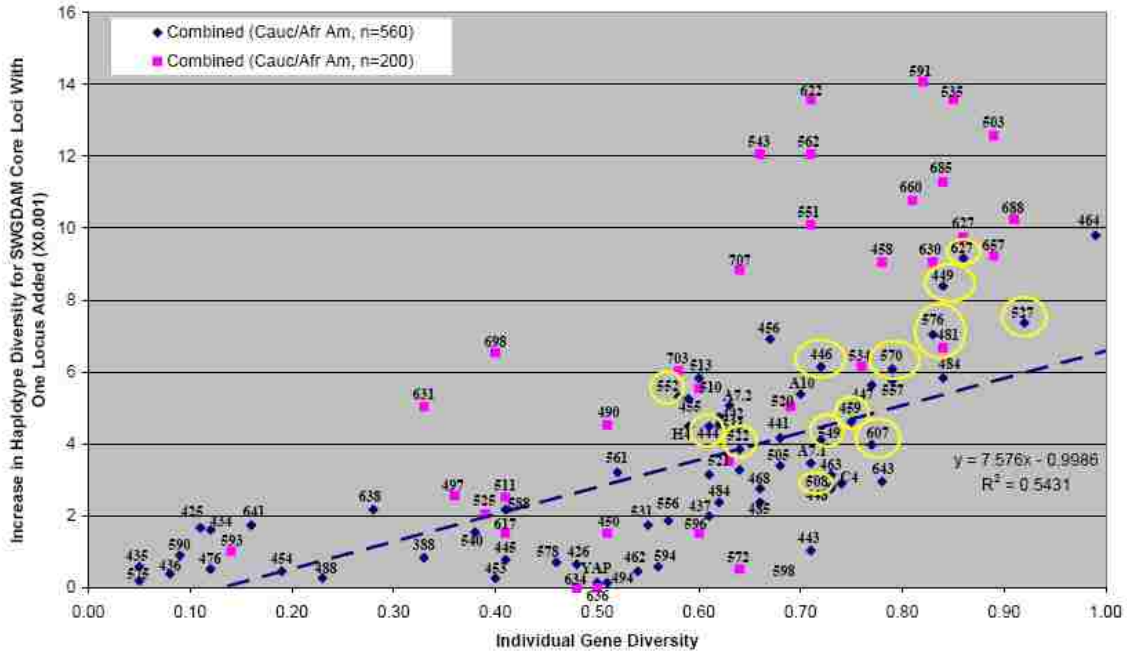

Figure 69. Evaluation of Individual Y-STR Locus Contribution to the Haplotype Diversity of Commonly Used Y-STRs

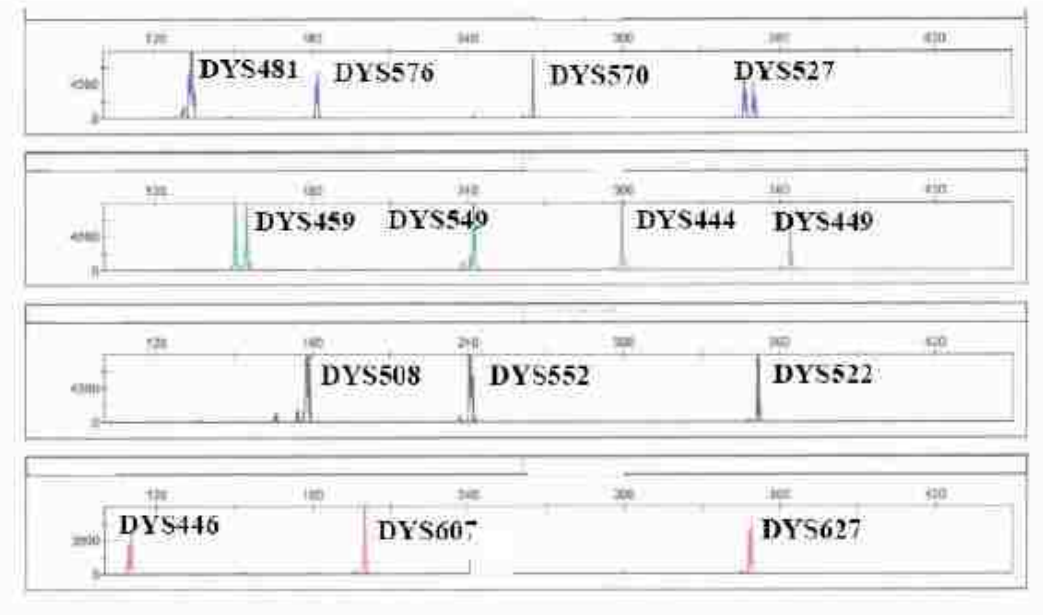

Figure 70. Ultra-High Discrimination (UHD) Y-STR Multiplex

APPENDIX B: TABLES

Table 1. Evaluation of the Correlation Between Age of the Stain and the Soret Band Hypsochromic Shift Using Various Age Intervals

Sample	r^2 value			
	15min-2days	15min-1 week	15min-1 month	15 min-1 year
	"Hours"	"Days"	"Weeks"	"Months"
22°C	0.9550	0.9481	0.9566	0.9626
37°C	0.9843	0.9667	0.9556	0.8430

Table 2. Comparison of the ΔλSoret For Bloodstains Stored at 22°C Using Two Different Spectrophotometers

Sample	λSoret – Microplate Reader	λSoret – UV Spectrophotometer	Difference
15 min	412.5	414.0	1.5
30 min	412.0	414.0	2.0
1 hour	412.0	413.7	1.7
3 hours	411.3	413.0	1.7
6 hours	411.0	411.7	0.7
18 hours	411.0	412.0	1.0
24 hours	410.8	411.8	1.0
48 hours	410.0	411.0	1.0
1 week	408.7	410.3	1.6
1 month	408.0	409.2	1.2
3 months	407.5	408.7	1.2
6 months	408.0	408.7	0.7
1 year	407.5	406.3	-1.2
	Total shift = 5nm	Total shift = 7.7nm	Average = 1.1nm

Table 3. Comparison of Hypsochromic Shift Correlation Values Using Two Different Spectrophotometers

	22°C		37°C	
	15min-48hrs	15min-1yr	15min-48hrs	15min-1yr
Microplate Reader	0.9462	0.9592	0.9858	0.8250
UV- Spec	0.9180	0.9577	0.9534	0.8130

Table 4. Comparison of λSoret for Standard (60 μl) and Small Bloodstains (< 1 μl)

	Average λSoret		
	15 minutes	48 hour	1 week
Full stain (60μl)	412.8	410.1	408.9
0.75 μl stain	412.0	408.0	406.0
0.5 μl stain	412.0	408.0	406.0

Table 5. Enzyme Candidates For Time Since Deposition Assays

Enzyme	Detection	Secondary Detection
Lactate dehydrogenase	NAD	MTT-formazan
Malate dehydrogenase	NAD	MTT-formazan
UDPglucose dehydrogenase	NAD	MTT-formazan
Glycerate dehydrogenase	NAD	MTT-formazan
Galactose dehydrogenase	NAD	MTT-formazan
Octanol dehydrogenase	NAD	MTT-formazan
Aldehyde dehydrogenase	NAD	MTT-formazan
Fumarate hydratase	NAD	MTT-formazan
Dihydrooroate dehydrogenase	NAD	MTT-formazan
L-glutamate dehydrogenase	NADP	MTT-formazan
Isocitrate dehydrogenase	NADP	MTT-formazan
Phosphogluconate dehydrogenase	NADP	MTT-formazan
Glucose-6-phosphate dehydrogenase	NADP	MTT-formazan
Aconitase	NADP	MTT-formazan
Phosphoglucomutase	NADP	MTT-formazan
L-xyulose reductase	NADP	MTT-formazan
Glycerol dehydrogenase	NADP	MTT-formazan
Carbonic anhydrase	4-MU	
Glycerol -3-phosphate dehydrogenase	MTT-formazan	
Alcohol dehydrogenase	MTT-formazan	
3-Hydroxybutyrate dehydrogenase	MTT-formazan	
Gluconate dehydrogenase	MTT-formazan	
Guanine deaminase	MTT-formazan	
Succinate dehydrogenase	MTT-formazan	
Purine nucleoside phosphorylase	MTT-formazan	
Aldehyde oxidase	NBT-formazan	
L-amino acid oxidase	NBT-formazan	
Sarcosine Oxidase	NBT-formazan	
Uricase	NBT-formazan	
Cytochrome-C oxidase	Indophenol blue (vis)	
Cholinesterase	Fast Red RT	
Acid phosphatase	Fast Blue BB	

Table 6. Time Required for Complete Loss of Enzyme Activity in Aged Bloodstains

Enzyme	Months to Reach 0 Activity
Glycerate dehydrogenase	10.1
Lactate dehydrogenase	11.4
Isocitrate dehydrogenase	11.8
Alcohol dehydrogenase	14.4
Phosphogluconate dehydrogenase	16.0
Malate dehydrogenase	20.7
L-xyulose reductase	28.7
3-hydroxybutyrate dehydrogenase	144.7
Phosphoglucomutase	Stable
Glucose-6-phosphate dehydrogenase	Stable
Gluconate dehydrogenase	Stable

Table 7. Characteristics of miRNA Panel and Normalizers for Body Fluid Identification Assays

microRNAs					
Sanger ID	Body Fluid Assay	Sequence	Entrez Gene ID	Mature sequence Sanger Accession #	Literature Ref.
hsa-miR-451	Blood Menstrual Blood	AAACCGUUACCAUUACUGAGUU	574411	MIMAT0001631	[55,59,61,121-123]
hsa-miR-16	Blood	UAGCAGCACGUAAAUAUUGGCG	--	MIMAT0000069	[41,59,124,125]
hsa-miR-135b	Semen	UAUGGCUUUUCAUUCCUAUGUGA	--	MIMAT0000758	[59,126,127]
hsa-miR-10b	Semen	UACCCUGUAGAACCGAAUUUGUG	406903	MIMAT0000254	[46,48,50,57,59]
hsa-miR-658	Saliva	GGCGGAGGGAAGUAGGUCCGUUGGU	724028	MIMAT0003336	none
hsa-miR-205	Saliva	UCCUUCAUUCCACCGGAGUCUG	--	MIMAT0000266	[42-45,50,52,59,128]
hsa-miR-124a	Vaginal Secretions	UAAGGCACGCGGUGAAUGCC	--	MIMAT0000422	[47,50,53,56,59,129]
hsa-miR-372	Vaginal Secretions	AAAGUGCUGCGACAUUUGAGCGU	442917	MIMAT0000724	[50,59,130]
hsa-miR-412	Menstrual Blood	ACUUCACCUGGUCCACUAGCCGU	574433	MIMAT0002170	none
Small non-coding RNAs (snRNA/snoRNAs) - Normalization					
RNU6b	All	CTGCGCAAGGATGACACGCAAATTCGTGAAGCGTTCCATATTTTT	26826	Not applicable	[131-133]
SNORD44	Blood - species	CCTGGATGATGATAGCAAATGCTGACTGAACATGAAGGTCTTAATTAGCTCTAACTGACT	26806	Not applicable	[131,134]

Table 8. Determination of Negative Result Threshold Values Through Assessment of Negative Controls

RT (-) samples

	miR451 50pg	miR16 50pg	miR135b 500pg	miR10b 500pg	miR658 50pg	miR205 50pg	miR124a 50pg	miR195 50pg	miR372 50pg	miR412 50pg	U6b 50pg	U6b 500pg	U44 50pg
Blood	Undet.	Undet.	Undet.	Undet.	40.0	40.1	37.3	45.6	Undet.	41.1	35.8	35.4	Undet.
Semen	Undet.	Undet.	Undet.	Undet.	40.1	39.5	37.3	46.9	Undet.	43.0	35.7	36.0	Undet.
Saliva	Undet.	Undet.	Undet.	Undet.	41.1	39.9	37.0	45.1	Undet.	42.6	35.3	35.4	Undet.
Vag.Sec	Undet.	Undet.	Undet.	Undet.	40.5	40.6	37.1	46.8	Undet.	40.7	35.6	35.5	Undet.
Mnstrl.Bld	Undet.	Undet.	Undet.	Undet.	42.6	40.9	37.6	Undet.	Undet.	42.1	36.2	35.4	Undet.
Avg	Undet.	Undet.	Undet.	Undet.	40.9	40.2	37.3	46.1	Undet.	41.9	35.7	35.5	Undet.
SD	N/A	N/A	N/A	N/A	1.1	0.6	0.2	0.9	N/A	1	0.3	0.3	N/A
Invalid Result	*N/A*	*N/A*	*N/A*	*N/A*	*≥37.5*	*≥38.5*	*≥36.5*	*≥43.0*	*N/A*	*≥39.0*	*>34.5*	*>34.5*	*N/A*

RT (+) samples

	miR451 50pg	miR16 50pg	miR135b 500pg	miR10b 500pg	miR658 50pg	miR205 50pg	miR124a 50pg	miR195 50pg	miR372 50pg	miR412 50pg	U6b 50pg	U6b 500pg	U44 50pg
Blood	*16.3*	*17.8*	37.9	39.4	37.5	36.4	33.1	18.5	37.9	32.5	24.8	22.3	28.0
Semen	31.6	30.2	*33.4*	*34.7*	39.6	34.0	33.8	36.0	38.2	32.4	30.2	29.2	43.2
Saliva	32.2	29.4	36.5	42.6	*27.7*	*27.1*	31.6	29.6	36.9	31.2	31.9	28.5	37.9
VagSec	34.4	32.4	40.7	39.3	33.6	29.9	*25.1*	*32.9*	*37.2*	31.9	28.3	27.5	33.9
Mnstrl.Bld	*24.4*	26.5	37.9	36.9	35.2	28.5	26.0	26.4	36.6	*31.7*	27.6	25.1	32.4

Undet. = undetected (Ct > 50); N/A = not applicable; SD = standard deviation

Threshold = Average – 3 SD (rounded to nearest .5 value)

RT (-) = negative reverse transcription reaction (no reverse transcriptase enzyme added)

Table 9. Sensitivity and Specificity of snRNAs and snoRNAs in Biological Stains

	Ct values											
Sample	U6b	U44	U26	U27	U28	U29	U30	U31	U38B	U43	U48	U90
Blood	24.8	28.3	27.0	27.2	30.5	27.3	39.4	35.6	33.0	30.2	32.0	35.3
Semen	29.2	43.2	43.2	39.6	42.1	38.0	29.8	26.6	41.4	33.6	40.8	42.3
Saliva	31.9	37.9	34.5	34.1	40.4	34.8	38.6	33.2	38.3	32.0	38.2	44.1
Vaginal Secretions	28.3	33.9	30.7	30.5	34.2	33.1	33.4	31.5	36.5	32.9	36.1	37.8
Menstrual Blood	27.6	32.4	28.4	28.4	30.6	28.9	29.2	27.2	32.5	29.3	30.2	34.4
Dog	23.7	41.7	44.0	28.1	42.6	40.2	47.1	35.0	38.1	29.3	38.8	40.4
Cat	24.6	42.3	42.5	36.3	42.8	41.1	42.3	42.3	40.9	31.1	39.4	42.5
Horse	25.1	48.9	41.5	38.8	40.2	39.3	45.1	28.3	41.4	33.0	39.6	41.5
Crane	25.9	42.0	48.0	38.6	40.9	48.3	47.1	Undet.	41.6	35.5	42.5	40.0
Cow	22.4	39.2	39.1	25.5	38.4	32.4	43.1	40.0	39.5	30.1	39.9	44.0
Sheep	22.9	40.7	38.9	26.3	40.3	34.3	44.1	27.7	41.2	28.6	39.6	39.7
Coyote	28.5	Undet.	49.2	33.2	43.7	44.2	Undet.	39.6	42.0	29.7	42.8	40.1
Pat. Cavy	29.7	42.4	Undet.	40.2	42.4	45.3	Undet.	40.8	47.0	28.5	44.0	39.3
Ferret	24.4	49.2	43.5	29.3	Undet.	36.0	Undet.	35.7	40.5	28.9	41.8	42.2
Deer	23.8	42.5	44.0	31.1	40.4	37.8	45.4	31.9	42.5	28.6	Undet.	41.4
Tortoise	29.6	40.2	46.8	40.6	42.6	47.0	41.5	42.3	35.8	32.6	36.6	38.1
Lamb	21.5	41.5	40.1	26.9	40.6	33.6	39.1	27.1	37.8	29.4	45.9	39.3
Chimpanzee	24.3	28.7	26.5	25.8	30.1	31.2	29.0	26.2	NT	29.7	NT	NT
Baboon	25.0	39.5	27.1	26.8	31.1	32.3	44.4	26.3	NT	29.7	NT	NT
Brown Lemur	25.2	Undet.	40.2	27.5	30.8	33.4	43.4	27.1	NT	35.7	NT	NT
Howler monkey	24.3	40.3	28.2	28.0	31.0	32.8	43.6	27.3	NT	30.3	NT	NT
Cynomolgus monkey	24.3	Undet.	26.6	26.4	30.0	30.8	44.8	27.1	NT	29.3	NT	NT
African Green monkey	25.1	48.9	26.6	28.4	30.2	31.1	40.7	26.4	NT	31.3	NT	NT
Spider Monkey	27.6	48.1	31.7	31.1	34.6	36.1	43.9	28.9	28.8	29.2	41.0	41.9
Rhesus macaque	22.8	43.3	27.0	27.9	30.5	32.8	44.6	25.7	29.2	28.4	28.2	39.2
Pig-tailed macaque	23.8	Undet.	32.5	27.4	30.4	36.9	47.7	26.6	35.7	29.7	29.8	39.1

Undet = undetected (Ct > 50) ; NT = not tested

Table 10. Summary of Conditions for Environmentally Compromised Samples

Outside, Covered (OC) – Exposed to heat, light and humidity						
Body Fluid	Exposure	Temperature Range		Humidity Range		Rain
		Low (^{o}F)	High (^{o}F)	Minimum	Maximum	(inches)
Blood	3 days	66	90	44	93	NA
	7 days	66	92	44	90	NA
	1 month	66	95	43	87	NA
Semen	3 days	66	92	45	93	NA
	7 days	66	93	45	91	NA
	1 month	66	96	44	88	NA
Saliva	3 days	66	92	45	93	NA
	7 days	66	93	45	91	NA
	1 month	66	96	44	88	NA
Vaginal Secretions	3 days	72	94	38	86	NA
	7 days	72	96	43	86	NA
	1 month	71	96	46	88	NA

Outside, Uncovered (OUC) – Exposed to heat, light, humidity and rain						
Body Fluid	Exposure	Temperature Range		Humidity Range		Rain
		Low (^{o}F)	High (^{o}F)	Minimum	Maximum	(inches)
Blood	1 day	66	88	38	84	0.63
	3 days	66	90	44	93	1.59
	7 days	66	92	44	90	2.70
Semen	1 day	66	89	42	94	1.59
	3 days	66	92	45	93	1.59
	7 days	66	93	45	91	2.70
Saliva	1 day	66	89	42	94	1.59
	3 days	66	92	45	93	1.59
	7 days	66	93	45	91	2.70
Vaginal Secretions	1 day	72	90	50	84	1.26
	3 days	72	91	46	85	1.28
	7 days	72	96	47	88	7.56

Table 11. miRNA Stability - Body Fluid Identification in Aged and Compromised Biological Fluid Samples

	Blood									
	22°C	22°C	37°C	37°C	OC	OC	OC	OUC	OUC	OUC
	1 year	18 months 2 years*	3 months	6 months	3 days	1 week	1 month	1 day	3 days	1 week
Blood assay (451-16)	+	+	-	+	-	+	NA	+	+	+
	Semen									
Semen assay (135b-10b)	+	+	+	+	+	+	-	+	-	-
	Saliva									
Saliva assay (658-205)	+	-	U6b-	U6b-	U6b-	U6b-	-	-	-	-
	Vaginal Secretions									
VagSec assay (124a-372)	+	+	+	+	+	-	U6b-	-	-	-

*2 year sample tested for blood, 18 month sample for all other body fluids

OC = outside, covered (heat, light, humidity); OUC = outside, uncovered (heat, light, humidity, rain); NA = not available

(+) = body fluid correctly identified; (-) body fluid not detected; U6b(-) = U6b value not acceptable, no further analysis performed

Table 12. Allele Recovery from Micro-Dissected Sperm Cells Using Various Amplification Cycles

# of Cells	36 cycles			32 cycles			28 cycles		
	50 RFU	100 RFU	150 RFU	50 RFU	100 RFU	150 RFU	50 RFU	100 RFU	150 RFU
1	11	11	10	2	2	1	1	0	0
5	19	19	19	16(3)	16(2)	9(1)	3	0	0
10	20(2)	20(2)	20(2)	17(3)	14(3)	10	0	0	0
20	20(2)	20(3)	20(3)	20	16	14	6	1	0
30	20(4)	20(4)	20(3)	2(2)	1(1)	1(1)	12	3	2
40	20(7)	20(7)	20(7)	16(1)	11(1)	11	18	11	9
50	19	19	19	20(1)	19(1)	18(1)	10(1)	6	3
60	20(2)	19(1)	18(1)	20	20	20	10	2	0
70	20(2)	20(2)	20(2)	18	13	12	20	20	15
80	20(1)	20(1)	20(1)	20	20	20	18	14	6
90	20	20	20	20(1)	20(1)	20(1)	15	6	1
100	19(1)	18(1)	18(1)	20	18	16	20	16	9
0	3(1)	3(1)	3(1)	1(1)	0	0	0	0	0
9947a	20	20	20	20	20	20	20	20	20
Blank	0	0	0	0	0	0	0	0	0

(#) = allelic drop-in (not originating from the donor in the study)

Table 13. Allele Recovery from Sperm Cells Isolated from a Sperm-Sperm (1:1) Mixture

# Cells	# Alleles Recovered (out of 14)		# Alleles Recovered (out of 14)		# Alleles Recovered (out of 14)	
	50 RFU		100 RFU		150 RFU	
	Male 1	Male 2	Male 1	Male 2	Male 1	Male 2
5	16	15	14	15	13	15
20	8	19	8	17	8	17
30	20	20	20	19	20	19
40	20	20	20	20	20	20
60	19	20	19	20	19	20
80	20	20	20	20	20	20
100	20	20	20	20	20	20
0	2	20	2	0	2	0
9947a	20		20		20	
Blank	0		0		0	

Table 14. Allele Recovery from Epithelial Cells Isolated from a 1:1 Buccal-Vaginal Epithelial Cell Mixture

# Cells	# Alleles Recovered (out of 14)		# Alleles Recovered (out of 14)		# Alleles Recovered (out of 14)	
	50 RFU		100 RFU		150 RFU	
	Male	Female	Male	Female	Male	Female
5	7	14	6	12	6	12
10	13	14	13	14	13	14
10	8	14	8	14	8	14
10	14	14	14	14	14	14
20	14	14	14	14	14	14
30	14	14	14	14	14	14
0	0	5	0	5	0	5
9947a	14		14		14	
Blank	0		0		0	

REFERENCES

1. Andrasko J. The estimation of age of bloodstains by HPLC analysis. J Forensic Sci; 1997; 42 (4): 601-607.

2. Inoue H, Takabe F, Iwasa M and Maeno Y. Identification of fetal hemoglobin and simultaneous estimation of bloodstain age by high-performance liquid chromatography. Int J Legal Med; 1991; 104 (3): 127-131.

3. Inoue H, Takabe F, Iwasa M, Maeno Y and Seko Y. A new marker for estimation of bloodstain age by high performance liquid chromatography. Forensic Sci Int; 1992; 57 (1): 17-27.

4. Kumagai R. Analysis of hemoglobin in bloodstains using high-performance liquid chromatography. Nihon Hoigaku Zasshi; 1993; 47 (3): 213-219.

5. Matsuoka T, Taguchi T and Okuda J. Estimation of bloodstain age by rapid determinations of oxyhemoglobin by use of oxygen electrode and total hemoglobin. Biol Pharm Bull; 1995; 18 (8): 1031-1035.

6. Anderson S, Howard B, Hobbs GR and Bishop CP. A method for determining the age of a bloodstain. Forensic Sci Int; 2005; 148 (1): 37-45.

7. Bauer M, Polzin S and Patzelt D. Quantification of RNA degradation by semi-quantitative duplex and competitive RT-PCR: a possible indicator of the age of bloodstains? Forensic Sci Int; 2003; 138 (1-3): 94-103.

8. Juusola J and Ballantyne J. Messenger RNA profiling: a prototype method to supplant conventional methods for body fluid identification. Forensic Sci Int; 2003; 135 (2): 85-96.

9. Juusola J and Ballantyne J. Multiplex mRNA profiling for the identification of body fluids. Forensic Sci Int; 2005; 152 (1): 1-12.

10. Juusola J and Ballantyne J. mRNA profiling for body fluid identification by multiplex quantitative RT-PCR. J Forensic Sci; 2007; 52 (6): 1252-1262.

11. Setzer M, Juusola J and Ballantyne J. Recovery and stability of RNA in vaginal swabs and blood, semen, and saliva stains. J Forensic Sci; 2008; 53 (2): 296-305.

12. Schneider PM, Bender K, Mayr WR, Parson W, Hoste B, Decorte R *et al.* STR analysis of artificially degraded DNA-results of a collaborative European exercise. Forensic Sci Int; 2004; 139 (2-3): 123-134.

13. Asamura H, Fujimori S, Ota M and Fukushima H. MiniSTR multiplex systems based on non-CODIS loci for analysis of degraded DNA samples. Forensic Sci Int; 2007; 173 (1): 7-15.

14. Asamura,H., Sakai,H., Ota,M. and Fukushima,H. MiniY-STR quadruplex systems with short amplicon lengths for analysis of degraded DNA samples. Forensic Science International: Genetics 1(1), 56-61. 2007.

15. Butler JM, Shen Y and McCord BR. The development of reduced size STR amplicons as tools for analysis of degraded DNA. J Forensic Sci; 2003; 48 (5): 1054-1064.

16. Coble MD and Butler JM. Characterization of new miniSTR loci to aid analysis of degraded DNA. J Forensic Sci; 2005; 50 (1): 43-53.

17. Dixon LA, Dobbins AE, Pulker HK, Butler JM, Vallone PM, Coble MD *et al.* Analysis of artificially degraded DNA using STRs and SNPs-results of a collaborative European (EDNAP) exercise. Forensic Sci Int; 2006; 164 (1): 33-44.

18. Eichmann C and Parson W. 'Mitominis': multiplex PCR analysis of reduced size amplicons for compound sequence analysis of the entire mtDNA control region in highly degraded samples. Int J Legal Med; 2008.

19. Hill CR, Kline MC, Coble MD and Butler JM. Characterization of 26 miniSTR loci for improved analysis of degraded DNA samples. J Forensic Sci; 2008; 53 (1): 73-80.

20. Opel KL, Chung DT, Drabek J, Butler JM and McCord BR. Developmental validation of reduced-size STR Miniplex primer sets. J Forensic Sci; 2007; 52 (6): 1263-1271.

21. Park MJ, Lee HY, Chung U, Kang SC and Shin KJ. Y-STR analysis of degraded DNA using reduced-size amplicons. Int J Legal Med; 2007; 121 (2): 152-157.

22. Tsukada K, Takayanagi K, Asamura H, Ota M, Kobayashi K and Fukushima H. Simultaneous PCR of Eight Loci for Very Short Y-STR Fragment Size. Progress in Forensic Genetics; 2004; 10 (322-324.

23. Babar IA, Slack FJ and Weidhaas JB. miRNA modulation of the cellular stress response. Future Oncol; 2008; 4 (2): 289-298.

24. Baehrecke EH. miRNAs: micro managers of programmed cell death. Curr Biol; 2003; 13 (12): R473-R475.

25. Bagnyukova TV, Pogribny IP and Chekhun VF. MicroRNAs in normal and cancer cells: a new class of gene expression regulators. Exp Oncol; 2006; 28 (4): 263-269.

26. Carrington JC and Ambros V. Role of microRNAs in plant and animal development. Science; 2003; 301 (5631): 336-338.

27. Carthew RW. Gene regulation by microRNAs. Curr Opin Genet Dev; 2006; 16 (2): 203-208.

28. Chen CZ and Lodish HF. MicroRNAs as regulators of mammalian hematopoiesis. Semin Immunol; 2005; 17 (2): 155-165.

29. Cheng HY and Obrietan K. Revealing a role of microRNAs in the regulation of the biological clock. Cell Cycle; 2007; 6 (24): 3034-3035.

30. Di LG, Calin GA and Croce CM. MicroRNAs: fundamental facts and involvement in human diseases. Birth Defects Res C Embryo Today; 2006; 78 (2): 180-189.

31. Jovanovic M and Hengartner MO. miRNAs and apoptosis: RNAs to die for. Oncogene; 2006; 25 (46): 6176-6187.

32. Klein ME, Impey S and Goodman RH. Role reversal: the regulation of neuronal gene expression by microRNAs. Curr Opin Neurobiol; 2005; 15 (5): 507-513.

33. Kloosterman WP and Plasterk RH. The diverse functions of microRNAs in animal development and disease. Dev Cell; 2006; 11 (4): 441-450.

34. Kusenda B, Mraz M, Mayer J and Pospisilova S. MicroRNA biogenesis, functionality and cancer relevance. Biomed Pap Med Fac Univ Palacky Olomouc Czech Repub; 2006; 150 (2): 205-215.

35. Lee CT, Risom T and Strauss WM. MicroRNAs in mammalian development. Birth Defects Res C Embryo Today; 2006; 78 (2): 129-139.

36. Lodish HF, Zhou B, Liu G and Chen CZ. Micromanagement of the immune system by microRNAs. Nat Rev Immunol; 2008; 8 (2): 120-130.

37. Mendell JT. MicroRNAs: critical regulators of development, cellular physiology and malignancy. Cell Cycle; 2005; 4 (9): 1179-1184.

38. O'Driscoll L. The emerging world of microRNAs. Anticancer Res; 2006; 26 (6B): 4271-4278.

39. Zhang B, Wang Q and Pan X. MicroRNAs and their regulatory roles in animals and plants. J Cell Physiol; 2007; 210 (2): 279-289.

40. Zhao Y and Srivastava D. A developmental view of microRNA function. Trends Biochem Sci; 2007; 32 (4): 189-197.

41. Calin GA, Cimmino A, Fabbri M, Ferracin M, Wojcik SE, Shimizu M *et al.* MiR-15a and miR-16-1 cluster functions in human leukemia. Proc Natl Acad Sci U S A; 2008; 105 (13): 5166-5171.

42. Feber A, Xi L, Luketich JD, Pennathur A, Landreneau RJ, Wu M *et al.* MicroRNA expression profiles of esophageal cancer. J Thorac Cardiovasc Surg; 2008; 135 (2): 255-260.

43. Gottardo F, Liu CG, Ferracin M, Calin GA, Fassan M, Bassi P *et al.* Micro-RNA profiling in kidney and bladder cancers. Urol Oncol; 2007; 25 (5): 387-392.

44. Gregory PA, Bert AG, Paterson EL, Barry SC, Tsykin A, Farshid G *et al.* The miR-200 family and miR-205 regulate epithelial to mesenchymal transition by targeting ZEB1 and SIP1. Nat Cell Biol; 2008.

45. Iorio MV, Visone R, Di LG, Donati V, Petrocca F, Casalini P *et al.* MicroRNA signatures in human ovarian cancer. Cancer Res; 2007; 67 (18): 8699-8707.

46. Ladeiro Y, Couchy G, Balabaud C, Bioulac-Sage P, Pelletier L, Rebouissou S *et al.* MicroRNA profiling in hepatocellular tumors is associated with clinical features and oncogene/tumor suppressor gene mutations. Hepatology; 2008.

47. Lukiw WJ. Micro-RNA speciation in fetal, adult and Alzheimer's disease hippocampus. Neuroreport; 2007; 18 (3): 297-300.

48. Ma L, Teruya-Feldstein J and Weinberg RA. Tumour invasion and metastasis initiated by microRNA-10b in breast cancer. Nature; 2007; 449 (7163): 682-688.

49. Negrini M and Calin GA. Breast cancer metastasis: a microRNA story. Breast Cancer Res; 2008; 10 (2): 203.

50. Rosenfeld N, Aharonov R, Meiri E, Rosenwald S, Spector Y, Zepeniuk M *et al.* MicroRNAs accurately identify cancer tissue origin. Nat Biotechnol; 2008; 26 (4): 462-469.

51. Subramanian S, Lui WO, Lee CH, Espinosa I, Nielsen TO, Heinrich MC *et al.* MicroRNA expression signature of human sarcomas. Oncogene; 2008; 27 (14): 2015-2026.

52. Tran N, McLean T, Zhang X, Zhao CJ, Thomson JM, O'Brien C *et al.* MicroRNA expression profiles in head and neck cancer cell lines. Biochem Biophys Res Commun; 2007; 358 (1): 12-17.

53. Baroukh N, Ravier MA, Loder MK, Hill EV, Bounacer A, Scharfmann R *et al.* MicroRNA-124a regulates Foxa2 expression and intracellular signaling in pancreatic beta-cell lines. J Biol Chem; 2007; 282 (27): 19575-19588.

54. Beuvink I, Kolb FA, Budach W, Garnier A, Lange J, Natt F *et al.* A novel microarray approach reveals new tissue-specific signatures of known and predicted mammalian microRNAs. Nucleic Acids Res; 2007; 35 (7): e52.

55. Bruchova H, Yoon D, Agarwal AM, Mendell J and Prchal JT. Regulated expression of microRNAs in normal and polycythemia vera erythropoiesis. Exp Hematol; 2007; 35 (11): 1657-1667.

56. Conaco C, Otto S, Han JJ and Mandel G. Reciprocal actions of REST and a microRNA promote neuronal identity. Proc Natl Acad Sci U S A; 2006; 103 (7): 2422-2427.

57. Garzon R, Pichiorri F, Palumbo T, Iuliano R, Cimmino A, Aqeilan R *et al.* MicroRNA fingerprints during human megakaryocytopoiesis. Proc Natl Acad Sci U S A; 2006; 103 (13): 5078-5083.

58. Krichevsky AM, Sonntag KC, Isacson O and Kosik KS. Specific microRNAs modulate embryonic stem cell-derived neurogenesis. Stem Cells; 2006; 24 (4): 857-864.

59. Landgraf P, Rusu M, Sheridan R, Sewer A, Iovino N, Aravin A *et al.* A mammalian microRNA expression atlas based on small RNA library sequencing. Cell; 2007; 129 (7): 1401-1414.

60. Liang Y, Ridzon D, Wong L and Chen C. Characterization of microRNA expression profiles in normal human tissues. BMC Genomics; 2007; 8 (166.

61. Masaki S, Ohtsuka R, Abe Y, Muta K and Umemura T. Expression patterns of microRNAs 155 and 451 during normal human erythropoiesis. Biochem Biophys Res Commun; 2007; 364 (3): 509-514.

62. Lagos-Quintana M, Rauhut R, Lendeckel W and Tuschl T. Identification of novel genes coding for small expressed RNAs. Science; 2001; 294 (5543): 853-858.

63. Lagos-Quintana M, Rauhut R, Meyer J, Borkhardt A and Tuschl T. New microRNAs from mouse and human. RNA; 2003; 9 (2): 175-179.

64. Gill P, Whitaker J, Flaxman C, Brown N and Buckleton J. An investigation of the rigor of interpretation rules for STRs derived from less than 100 pg of DNA. Forensic Sci Int; 2000; 112 (1): 17-40.

65. Gill P. Application of low copy number DNA profiling. Croat Med J; 2001; 42 (3): 229-232.

66. Whitaker JP, Cotton EA and Gill P. A comparison of the characteristics of profiles produced with the AMPFlSTR SGM Plus multiplex system for both

standard and low copy number (LCN) STR DNA analysis. Forensic Sci Int; 2001; 123 (2-3): 215-223.

67. Casciola-Rosen L and Nagaraju K. Immunoblotting of single cell types isolated from frozen sections by laser microdissection. Methods Enzymol; 2002; 356 (70-79.

68. Di MD, Giuffre G, Staiti N, Simone A, Le DM and Saravo L. Single sperm cell isolation by laser microdissection. Forensic Sci Int; 2004; 146 Suppl (S151-S153.

69. Dietmaier W, Hartmann A, Wallinger S, Heinmoller E, Kerner T, Endl E *et al.* Multiple mutation analyses in single tumor cells with improved whole genome amplification. Am J Pathol; 1999; 154 (1): 83-95.

70. Lu L, Neff F, Dun Z, Hemmer B, Oertel WH, Schlegel J *et al.* Gene expression profiles derived from single cells in human postmortem brain. Brain Res Brain Res Protoc; 2004; 13 (1): 18-25.

71. Persson A, Backvall H, Ponten F, Uhlen M and Lundeberg J. Single cell gene mutation analysis using laser-assisted microdissection of tissue sections. Methods Enzymol; 2002; 356 (334-343.

72. Ponten F, Williams C, Ling G, Ahmadian A, Nister M, Lundeberg J *et al.* Genomic analysis of single cells from human basal cell cancer using laser-assisted capture microscopy. Mutat Res; 1997; 382 (1-2): 45-55.

73. Roehrl MH, Becker KF, Becker I and Hofler H. Efficiency of single-cell polymerase chain reaction from stained histologic slides and integrity of DNA in archival tissue. Diagn Mol Pathol; 1997; 6 (5): 292-297.

74. Suarez-Quian CA, Goldstein SR, Pohida T, Smith PD, Peterson JI, Wellner E *et al.* Laser capture microdissection of single cells from complex tissues. Biotechniques; 1999; 26 (2): 328-335.

75. Saiki RK, Gelfand DH, Stoffel S, Scharf SJ, Higuchi R, Horn GT *et al.* Primer-directed enzymatic amplification of DNA with a thermostable DNA polymerase. Science; 1988; 239 (4839): 487-491.

76. Cheng J, Waters LC, Fortina P, Hvichia G, Jacobson SC, Ramsey JM *et al.* Degenerate oligonucleotide primed-polymerase chain reaction and capillary electrophoretic analysis of human DNA on microchip-based devices. Anal Biochem; 1998; 257 (2): 101-6.

77. Cheung VG and Nelson SF. Whole genome amplification using a degenerate oligonucleotide primer allows hundreds of genotypes to be performed on less than one nanogram of genomic DNA. Proc Natl Acad Sci U S A; 1996; 93 (25): 14676-9.

78. Dean FB, Nelson JR, Giesler TL and Lasken RS. Rapid amplification of plasmid and phage DNA using Phi 29 DNA polymerase and multiply-primed rolling circle amplification. Genome Res; 2001; 11 (6): 1095-9.

79. Dean FB, Hosono S, Fang L, Wu X, Faruqi AF, Bray-Ward P *et al.* Comprehensive human genome amplification using multiple displacement amplification. Proc Natl Acad Sci U S A; 2002; 99 (8): 5261-6.

80. Huang Q, Schantz SP, Rao PH, Mo J, McCormick SA and Chaganti RS. Improving degenerate oligonucleotide primed PCR-comparative genomic hybridization for analysis of DNA copy number changes in tumors. Genes Chromosomes Cancer; 2000; 28 (4): 395-403.

81. Keohavong P and Thilly WG. Fidelity of DNA polymerases in DNA amplification. Proc Natl Acad Sci U S A; 1989; 86 (23): 9253-9257.

82. Kittler R, Stoneking M and Kayser M. A whole genome amplification method to generate long fragments from low quantities of genomic DNA. Anal Biochem; 2002; 300 (2): 237-244.

83. Kuukasjarvi T, Tanner M, Pennanen S, Karhu R, Visakorpi T and Isola J. Optimizing DOP-PCR for universal amplification of small DNA samples in comparative genomic hybridization. Genes Chromosomes Cancer; 1997; 18 (2): 94-101.

84. Lasken RS and Egholm M. Whole genome amplification: abundant supplies of DNA from precious samples or clinical specimens. Trends Biotechnol; 2003; 21 (12): 531-5.

85. Sanchez-Cespedes M, Cairns P, Jen J and Sidransky D. Degenerate oligonucleotide-primed PCR (DOP-PCR): evaluation of its reliability for screening of genetic alterations in neoplasia. Biotechniques; 1998; 25 (6): 1036-8.

86. Sussman HE. Whole-genome Amplification Easy as Phi: Amersham Biosciences amplifies genomic DNA with a unique DNA polymerase. The Scientist; 2003; 17 (16): 54.

87. Telenius H, Carter NP, Bebb CE, Nordenskjold M, Ponder BA and Tunnacliffe A. Degenerate oligonucleotide-primed PCR: general amplification of target DNA by a single degenerate primer. Genomics; 1992; 13 (3): 718-25.

88. Zhang L, Cui X, Schmitt K, Hubert R, Navidi W and Arnheim N. Whole genome amplification from a single cell: implications for genetic analysis. Proc Natl Acad Sci U S A; 1992; 89 (13): 5847-5851.

89. Ballantyne KN, van Oorschot RA and Mitchell RJ. Comparison of two whole genome amplification methods for STR genotyping of LCN and degraded DNA samples. Forensic Sci Int; 2006.

90. Hanson EK and Ballantyne J. Whole genome amplification strategy for forensic genetic analysis using single or few cell equivalents of genomic DNA. Anal Biochem; 2005; 346 (2): 246-257.

91. Jiang Z, Zhang X, Deka R and Jin L. Genome amplification of single sperm using multiple displacement amplification. Nucleic Acids Res; 2005; 33 (10): e91.

92. Sorensen KJ, Turteltaub K, Vrankovich G, Williams J and Christian AT. Whole-genome amplification of DNA from residual cells left by incidental contact. Anal Biochem; 2004; 324 (2): 312-4.

93. Rook MS, Delach SM, Deyneko G, Worlock A and Wolfe JL. Whole genome amplification of DNA from laser capture-microdissected tissue for high-throughput single nucleotide polymorphism and short tandem repeat genotyping. Am J Pathol; 2004; 164 (1): 23-33.

94. Comey CK, Presely KW, Smerick JB, Sobieralski CA, Stanley DM and Baechtel FS. Extraction Strategies for Amplified Fragment Length Polymorphism Analysis. J Forensic Sci; 1994; 39 (1254-1269.

95. Chomczynski P and Sacchi N. Single-step method of RNA isolation by acid guanidinium thiocyanate-phenol-chloroform extraction. Anal Biochem; 1987; 162 (1): 156-159.

96. Hanson EK and Ballantyne J. A highly discriminating 21 locus Y-STR "megaplex" system designed to augment the minimal haplotype loci for forensic casework. J Forensic Sci; 2004; 49 (1): 40-51.

97. Hanson EK, Berdos PN and Ballantyne J. Testing and evaluation of 43 "noncore" Y chromosome markers for forensic casework applications. J Forensic Sci; 2006; 51 (6): 1298-1314.

98. Hanson EK and Ballantyne J. Population Data for a Novel, Highly Discriminating Tetra-Local Y-Chromosome Short Tandem Repeat: DYS503. J Forensic Sci; 2007; 52 (2): 498-499.

99. Hanson EK and Ballantyne J. Population data for 48 'Non-Core' Y chromosome STR loci. Leg Med (Tokyo); 2007.

100. Hanson EK and Ballantyne J. An ultra-high discrimination y chromosome short tandem repeat multiplex DNA typing system. PLoS ONE; 2007; 2 (1): e688.

101. Lim LP and Linsley PS. Mustering the micromanagers. Nat Biotechnol; 2007; 25 (9): 996-997.

102. Doleshal M, Magotra AA, Choudhury B, Cannon BD, Labourier E and Szafranska AE. Evaluation and Validation of Total RNA Extraction Methods for MicroRNA Expression Analyses in Formalin-Fixed, Paraffin-Embedded Tissues. J Mol Diagn; 2008; 10 (3): 203-211.

103. Salamonsen LA and Woolley DE. Menstruation: induction by matrix metalloproteinases and inflammatory cells. J Reprod Immunol; 1999; 44 (1-2): 1-27.

104. Tabibzadeh S. The signals and molecular pathways involved in human menstruation, a unique process of tissue destruction and remodelling. Mol Hum Reprod; 1996; 2 (2): 77-92.

105. Lowe A, Murray C, Whitaker J, Tully G and Gill P. The propensity of individuals to deposit DNA and secondary transfer of low level DNA from individuals to inert surfaces. Forensic Sci Int; 2002; 129 (1): 25-34.

106. van Oorschot RA and Jones MK. DNA fingerprints from fingerprints. Nature; 1997; 387 (6635): 767.

107. Wickenheiser RA. Trace DNA: a review, discussion of theory, and application of the transfer of trace quantities of DNA through skin contact. J Forensic Sci; 2002; 47 (3): 442-450.

108. Kayser M, Caglia A, Corach D, Fretwell N, Gehrig C, Graziosi G *et al.* Evaluation of Y-chromosomal STRs: a multicenter study. Int J Legal Med; 1997; 110 (3): 125-129.

109. SWGDAM Y-STR Subcommittee. Report on the Current Activities of the Scientific Working Group on DNA Analysis Methods Y-STR Subcommittee. Forensic Science Communications; 2007; 6 (3).

110. Hanson EK and Ballantyne J. Comprehensive annotated STR physical map of the human Y chromosome: Forensic implications. Leg Med (Tokyo); 2006; 8 (2): 110-120.

111. Kayser M, Kittler R, Erler A, Hedman M, Lee AC, Mohyuddin A *et al.* A comprehensive survey of human Y-chromosomal microsatellites. Am J Hum Genet; 2004; 74 (6): 1183-1197.

112. Bauer M and Patzelt D. Evaluation of mRNA markers for the identification of menstrual blood. J Forensic Sci; 2002; 47 (6): 1278-82.

113. Bauer M and Patzelt D. Protamine mRNA as molecular marker for spermatozoa in semen stains. Int J Legal Med; 2003; 117 (3): 175-9.

114. Nussbaumer C, Gharehbaghi-Schnell E and Korschineck I. Messenger RNA profiling: a novel method for body fluid identification by real-time PCR. Forensic Sci Int; 2006; 157 (2-3): 181-186.

115. Sanger Institute, http://microrna.sanger.ac.uk/. 2008.

116. Huberty C. Applied Discriminant Analysis (Wiley Series in Probability and Statistics).: Wiley-Interscience, 1994.

117. Gill P. LCN DNA: proof beyond reasonable doubt? - a response. Nat Rev Genet; 2008.

118. Kloosterman AD and Kersbergen P. Efficacy and limits of genotyping low copy number (LCN) DNA samples by multiplex PCR of STR loci. J Soc Biol; 2003; 197 (4): 351-359.

119. Lucy D, Curran JM, Pirie AA and Gill P. The probability of achieving full allelic representation for LCN-STR profiling of haploid cells. Sci Justice; 2007; 47 (4): 168-171.

120. McCartney C. LCN DNA: proof beyond reasonable doubt? Nat Rev Genet; 2008; 9 (5): 325.

121. Dore LC, Amigo JD, Dos Santos CO, Zhang Z, Gai X, Tobias JW *et al.* A GATA-1-regulated microRNA locus essential for erythropoiesis. Proc Natl Acad Sci U S A; 2008; 105 (9): 3333-3338.

122. Xue X, Zhang Q, Huang Y, Feng L and Pan W. No miRNA were found in Plasmodium and the ones identified in erythrocytes could not be correlated with infection. Malar J; 2008; 7 (47.

123. Zhan M, Miller CP, Papayannopoulou T, Stamatoyannopoulos G and Song CZ. MicroRNA expression dynamics during murine and human erythroid differentiation. Exp Hematol; 2007; 35 (7): 1015-1025.

124. Calin GA, Dumitru CD, Shimizu M, Bichi R, Zupo S, Noch E *et al.* Frequent deletions and down-regulation of micro- RNA genes miR15 and miR16 at 13q14 in chronic lymphocytic leukemia. Proc Natl Acad Sci U S A; 2002; 99 (24): 15524-15529.

125. Linsley PS, Schelter J, Burchard J, Kibukawa M, Martin MM, Bartz SR *et al.* Transcripts targeted by the microRNA-16 family cooperatively regulate cell cycle progression. Mol Cell Biol; 2007; 27 (6): 2240-2252.

126. Bandres E, Cubedo E, Agirre X, Malumbres R, Zarate R, Ramirez N *et al.* Identification by Real-time PCR of 13 mature microRNAs differentially expressed in colorectal cancer and non-tumoral tissues. Mol Cancer; 2006; 5 (29.

127. Chim SS, Shing TK, Hung EC, Leung TY, Lau TK, Chiu RW *et al.* Detection and characterization of placental microRNAs in maternal plasma. Clin Chem; 2008; 54 (3): 482-490.

128. Sempere LF, Christensen M, Silahtaroglu A, Bak M, Heath CV, Schwartz G *et al.* Altered MicroRNA expression confined to specific epithelial cell subpopulations in breast cancer. Cancer Res; 2007; 67 (24): 11612-11620.

129. Karginov FV, Conaco C, Xuan Z, Schmidt BH, Parker JS, Mandel G *et al.* A biochemical approach to identifying microRNA targets. Proc Natl Acad Sci U S A; 2007; 104 (49): 19291-19296.

130. Voorhoeve PM, le SC, Schrier M, Gillis AJ, Stoop H, Nagel R *et al.* A genetic screen implicates miRNA-372 and miRNA-373 as oncogenes in testicular germ cell tumors. Cell; 2006; 124 (6): 1169-1181.

131. Wong L, Lee K, Russell I and Chen C. Endogenous Controls for Real-Time Quantitation of miRNA Using TaqMan$^{(R)}$ MicroRNA Assays. Applied Biosystems TechNotes; 2008; 15 (1): 15.

132. Peltier HJ and Latham GJ. Normalization of microRNA expression levels in quantitative RT-PCR assays: identification of suitable reference RNA targets in normal and cancerous human solid tissues. RNA; 2008; 14 (5): 844-852.

133. Brow DA and Guthrie C. Spliceosomal RNA U6 is remarkably conserved from yeast to mammals. Nature; 1988; 334 (6179): 213-218.

134. Kiss-Laszlo Z, Henry Y, Bachellerie JP, Caizergues-Ferrer M and Kiss T. Site-specific ribose methylation of preribosomal RNA: a novel function for small nucleolar RNAs. Cell; 1996; 85 (7): 1077-1088.